Dissertation

submitted to the

Combined Faculty of Natural Sciences and Mathematics

of the Ruperto Carola University Heidelberg, Germany

for the degree of

Doctor of Natural Sciences

presented by

M.Sc. Sabeth Maria Sheela Fischer

Born in: Weingarten, Baden-Württemberg, Germany

Oral examination: 26th April 2024

Impact of neurotoxic substances on the development and behavior of zebrafish embryos

Case studies with nicotine, desnitro-imidacloprid

and three antidepressants

Referees: **Prof. Dr. Thomas Braunbeck**

                        Prof. Dr. Joachim Sturve

Declaration

The applicant, Sabeth Maria Sheela Fischer, declares that she is the sole author of the submitted dissertation and that no other sources for help apart from those specifically referred to have been used. Additionally, the applicant declares that she has not applied for permission to enter examination procedure at another institution and that this dissertation has not been presented to other faculty and has not been used in its current or in any other form in another examination.

09.02.2024

Date   Signature

SUMMARY

The zebrafish embryo as an alternative complex vertebrate model can be utilized as a valuable tool for assessing developmental neurotoxicity. Analysis of embryonic behavior in particular is a method that can be used to detect even subtle changes that may later have serious effects on the fitness of the organism. Behavioral screening studies, in which the coiling activity or locomotion of embryos was examined, have proven to be suitable for identifying suspected developmental neurotoxic substances. As the activity level of the embryo is highly dependent on the developmental stage, experiments observing the full range of coiling behavior development exert the potential to discriminate different modes of action. However, since behavior is a sensitive endpoint, it can be influenced by various confounding factors. To allow a better comparison of results between laboratories, it is important to minimize possible deviations by standardizing a protocol.

Implementing the generalized additive modeling (GAM) approach is a beneficial option to minimize the influence of confounding factors in data analysis, which was my first aim of this dissertation. For this purpose, I chose nicotine as proof-of-concept substance for developmental neurotoxicity in tail coiling behavior experiments. The exposure concentrations were below acute median effective concentrations as previously determined by fish embryo toxicity (FET) tests. The analysis with GAM resulted in a flexible description of the trend of the behavior over the whole time period (21-47 hpf). By accounting natural variability of the fish into the model, I was able to pool the replicates which leads to higher robustness towards outliers by increasing sample size. In addition, I could discriminate the treatment-related alterations in the tail coiling behavior from several cofounding factors. My results revealed a biphasic response in the frequency with low concentrations showing an increase in activity which returned to control levels with a higher treatment. Concurrently, the duration of the movements was monotonically decreasing with increasing concentrations. To base these findings on morphological level, I furthermore inspected the integrity of corresponding secondary motoneurons (zn8 antibody) and skeletal muscle by using the birefringence properties arising from the ultrastructure of the sarcomeres. Here, the measured intensity of linear polarized light passing through the muscles can be used as a proxy for the degree of organization of the developing muscle. I detected a reduced motoneuron integrity as well as a diminished integrity of the muscles at higher nicotine concentrations. Both structural endpoints align with the behavior outcomes. However, the coiling assay has again proven to be more sensitive.

As the tail coiling assay amended with the GAM approach has been shown to be suitable to detect developmental neurotoxic effects, I next investigated a suspected metabolite of the neonicotinoid insecticide imidacloprid, namely desnitro-imidacloprid. The mode of action of both, the parent compound and the metabolite, are the binding at the nicotinic acetylcholine receptors (nAChRs). In *in vitro* experiments, desnitro-imidacloprid revealed a higher selectivity for mammalian receptors instead of insect receptors and was compared to the impact of nicotine treatment. Therefore, I investigated the developmental neurotoxic potential of this compound for vertebrates with zebrafish embryos as model organisms. Since acute exposure in the FET test at relevant concentrations has not demonstrated severe morphological impacts, I further utilized the sensitive coiling assay for a more in depth examination. Also here, I could not detect a significant alteration compared to the control. Even through, the compound was detected by target chemical analysis in the embryo's body, it showed no tendency to bioaccumulate. I suspect that possible reasons for the absences of effects could be quick metabolization by the embryo or a dissimilar affinity of desnitro-imidacloprid to mammalian and zebrafish nAChR. At least for zebrafish, I conclude that desnitro-imidacloprid does not show a comparable developmental neurotoxic potential like nicotine. Additionally, it illustrates the discrepancies of translating cell-based to whole organism findings.

In the last topic of my dissertation, I deal with the pollution of water bodies by contaminants, focusing on pharmaceuticals. Monitoring studies pointed out that a large proportion of anthropogenic substances detected in the aquatic environment have shown neuroactive modes of action. These also include antidepressants which are designed to interfere with neurotransmitter homeostasis. As the nervous system of vertebrates is highly conserved, fish can be adversely affected by exposure. In general, the development of the nervous system is particularly vulnerable to chemical stressors and can lead to long-lasting population-relevant impairments. In order to evaluate the risk of such psychoactive substances for fish, I investigated the impact of the most commonly prescribed and environmentally relevant antidepressant agents sertraline, paroxetine and venlafaxine on the developing zebrafish embryo. I could see shared effects of all three compounds in the FET test. This included cardiotoxicity which manifested in reduced heartbeat as well as pericardiac edema. Moreover, beginning degeneration of the fin seam was visible which I assume can be based on insufficient nutrient supply through weak cardiac performance. In addition, I could observe a loss of equilibrioception which became observable with the first unsuccessful swimming attempts. To study sublethal developmental neurotoxic effects of antidepressant exposure on embryonic behavior, I selected low concentrations which are based on previously determined EC_{10} values from the FET test. In the subsequent coiling assay, I could see a reduced ability to move with increasing concentrations for all antidepressants. Similarly to nicotine, low environmentally relevant concentrations of paroxetine showed the ability to induce hyperactive movements. In contrast, on day four (107 – 109 hpf) I could detect lower visual-motor response to a light stressor in a concentration dependent manner for all substances. To this end, I concluded that antidepressants could lower the fish embryos´ fitness by impacting heart health and equilibrium while swimming. In the case of sertraline, embryonic behavioral alterations have been visible at concentrations of 0.1 µg/L which was measured several times in contaminated water bodies. My findings suggest that antidepressants can pose a realistic threat to fish in the aquatic environment.

In my opinion, using zebrafish embryos to detect developmental neurotoxicity is one essential element of a testing strategy. Because neurotoxic substances can cause long-lasting damage during development, even at low concentrations, it is important to have a highly sensitive test method. Behavior as an endpoint, and in particular the observation of the coiling movement, has been shown to be the most sensitive and suitable for this purpose amongst the test methods used. For economic, time and ethical reasons, the number of *in vivo* models for testing the safety of chemicals is gradually going to be restricted. The zebrafish embryo as a complex vertebrate organism can be a valuable link between *in silico* or *in vitro* and *in vivo* outcomes.

ZUSAMMENFASSUNG

Der Embryo des Zebrabärblings, als alternatives komplexes Wirbeltiermodel, kann als wertvolles Werkzeug für die Bewertung von Entwicklungsneurotoxizität genutzt werden. Vor allem kann die Analyse von embryonalem Verhalten verwendet werden um sogar subtile Veränderungen, die möglichweise schwerwiegende Auswirkungen auf die Fitness des Organismus haben, zu detektieren. Screening-Studien zum Verhalten, in welchen die Aktivität der Schwanzbewegung (im Folgenden als „Coiling" bezeichnet) und der Fortbewegung des Embryos untersucht wurden, haben gezeigt, dass diese sich zur Identifizierung mutmaßlicher entwicklungsneurotoxischer Substanzen eignet. Da das Aktivitätsniveau der Embryonen maßgeblich vom Entwicklungsstadium abhängt, bieten Experimente, bei denen das gesamte Spektrum der Entwicklung des Coiling-Verhaltens beobachtet wird, die Möglichkeit, verschiedene Wirkmechanismen zu unterscheiden. Allerdings kann das Verhalten von verschiedenen Störfaktoren beeinflusst werden, gerade weil es ein sensitiver Endpunkt ist.

Das erste Ziel meiner Dissertation war es einen generalisierten additiven Modellansatz (Generalized Additive Model, GAM) einzuführen, der die Möglichkeit bietet diese Störgrößen in der Datenanalyse zu minimieren. Zu diesem Zweck habe ich Nikotin als „Proof-of-Concept" Substanz für die Prüfung der Entwicklungsneurotoxizität in den Experimenten zum Coiling-Verhalten gewählt. Die Belastungskonzentrationen lagen unter der akuten medianen wirksamen Konzentration (EC_{50}), welche zuvor im Fischembryotoxizitätstest (FET-Test) bestimmt wurde. Die Auswertung mit GAM resultierte in einer flexiblen Beschreibung des Verlaufs des Verhaltens über den ganzen Zeitabschnitt hinweg (21-47 hpf). Durch die in das Model miteinbezogene natürliche Variabilität der Fische, war es mir möglich die Replikate kombinieren, was zu einer höheren Robustheit gegenüber Ausreißern durch die vergrößerte Probengröße führte. Zusätzlich konnte ich behandlungsbedingte Veränderung im Coiling-Verhalten zu einigen Störfaktoren abgrenzen. Die in meinen Experimenten gemessene Coiling-Frequenz weist einen biphasischen Verlauf in Abhängigkeit von der Konzentration auf, welche bei niedrigen Konzentrationen eine erhöhte Aktivität aufweist und mit steigender Konzentration wieder auf das Niveau der Kontrolle sinkt. Hingegen sinkt die Dauer der Bewegung monoton mit steigenden Konzentrationen. Um diese Ergebnisse mit der morphologischen Ebene in Verbindung zu bringen, habe ich die Integrität der entsprechenden sekundären Motoneurone (zn8 Antikörper) sowie der Skeletmuskulatur anhand der Doppelbrechungseigenschaften untersucht, welche sich aus der Ultrastruktur der Sarkomere ergeben. Hierbei wurde die gemessene Intensität des linear polarisierten Lichts, welche durch den Muskel dringt, stellvertretend für den Grad der Organisation des sich entwickelnden Muskels genutzt. Ich detektierte eine reduzierte Integrität der Motoneurone sowie eine verminderte Unversehrtheit der Muskeln bei hohen Nikotinkonzentrationen. Beide strukturellen Endpunkte korrelierten mit den Verhaltensergebnissen. Jedoch hat sich der Coiling-Assay als am sensitivsten herausgestellt.

Da sich der Coiling-Assay mit samt der GAM Methode als geeignet zur Detektion von entwicklungsneurotoxischen Effekten erwiesen hat, habe ich als nächstes den verdächtigen Metaboliten Desnitro-Imidacloprid, des neonikotinoiden Insektizid Imidacloprid, untersucht. Die Wirkungsweise beider Substanzen, dem Ausgangsstoff und dem Metaboliten, ist die agonistische Bindung an den nikotinischen Acetylcholinrezeptor (nAChR). In *in vitro* Experimenten zeigte Desnitro-Imidacloprid jedoch eine höhere Selektivität zu Säugetier- anstelle von Insektenrezeptoren und wurde mit den Auswirkungen einer Nikotinbehandlung verglichen. Deshalb habe ich das entwicklungsneurotoxische Potenzial dieser Verbindung auf Wirbeltiere mit dem Embryo des Zebrabärblings als Modelorganismus untersucht. Da der Akut-Toxizitätstest keine schwerwiegenden morphologischen Effekte aufgezeigt hat, habe ich den sensitiven Coiling-Assay für eine weiterführende Untersuchung genutzt. Ebenso hier konnte ich keine signifikante Veränderung zur Kontrolle feststellen. Auch wenn die Substanz durch chemische Analyse im Körper des Embryos detektierbar war, war keine Bioakkumulation zu erkennen.

Ich vermute, dass mögliche Gründe für das Ausbleiben von Effekten entweder eine schnelle Verstoffwechselung durch den Embryo sein kann oder aber, dass Desnitro-Imidacloprid eine ungleiche Affinität zu Säugetier und Zebrabärblings nAChR aufweist. Zumindest für den Zebrabärbling kann ich hiermit schlussfolgern, dass Desnitro-Imidacloprid kein vergleichbares entwicklungsneurotoxisches Potential, welches vergleichbar mit Nikotin ist, besitzt. Außerdem zeigt dies, wie schwierig es ist, zellbasierte Ergebnisse auf einen ganzen Organismus zu übertragen.

Im letzten Thema meiner Dissertation beschäftigte ich mich mit der Wasserverschmutzung durch Schadstoffe mit Fokus auf Pharmazeutika. Beobachtungsstudien betonen, dass ein hoher Anteil von menschengemachten Substanzen, die in der aquatischen Umwelt detektiert wurden, eine neurotoxische Wirkungsweise aufweisen. Diese Substanzen schließen Antidepressiva mit ein, die dafür hergestellt wurden mit dem Gleichgewicht von Neurotransmittern zu interferieren. Da das Nervensystem in der gesamten Wirbeltierklasse hochkonserviert ist, können Fische negativ beeinträchtigt werden. Im Allgemeinen ist das sich entwickelnde Nervensystem besonders anfällig für chemische Stressoren und kann deshalb anfällig für langanhaltenden, populationsrelevanten Schädigungen sein. Um das Risiko solcher psychoaktiven Substanzen für den Fisch zu bewerten, habe ich die Auswirkungen der meistverschriebenen und umweltrelevanten Antidepressiva Sertralin, Paroxetin und Venlafaxin auf den sich entwickelnden Embryo des Zebrabärbling untersucht. Im FET-Test konnte ich Effekte sehen, die bei allen drei Verbindungen gleichermaßen auftraten. Dazu zählte eine Kardiotoxizität, welche sich durch verringerten Herzschlag und Perikardium-Ödeme zeigte. Außerdem war eine beginnende Degradation des Flossensaums zu erkennen, wobei ich annehme, dass diese auf die ungenügende Nährstoffversorgung durch den schwachen Herzschlag zurückzuführen ist. Zusätzlich konnte ich einen Verlust des Gleichgewichts feststellen, welcher bei den ersten Schwimmversuchen beobachtbar wurde. Um die subletalen entwicklungsneurotoxischen Effekte der Antidepressiva auf das embryonische Verhalten untersuchen zu können, wählte ich geringe Wirkungskonzentrationen (EC_{10}) aus, welche ich zuvor im FET-Test bestimmt hatte. Im nachfolgenden Coiling-Assay konnte ich bei allen Antidepressiva eine reduzierte Fähigkeit zur Bewegung mit steigenden Konzentrationen feststellen. Wie bei Belastung mit Nikotin, induzieren auch geringe und umweltrelevante Konzentrationen von Paroxetin hyperaktive Bewegungen. Im Gegensatz dazu, konnte ich für alle Substanzen am vierten Tag (107-109 hpf) eine konzentrationsabhängige geringere visuell-motorische Reaktion gegenüber Lichtreizen feststellen. Deshalb nehme ich an, dass diese Antidepressiva die Fitness der Embryonen durch beeinträchtigte Herzgesundheit und Gleichgewicht beim Schwimmen verringern können. Bei Sertralin war eine Veränderung des Embryonalverhalten schon bei Konzentrationen von 0,1 µg/L sichtbar, welche schon mehrmals in belasteten Gewässern gemessen werden konnte. Meine Ergebnisse legen nahe, dass Antidepressiva ein realistisches Risiko für Fische in der aquatischen Umwelt darstellen können.

Meiner Meinung nach ist der Embryo des Zebrabärblings ein essenzielles Element zur Testung von Entwicklungsneurotoxizität. Da neurotoxische Substanzen langwierige Schäden in der Entwicklung anrichten können, ist es wichtig, hochsensible Methoden zu etablieren. Verhalten als Endpunkt, und speziell die Beobachtung der Coiling-Bewegung, zeigte sich als sensitivste Methode für dieses Vorhaben. Aus wirtschaftlichen, zeitlichen und ethischen Gründen wird die Zahl der *in vivo* Modelle zur Prüfung der Sicherheit von Chemikalien allmählich eingeschränkt. Der Embryo des Zebrabärblings kann hier als komplexer Wirbeltierorganismus ein wertvolles Bindeglied zwischen *in silico* oder *in vitro* und *in vivo* Untersuchungen sein.

TABLE OF CONTENT

LIST OF FIGURES

LIST OF TABLES

ABBREVIATION

ACh	Acetylcholine
AChR	Acetylcholine receptor
AFT	Acute fish Toxicity
ANOVA	Analysis of variance
A-zone	Anisotropic zone (muscle)
BCF	Bioconcentration factor
CaP	Caudal primary (motoneuron)
CEC	Contaminants of emerging concern
CI	Confidence interval
CYP	Cytochrome P450
DCA	3,4-dichloranilin
DIN	Deutsche Institut für Normung
DMSO	Dimethyl sulfoxide
dn-imi	Desnitro-imidacloprid
DNT	Developmental neurotoxicity
dpf	Days post fertilization
EC	Effective concentration
ECHA	European Chemical Agency
EFSA	European Food Safety Authority
EURL ECVAM	European Union Reference Laboratory for Alternatives to Animal Testing
FET	Fish embryo acute toxicity
fps	Frames per second
GAM	Generalized additive model
GFP	Green fluorescent protein
HTR	5-hydroxytryptamin (serotonin) receptor
hpf	Hours post fertilization
hs	Hemi septum
IC	Internal concentration
isl1	Insulin gene enhancer protein 1
ISO	International Organization for Standardization
I-zone	Isotropic zone (muscle)
LC	Lethal concentration

LMM	Linear mixed model
MiP	Middle primary (motoneuron)
mnx1	Motor neuron and pancreatic homeobox1
NC	Negative control
nc	Notochord
NGS	Normal goat serum
OECD	Organization for Economic Co-operation and Development
ON	Over night
PFA	Paraformaldehyde
PBS	Phosphate-buffered saline
REACH	Registration, Evaluation, Authorization and Restriction of Chemicals
RoP	Rostral primary (motoneuron)
rpm	Rounds per minute
RT	Room temperature
SC	Solvent control
sc	Spinal cord
SE	Standard error
SD	Standard diviation
SERT	Serotonin transporter
SNRI	Selective serotonin-noradrenalin-reuptake-inhibitor
SSRI	Selective serotonin reuptake-inhibitor
TG	Test guidelines
tg	Transgenic
TH	Tyrosine hydroxylase
PPP	Plant protection products
PBT	Persistent, bioaccumulative and toxic
POP	Persistent organic pollutants
VMR	Visual-motor response
VaP	Variable primary (motoneuron)
5-HT	5-hydroxytryptamine (serotonin)

1 GENERAL INTRODUCTION

1.1 Chemical testing in the EU

Chemicals are regulated in the European Union by sophisticated frameworks. The basis is the Registration, Evaluation, Authorization and Restriction of Chemicals (REACH) Regulation (EC, No 1907/2006), which is coordinated and monitored by the European Chemical Agency (ECHA). All chemicals with a production volume of more than 1 ton per year must be registered under REACH. To this end, the manufacturer or distributor must provide detailed information on the substance, including ecotoxicological data and risk analyses. The scope of this data depends primarily on the annual production volume. Depending on this, the requirements of the tests are increased in a tiered principle. According to ECHA, more than 21,000 chemicals were registered on the European market after the deadline in 2018 (ECHA, 2018). Following authorization, various other regulations apply depending on the use of the substance, such as the Plant Protection Products Regulation (Regulation (EC) No 1107/2009), before the products are placed on the European market.

From a regulatory point of view, standardized tests are essential to objectively assess the hazard of a substance. Guidelines for chemicals testing were published by the Organization for Economic Co-operation and Development (OECD) and accepted and adopted by its members in 1984. It addresses physical chemical properties, environmental fate, and human health effects as well as the assessment of chemicals on biota.

1.2 Neurotoxicity and developmental neurotoxicity

More than thousands of chemicals are suspected to have a serious potential for neurotoxicity, but only a small proportion of cases have been documented so far (Grandjean and Landrigan, 2006, Tilson et al., 1995). Neurotoxicity is generally defined as "any adverse effect on the chemistry, structure or function of the nervous system, during development or at maturity, induced by chemicals or physical influences" (Ladefoged and Miljöstyrelsen, 1995). Functional neurotoxic impairments by chemicals can disrupt neurotransmission and thus cognitive, sensory and motor functions. Damage to the anatomy of the brain or the organization of the nervous system can be caused by the loss of neurons which is termed as structural neurotoxicity (Costa et al., 2008). Additionally underlying modes of action can be oxidative stress or disrupted function of mitochondria (Bal-Price et al., 2015). If damage to the nervous system occurs during developmental processes, it is called developmental neurotoxicity. Organisms are particularly sensitive to external stress factors in their early stages. The reason is that the development and organization of the nervous system is a carefully coordinated process based on closely harmonized spatial and temporal steps. A disruption in this delicate time window, before organs and structures are mature, can lead to harmful and long-lasting effects later in life even though the stressor is absent (Bal-Price et al., 2015, Rice and Barone, 2000).

Proven neurotoxic substances for humans are listed in the review of Grandjean and Landrigan (2006) and compile over 200 chemicals including metals (*e.g.* lead, mercury, arsenic or cyanide), solvents (*e.g.* methanol, chloroform or xylene) and pesticides (*e.g.* aldicarb, DDT or chlorpyrifos). It has to be noted that pharmaceuticals, food additives, microbial toxins and biogenic toxics were excluded from this assessment. Substances that have only shown adverse impacts in laboratory animals, as well as additional more than 1000 chemicals, are not considered (Grandjean and Landrigan, 2006).

The major challenge of identifying developmental toxicity is the fact that commonly used toxicological screening methods might miss some adverse outcomes, due to the lack of neurotoxic indications in mature organisms (Claudio et al., 2000). Whereas low dose exposure in early life stages can cause server consequences later in life, the same dosage might be harmless for adult organisms. Fritsche et al. (2015) estimated that only 5 out of 200 compounds which adversely affected brain and nervous system developmental are reported.

A monitoring study of aquatic pollutants has exhibited that the largest group of the chemicals found in the samples, have a known neuroactive mode of action (Busch et al., 2016). Most of these compounds are pesticides and pharmaceuticals. Therefore, there is a realistic threat to aquatic ecosystems to be negatively affected by these chemicals.

The current assessment of the developmental neurotoxicity of chemicals is not mandatory by law and is only carried out if there is reasonable suspicion based on potential neurotoxic mode of action, structure-activity relationship or suspicious results from animal studies. Developmental neurotoxicity testing is based on OECD TG No. 426 (OECD, 2007), where rodents are exposed daily to a potential neurotoxic substance during pregnancy. Besides the morbidity and mortality of the litter, behavioral and neuropathologic assessments are evaluated during development. For suspicious pesticides, developmental neurotoxicity evaluation can be included as an extension to the one-generation reproduction toxicity study (Test No. 443; OECD, 2018). This study is a comprehensive evaluation of the parental animals and their first generation of offsprings up to maturation, in which reproductive and developmental toxicity is investigated. Such test protocols take several months, are costly, and require a considerable number of rodents.

However, *in vivo* toxicity studies on vertebrates are still necessary under the EU chemical regulation. The objective is to support and implement alternative solutions which are, whenever possible, compatible with the 3 Rs principle – Replace, Reduce, Refine (Russell and Burch, 1959). The challenge of testing the high number of potentially harmful chemicals requires systematic and efficient tests. Currently, proposals for *in vitro* test batteries for developmental neurotoxicity are being examined and discussed (Juberg et al., 2023, Masjosthusmann et al., 2020). The zebrafish and especially its embryo is increasingly being recommended for this purpose as an alternative method to complement the test battery (de Oliveira et al., 2021, Fritsche et al., 2015, Nishimura et al., 2015).

1.3 Zebrafish embryo as an alternative method

The small teleost zebrafish (*Danio rerio*) offers several advantages: The ability to genetic modification, short generation time and easy husbandry and handling. In addition, females lay a large number of eggs several times a week. External reproduction enables monitoring the developmental steps of a vertebrate through its transparent chorion and body in a non-invasive way. Additionally, given that the zebrafish embryos are considered as non-protected life-stages (Strähle et al., 2012) according to current EU animal welfare legislation (EU, 2010) they have received increasing attention for chemical testing, which, as a non-protected vertebrate model, can serve as an excellent surrogate to mammalian models (Bauer et al., 2021, Braunbeck et al., 2015, Embry et al., 2010, Jarque et al., 2020, Nishimura et al., 2016, Strähle et al., 2012).

For these reasons, the fish embryo acute toxicity (FET) test is especially suitable as an alternative method. It was validated from 2008 to 2012 and finally approved by the OECD one year later under Test Guideline No. 236 (Busquet et al., 2014, OECD, 2007, OECD, 2013). In Germany, the FET test is

already used for testing wastewater samples since 2005 (DIN, 2001). However, originally, this test was meant to be a full replacement method for the acute fish toxicity (AFT) test (OECD TG No. 203) for chemical testing. This *in vivo* toxicity test is based on adult stages of fish with the apical endpoint of mortality, *i.e.,* lethal concentrations of 50 % (LC_{50}). Comparative studies and meta-analyses showed a high correlation between the results of the AFT and FET tests in terms of their sensitivity (Belanger et al., 2013, Lammer et al., 2009a). Additionally, great effort has been put into research to identify and, if necessary, overcome limitations and difficulties of this alternative method (Braunbeck et al., 2015, Embry et al., 2010, Kais et al., 2017, Kais et al., 2013, Lammer et al., 2009b, Pelka et al., 2017, Simeon et al., 2020, von Hellfeld et al., 2020).

Although the European Union Reference Laboratory for Alternatives to Animal Testing (EURL ECVAM) recommended the test for aquatic acute toxicity testing (Joint Research Centre, , 2014), the FET test became a refinement method. Further evaluation in a regulatory context concluded that the test cannot be considered to have the potential to fully replace the AFT test yet and should therefore be only used in a weight of evidence approach. Reasons for the outcome include the occurring underestimation of toxicity for substances with a neurotoxic mode of action (Sobanska et al., 2018). One of the underlying reasons for this limitation is the embryos' lack of sensitivity to neurotoxic modes due to the lack of gill respiration, which only develops post-embryonically. The neurotoxic effect of respiratory failure syndrome, in which the gills are not sufficiently ventilated due to spasms, does not occur in embryos with skin respiration. Kämmer and colleagues proofed a higher sensitivity to neurotoxic compounds when post-embryonic fish develop gill respiration later on (Kämmer et al., 2022).

1.4   Testing developmental neurotoxicants in zebrafish embryo

The lack of sensitivity to neurotoxic substances can be counteracted with additional and more sensitive endpoints. Over the years, the zebrafish has proven to be an effective model organism for the screening of developmental neurotoxic substances, as the basic characteristics of the neurological system are highly conserved in vertebrates (Bailey et al., 2013, Bal-Price et al., 2018, d'Amora and Giordani, 2018, Fritsche et al., 2015, Legradi et al., 2018, Nishimura et al., 2015, Sachana et al., 2021). In addition to the frequently proposed integration of behavioral endpoints, the zebrafish embryo is also particularly suitable for combining structural, genetic and physiological measurements to strengthen the evidence base (Atzei et al., 2021, Basnet et al., 2019, Klüver et al., 2015, Sloman and McNeil, 2012). Furthermore, on this basis it can combine human-health related and ecologically important questions concerning neurotoxic contaminants in the (aquatic) environment.

However, it is essential to know the underlying and normal development of the zebrafish before assessing developmental neurotoxic consequences, I will outline the most important steps in the development below. In combination with each section, I will also address possible applications and tests.

1.4.1   Neurogenesis and the assessment of motoneuron integrity

Like other vertebrates, zebrafish develop their central and peripheral neural system from ectodermal cells. The intrinsic mesodermal signaling for differentiation to neuroectoderm is an antagonistic mechanism which blocks epidermal fate (Wilson and Hemmati, 1997). In zebrafish embryos, the evolved cells of the neural plate form a solid neural keel. This is followed by the formation of a lumen, the neurocoele in the trunk region which inflates to a tube-like structure during gastrulation (Papan and

Campos-Ortega, 1994, Schmitz et al., 1993, Strähle and Blader, 1994). This differs from the process of folding and invagination in most vertebrates (Araya et al., 2016). During neurulation, the anterior part of the neural tube expands, leading to the formation of three distinct areas that correspond to the future forebrain, midbrain, and hindbrain. The remaining posterior part forms the neural tube and finally the spinal cord. These processes are highly conserved in vertebrates (Kimmel, 1993, Lowery and Sive, 2004).

Following the formation of the central nervous system, the peripheral nervous system develops, which includes the motoneurons that are necessary for motor behavior. In zebrafish, these develop at two different times and are therefore referred to as primary and secondary motoneurons.
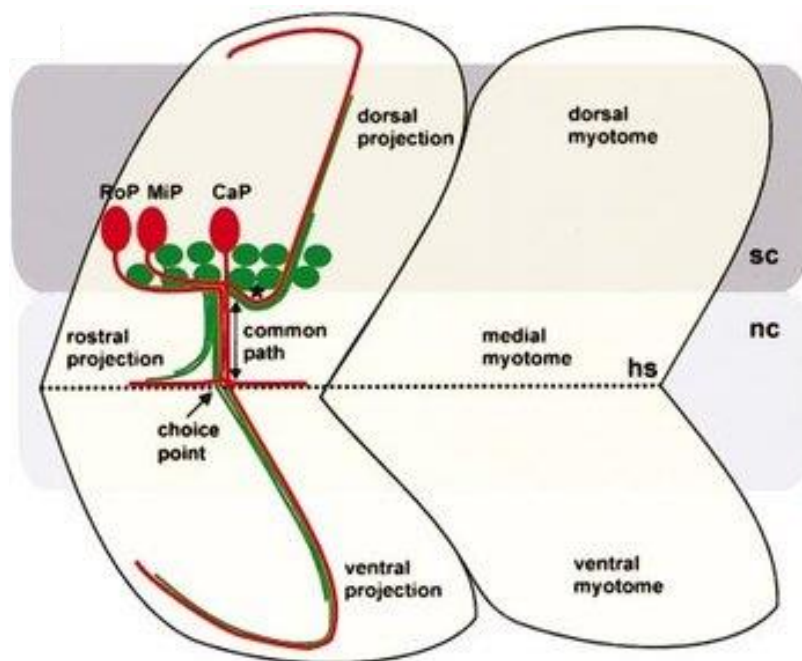
Figure 1: Schematic illustration of the projection pattern of motoneurons in zebrafish embryos at day 3. The image shows a lateral view of the spinal cord (sc), notochord (nc), dorsal and ventral myotomes and motoneurons. The somas of the three different primary motoneurons (red), Rostral Primary axon (RoP), Middle Primary axon (MiP) and Caudal Primary axon (CaP), are located in the spinal cord. They develop and extend along a common pathway and project their axons to rostral, ventral, or dorsal target myotomes. The secondary motoneurons (green) follow the predetermined pathways of the primary motoneurons. Horizontal septum (hs) is indicated by a dashed line. Figure was adapted with permission (9.4) from Ott et al. (2001).

First, primary motoneurons occurs at the segmentation stage around 10 h post fertilization (hpf) (Kimmel et al., 1995, Myers et al., 1986, Westerfield et al., 1986). Three neurons in each spinal hemi-segment (Fig. 1), which can be identified and named by their position of the soma in the spinal cord, project their axons into the periphery and innervate muscle pioneers (Melancon et al., 1997, Westerfield et al., 1986). In general, the most Rostral Primary axon (RoP) projects to the medial region along the horizontal myoseptum, the Middle Primary axon (MiP) projects to the dorsal region, and the Caudal

Primary axon (CaP) projects to the ventral part of the muscle segment (Eisen, 1991a, Eisen, 1991b). There is also a fourth primary motoneuron, called the Variable Primary (VaP). However, it has been shown that 85 % of those undergo apoptosis before the second day of development (Eisen et al., 1990). The secondary motoneurons project their axons onto the predetermined pathways of primary motoneurons 6 h later. The somata of the latter motoneurons are generally smaller in size and more numerous than those of the primary motoneurons (Myers et al., 1986). Buss and Drapeau hypothesized primary motoneurons only innervate slow muscles, whereas secondary motoneurons project their axons to various kinds of fibers (Buss and Drapeau, 2000).

Zebrafish offer a wide range of possibilities for studying the nervous system, and fluorescent transgenic lines in particular have significantly expanded the possibilities (Linney et al., 2004). In their article, Choe and colleagues provided an overview of various representative transgenic zebrafish lines used in biomedical research, including important model lines for investigating the nervous system (Choe et al., 2021). By labelling different genes that are important for the development, guidance and formation of the nervous system, specific subgroups of neurons can be tagged and visualized in real time. For motoneurons, there are many different established transgenic (tg) lines such as tg(mxn1:GFP), which combine biofluorescence with the expression of the transcription factor (*motor neuron and pancreatic homeobox 1* (mxn1)), which is expressed in postmitotic spinal cord neurons (Bello-Rojas et al., 2019). The tg(isl1a:GFP) line is used to label and monitor the development of primary motoneurons as this transcription factor *insulin gene enhancer protein 1* (isl1) is solely expressed in the earlier wave of neurulation (Hutchinson and Eisen, 2006).

Another approach, which is frequently combined with transgenic lines, consists of labelling the structure of the neurons with antibodies. Primary and secondary motoneurons are often stained with the antibodies znp-1 or zn8, formerly zn5, respectively (Eisen et al., 1990, Melancon et al., 1997, Menelaou et al., 2015, Menelaou and Svoboda, 2009, Muth-Kohne et al., 2012, Myers et al., 1986, Svoboda et al., 2002, Welsh et al., 2009). The first one (znp-1) is also called anti-syt2 because it is targeting synaptotagmin which is a transmembrane protein in the pre-synapse involved in vesicle exocytosis whereas the second antibody (zn8) binds to the protein neurolin or DM-GRASP (Fig. 2) which plays an important role in pathfinding in developing secondary motoneuron (Ott et al., 2001).
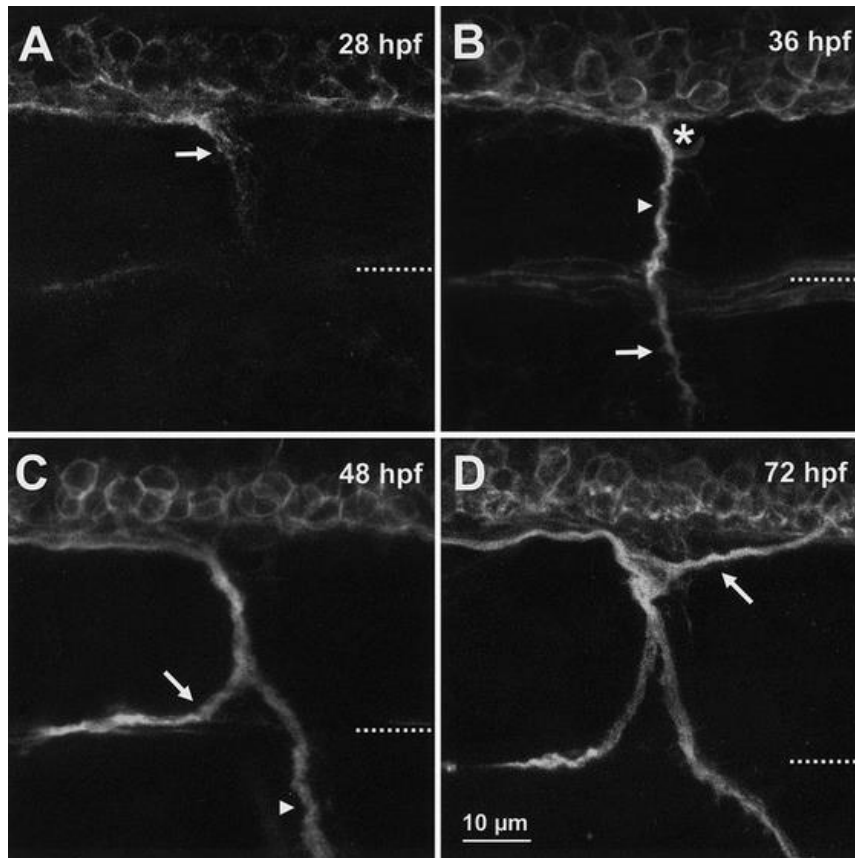
Figure 2: Development of secondary motoneurons shown by neurolin expression pattern. A to D show the lateral view of a zebrafish embryo 28, 36, 48 and 72 hours post fertilization (hpf). Arrowheads indicate the common pathway of all motoneurons, while arrows sequentially indicate the first outgrowth of a secondary motoneuron axon, ventral, horizontal, and dorsal projections. The dashed lines mark the horizontal myoseptum of the respective myotome. Scale bar indicates 10 µm. Figure was adapted with permission (9.4) from Ott et al. (2001).

1.4.2 Myogenesis and assessment of muscle integrity

In vertebrate embryonic development, somites form from the mesoderm after gastrulation, which is paraxial to the ventral notochord and dorsal neural tube. The paraxial mesoderm condenses segments from cranial to caudal into defined units called somites. Each somite is associated with a segment of the neural tube referred to as a neuromere. The somites further differentiate into dermatomes, sclerotomes, and myotomes. While the sclerotome is the basis for cartilage and bone, the dermatome is responsible for the skin and the myotome for the muscles (Holley and Nüsslein-Volhard, 1999).

Simultaneously to neurogenesis of the primary motoneurons, zebrafish somitogenesis begins at 10 hpf when raised at 28.5 °C (Kimmel et al., 1995, Mendieta-Serrano et al., 2022). At this point, some of the adaxial cells of the myotome first differentiate into slow muscles, triggered by signaling molecules of the notochord (Blagden et al., 1997). Devoto and colleagues showed that this subtype of fibers migrates through the myotome and builds a superficial monolayer on the somite (Fig. 3; Devoto et al., 1996). Because of their high content of the red pigment myoglobin, which improves oxygen supply, slow

muscles are also called red fibers. In addition, they contain a large number of mitochondria. Together, this enables aerobic and continuous motion without fatigue.
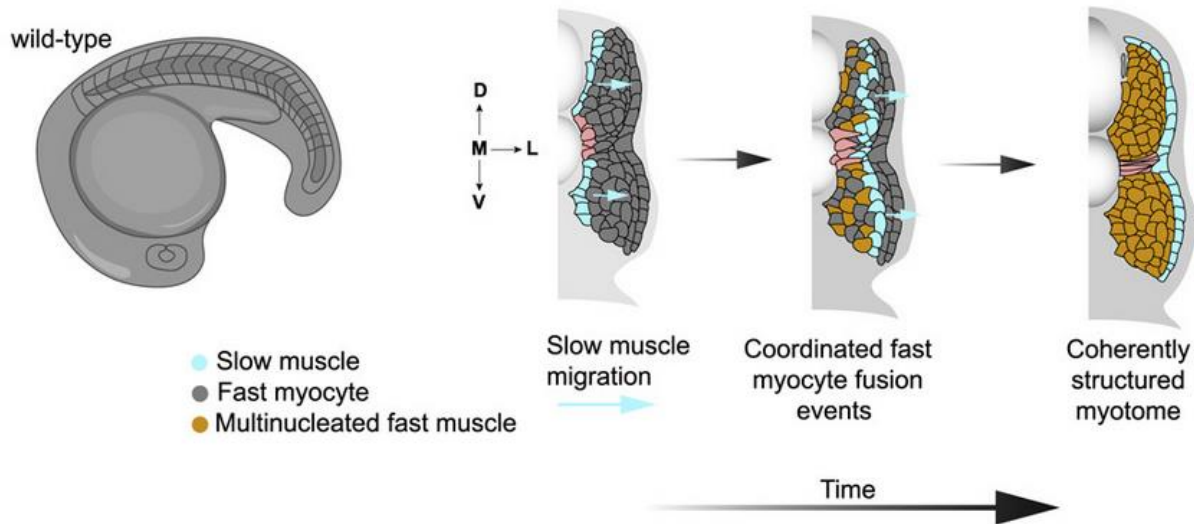
Figure 3: Dynamics of slow and fast muscle development in zebrafish embryo. The image depicts the lateral view of a schematic zebrafish embryo on the left side. On the right, three transversal sections of the trunk are shown in a chronological order of development to illustrate the migration and differentiation of the slow and the fast muscles. M= middle, L=lateral, D=dorsal, V=ventral. Figure was used with permission from Mendieta-Serrano et al. (2022).

Fast muscles, which evolve later in time, make up the majority of total muscle mass, lie deeper in the body, and are much thicker in diameter. Unlike slow muscles, these muscles obtain their glycose and thus ATP through anaerobic glycolysis. Cell fusion of mononuclear myocytes leads to polynucleated fibers which in turn contain many myofibrils (Johnston et al., 2011, Johnston et al., 1977, Mendieta-Serrano et al., 2022).

The basic contractile units of these myofibrils are the sarcomeres. Within the sarcomere, two proteins play key roles for muscle contraction, namely myosin and actin. These proteins are arranged in a well-organized and repetitive way. Therefore, the sarcomeres can be divided into different zones, illustrated in Figure 4. In the I-zone (isotropic zone), only actin filaments are present, while the A-zone (anisotropic zone) denotes a region around the center of the sarcomere where myosin and actin filaments partly overlap. These zones are named according to their optical properties.

In general, light propagation in a material is described by the refractive index. Materials which are optically anisotropic exhibit different refractive indices, depending on the direction of propagation and the light polarization. If linearly polarized light propagates through these so called birefringent materials, the polarization direction gets rotated. This effect can be used in polarization light microscopy to selectively image zones or layers of material. Figure 5 illustrates such an experimental polarization microscopy setup. A sample is placed between two optical filters which transmit solely light with a certain polarization direction. From the left, unpolarized light propagates through the first filter, named polarizer, and gets polarized. When the light from the polarizer propagates through the muscle sample,

it is altered differently by the I-zones and A-zones, respectively. In an I-zone, the light polarization direction is not effected. Hence, the light collected from an I-zone is fully absorbed by the second filter, called analyzer, when the two filters are crossed orientation. Subsequently, the corresponding region appears dark in the resulting image. The optical anisotropy of the A-zone, in contrast, can alter the light polarization direction. As a result, light collected from an A-zone can partially pass the analyzer and allow to image the A-zones of the muscle sample. The magnitude of light which can pass the analyzer depends on the relative orientation of incident light polarization and optical axis of the A-zone.
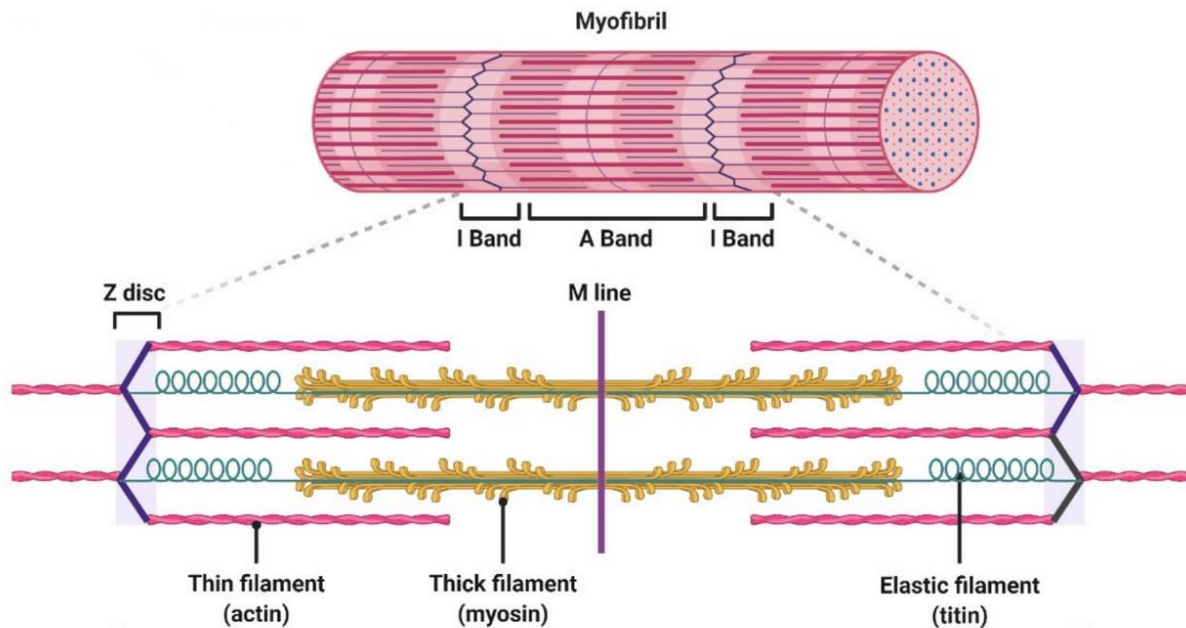
Figure 4: The structure of a sarcomere in a straited muscle. Depicted is a myofibril with its isotropic zone (I-band) and anisotropic zone (A-band). The magnification shows a sacromere, the smallest contractil units of the myofibril. The z-disk (German *zwischen* meaning *between*) is the anchor for the filaments such as titin (blue) and actin (pink). In the middle of the sarcomere (M line) there is myosin (yellow). In polarization microscopy, the overlapping zone of actin and myosin appear bright (part of A-band), whereas actin alone appears darker (I-band). The z-disc (German *zwischen* meaning *between*) is the anchor for the filaments consisting of actinin and desmin. Figure is adapted with permission (9.4) from Santiago et al. (2021).

The highly organized structure of muscles can give insights into functionality of the muscle itself but also for the right development and connectivity with the corresponding motoneurons. Overstimulation due to receptor blockage or reduced degradation of neurotransmitters can lead to an increase in the calcium level in the muscle and thus to excitotoxicity and degeneration (Behra et al., 2002, Engel et al., 1982). This in turn becomes visible in an altered structure. Therefore, in zebrafish research, these optical properties of the muscles are used to assess the health of the muscles by determining the birefringence potential of the muscle tissue (Konemann et al., 2022, Shahid et al., 2016, Smith et al., 2013).
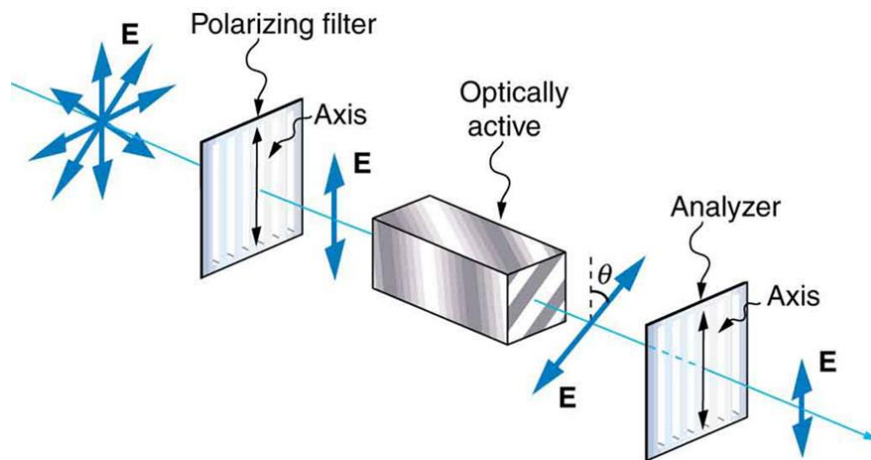
Figure 5: Simplified principle of polarization microscopy. Unpolarized light with the electric field vector E passes through a polarization filter with vertical polarization plane axis. Linearly polarized light strikes an optically active object that rotates the light polarization by an angle. The different polarization axes are depicted with blue arrows. An analyzer detects the changes in the axis of polarization. Figure was used with permission (9.4) from College Physics (2016) by OpenStax.

1.4.3 Early motor behavior and its assessment

Functional impairments of the nervous system by chemical stressors are detectable by behavioral measurements. During development these alterations can persist into adulthood even though the stressor is absent. Therefore, the detection of a deviation from the normally stereotypical activity patterns in the life phases can serve as an important early warning system.

Shortly after the innervation of muscle fibers by the first wave of motoneurons, earliest movements are observable in the developing embryo at 17 hpf (Saint-Amant and Drapeau, 1998). These distinct side-to-side movements, in the literature referred to as tail coils, result from a basic, glycine and electrically coupled neuronal circuit within the spinal cord and gap junctions (Downes and Granato, 2006, Hirata et al., 2005, Saint-Amant and Drapeau, 1998). Especially these stereotypic occurrence and regular patterns of tail coils have been increasingly used as a neurobehavioral endpoint in the so-called spontaneous tail coiling (STC) assay to assess the neuroactive potential of chemical compounds (de Oliveira et al., 2021, Lacchetti et al., 2022, Ogungbemi et al., 2021, Ogungbemi et al., 2020a, Vliet et al., 2017, von Hellfeld et al., 2023, Weichert et al., 2017, Zhang et al., 2021, Zindler et al., 2019a). In most cases, the frequency of movements at one time point has been quantified to detect behavioral abnormalities after exposure to chemical stressors, making this an extremely rapid method. However, such a single point in time could lead to an underestimation of the actual risk since contaminants may need more time to cross the chorion and the embryo due to their specific physicochemical properties (de Koning et al., 2015, Pelka et al., 2017). Therefore, observing the evolving tail coiling behavior over a longer period can be more conclusive (von Hellfeld et al., 2023, von Hellfeld et al., 2022, Zindler et al., 2019a, Zindler et al., 2019b).

Shortly after the first spontaneous tail movements, zebrafish develop the ability to perceive external stimuli. The first type of reactivity is the touch response at 21 hpf (Brustein et al., 2003). As this test is particularly simple to perform, this behavior pattern was also used to investigate a wide range of different substances such as pesticides, nanoparticles, pharmaceuticals and industrial chemicals (Ames et al., 2023, Hua et al., 2022, Smith et al., 2013, Stehr et al., 2006, Sylvain et al., 2010). Other developing responses include the photo-motor reaction to changing ambient light conditions which are first apparent as early as 23 hpf (Zindler et al., 2019b) which is mediated by deep brain photoreceptors (Fernandes et al., 2012). This basic behavior is also called dark photokinesis and is an undirected hyperactive motor behavior to escape the dark spaces (Ganzen et al., 2017, Kalueff et al., 2013). At around 3 days post fertilization (dpf), zebrafish embryos begin to show directional and visually mediated behaviors. These include the so-called light-seeking behavior as well as the optokinetic response, in which the eyes of an immobilized embryo are able to follow a rotating object, and the optomotor response, in which the embryo is induced to swim in the direction of a stimulus. The visual-motor response (VMR) is a stereotypical startle response that is a sudden reaction to an intense sensory stimulus. The VMR is often carried out with light stimuli and is therefore similar to the widely used light-dark transition test (Basnet et al., 2019, Kimmel et al., 1974, Ogungbemi et al., 2019). In general, a lower variability between individuals and an increasing robustness of the reactions can be observed from day 5 onwards (Ganzen et al., 2017, Hill et al., 2023).

1.5 Analysis of highly variable biological data with generalized additive modeling

The analysis of data sets which are recorded over a certain period of time – often the case for behavioral or biomedical longitudinal studies – is often quite complex. To be able to analyze trends in the data sets rather than looking on single time points separately, commonly employed nested analysis of variance (ANOVA) for repeated measurements is used. Even though it is a straightforward approach which has been thoroughly tested, some prerequisites must be met by the data beforehand to obtain a robust model. These include the type of distribution, the homogeneity of variance and that the data follow a linear trend (Diaz-Garzon Marco et al., 2020). Another limitation is the inability to deal with missing data in the time series of an observed subject (i.e. individual persons or animals). This so-called incomplete observation of one subject must be entirely excluded from the analysis. This can lead to an increase in the number of laboratory animals or clients involved to still achieve statistical power, which in turn can lead to ethical or financial difficulties (Zhang and Hartmann, 2023).

In the last decades, other techniques including linear mixed model have been increasingly utilized to overcome the limitation of incomplete unbalanced data. One other major advantage of the linear mixed-model (LMM) is the ability to differentiate and incorporate fixed effects (e.g., treatment-related effects like drug administration) and random effects (e.g., variability between individuals which cannot be explained by the experimental treatment such as age or weight). However, the linearity of the response variable over time is still a crucial assumption and most biological observations follow other trends (Diaz-Garzon Marco et al., 2020).

In this case the generalized additive model (GAM), first introduced by Hastie and Tibshirani (1986), is a well-suited alternative approach. It is a derivation and a mixture of (generalized) linear model and mixed model approaches. Key advantage is that GAM relaxes the linear and normality assumptions ("generalized"). For this purpose, the model uses a combination or sum of different functions

("additive"), called smooth functions. By overlaying these functions with different weights, dynamically changing trends in the data can be described more flexible. Additionally, random effects, e.g. variability on individual or replicate level, can be identified and distinguished from treatment-related, the fixed effects which is the focus of the observation (Hastie and Tibshirani, 1986, Mundo et al., 2022).

The adaptive and data-driven nature of GAM has increased its popularity, especially in fields like health, biomedical, ecology and environmental sciences where the presence of multiple influencing variables in longitudinal datasets is common (Guisan et al., 2002, Pedersen et al., 2019, Ravindra et al., 2019).

2 AIMS OF THE STUDY

I divided the content of this dissertation into three different parts, associated with three different case studies. The compounds selected for the case studies were nicotine, the metabolite desnitro-imidacloprid and the three antidepressants sertraline, paroxetine and venlafaxine. While nicotine and desnitro-imidacloprid are agonists of the nicotinic acetylcholine receptor (nAChR), the antidepressants mainly act on neurotransmitter homeostasis by inhibiting the reuptake of serotonin. Venlafaxine additionally blocks the reuptake of norepinephrine and dopamine, however to a lesser extent. As the listed substances are neuroactive, they have the ability to interact with the vertebrate nervous system and thus could cause neurotoxicity. To assess the actual developmental neurotoxicity of these substances, I used the zebrafish embryo as a model organism. In addition to the investigation of the acute toxic profile of the substances, I focused on embryonic behavioral alterations.

The following objectives were addressed in the individual case studies:

(1) My first case study covered the investigation of the suitability of using the generalized additive modeling for the analysis of the time course of coiling development in zebrafish embryos. The generalized additive modeling should provide a better description and visualization of underlying trends and patterns, which, in turn, should improve both the effectiveness of the assay and our understanding of adverse outcomes. To obtain further information, I included skeletal muscle and secondary motoneuron integrity as additional structural endpoints. For this proof-of-concept study, I chose nicotine which is a well-known and examined developmental neurotoxin. Afterwards, the modeling approach was used for the following coiling experiments.

(2) Next, I performed a case study on the effects of desnitro-imidacloprid, a metabolite of the neonicotinoid pesticide imidacloprid. As desnitro-imidacloprid is suspected to have a similar toxic potential as nicotine, I first compared the acute toxicity of the two substances on the zebrafish embryo development in the FET test. In addition, the water concentrations and the internal concentrations in the body of the embryos were measured (in cooperation with Cyprotex in UK) and analyzed in order to assess the uptake and accumulation of the substance which were administered via the water. To gain an insight into the potential developmental neurotoxicity of this metabolite, I investigated the effect on early coiling behavior and also compared it with nicotine.

(3) In the last case study, I analyzed the effects of the most commonly prescribed antidepressants venlafaxine, paroxetine, and sertraline. These neuroactive compounds are becoming an emerging concern due to the increasing aquatic environmental contamination. Thus, I first analyzed the acute toxicity in the developing zebrafish embryo with the FET test to characterize the hazard of the compounds. Subsequently, I investigated the impact of low concentrations of the substances on the spontaneous coiling movements and the visual-motor responses triggered by light. Both pre and post-hatching motor behaviors can be a potential indicator for embryonic neurodevelopmental impairments and can provide information of the fitness of the organism.

3 GENERAL MATERIAL & METHODS

3.1 Chemicals and test substances

I supplied all chemicals used by Sigma-Aldrich (Deisenhofen, Germany) unless I have stated it otherwise. These included tricaine (3-aminobenzoic acid ethyl ester methane sulfonate, CAS number 886-86-2). 3,4-Dichloraniline (DCA, CAS no. 95-76-1), paraformaldehyde (PFA, CAS no. 3025-89-4), Triton X-100 (CAS no. 9002-93-1, Carl Roth, Karlsruhe, Germany), and Hoechst 3342 (CAS no. 23491-52-3). The stock solutions I prepared were at the following concentrations: tricaine at 400 mg/L (buffered with 480 mg/L NaHCO3) and DCA at 200 mg/L were stored at 4 °C. I aliquoted PFA with 40 g/L (in 1× phosphate-buffered saline (PBS) see below), Normal Goat Serum (NGS, CAS no. 999999-99-4, Merck KGaA, Darmstadt, Germany), and stock of Hoechst 3342 with 2 mg/L (in 1× PBS + 0.5 % Triton X-100) and stored them at -20 °C. I also divided the first zn8 antibody (Developmental Studies Hybridoma Bank, Cat# zn-8, RRID:AB_531904, Iowa city, Iowa, USA) and the secondary goat anti-mouse antibody (Alexa fluor 568, Thermo Fisher, Dreieich, Germany) into 5 µl each and stored at -20 °C. I stored dimethyl sulfoxide (DMSO, CAS no. 67-68-5, Carl Roth) and water-free glycerol (CAS no. 56-81-5, neoFroxx, Einhausen, Germany) at room temperature (RT) until usage.
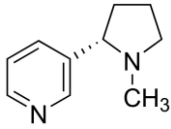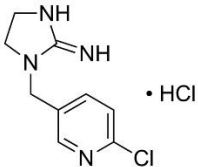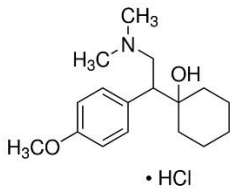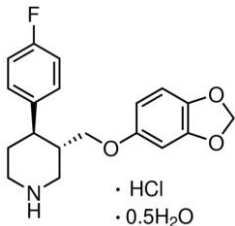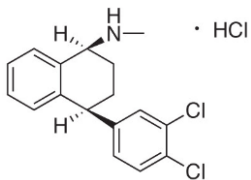
I prepared the dilution water with ultra-purified water (Milli-Q®, Merck KGaA, Darmstadt, Germany) with different salts (for 1 L dilution water: 294 mg $CaCl_2×H_2O$, 123.3 mg $MgSO_4×7H_2O$, 64.7 mg $NaHCO_3$, 5.7 mg KCl) according to stated water parameter in Annex 2 in TG 203 Section 2 (OECD, 2019). I aerated the water daily before use and adjusted the pH to 7.72 ± 0.02.

For the 10× PBS stock solution, I weighed 40.03 g NaCl, 10.789 g Na_2HPO_4, 1.006 g KCl, 1.0215 g KH_2PO_4 and dissolved the salts in 0.5 L ultra-purified water. The 1 x PBS solution was diluted with ultra-purified water and the pH was adjusted to 7.4.

I listed the test chemicals with additional information in Table 1. In the following text, I am going to further refer them to as nicotine, desnitro-imidacloprid, venlafaxine, paroxetine, and sertraline.

I prepared the stock solutions of the test chemicals as follows: for the nicotine I prepared two stock solutions, one without and one with 100 % DMSO, stored at 4 °C. Desnitro-imidacloprid as well as sertraline were only dissolved in 100 % DMSO and stored at -80 °C and -20 °C, respectively. Stock solutions of paroxetine and venlafaxine were prepared with dilution water and stored at 4 °C, while the latter had to be renewed every month. All substances were protected from light to minimize photodegradation. Final exposure concentrations of the test chemical in the different assays can be found in Table 2.

Table 1: List of test substances used in the experiments. I took the information on physicochemical properties as well as molecular structures from SDS sheets, Pubchem[a] and DrugBank[b] webpages.

Compound	Molecular structure	Molecular weight [g/mol]	Log Kow	CAS Number	Supplier
(-)-Nicotine		162.23	1.17	54-11-5	Sigma-Aldrich
Desnitro-Imidacloprid hydrochloride		247.12	0.57	127202-53-3	Sigma-Aldrich
Venlafaxine hydrochloride		313.86	3.3	99300-78-4	Sigma-Aldrich
Paroxetine hydrochloride hemihydrate		374.83	2.53	110429-35-1	Sigma-Aldrich
Sertraline hydrochloride		342.69	5.06	79559-97-0	LKT Laboratories[c]

[a] https://pubchem.ncbi.nlm.nih.gov/
[b] https://go.drugbank.com/
[c] Saint Paul, Minnesota, USA

Table 2: Exposure concentrations of the compounds used in the different assays.

Compound	Test	Concentrations	Solvent
DCA [a]	FET	4 mg/L	-
Nicotine	FET	6.25, 12.5, 25, 50, 100, 200, 400 µM	0.1 % DMSO
	Coiling assay	5, 10, 20, 40 µM	0.1 % DMSO
	Coiling assay	5, 10, 20, 40 µM	-
	Muscle & motoneuron integrity	5, 10, 20, 40, 80 µM	-
Desnitro-Imidacloprid	FET, IC, Coiling assay	6.25, 12.5, 25, 50, 100 µM	0.1 % DMSO
Sertraline	FET	0.1, 1, 10, 100, 1 000, 5 000, 10 000 µg/L	0.1 % DMSO
	Coiling assay, VMR	0.01, 0.1, 1, 10, 10 µg/L	0.01 % DMSO
Paroxetine	FET	0.625, 1.25, 2.5, 5, 10, 20 mg/L	-
	Coiling assay	0.01, 0.1, 1, 10, 100, 1 000, 2 000 µg/L	-
	VMR	0.1, 1, 10, 100, 1 000 µg/L	
Venlafaxine	FET [b]	88, 132, 198, 296, 444, 667, 1 000 mg/L	-
	Coiling assay, VMR	0.1, 1, 10, 25 mg/L	-

FET – Fish Embryo Acute Toxicity, VMR – Visual Motor Response, IC – Internal concentration

[a] DCA - 3,4-dichloroaniline; was used as a positive control; [b] FET test for venlafaxine was conducted by Saskia Hagstotz who was supervised by Katarina Brotzmann.

3.2 Fish husbandry, maintenance and egg production

For my experiments, we[1] used breeding stocks of adult wild-type zebrafish (*Danio rerio*) from the "Westaquarium" strain received from our in-house breeding facilities of the Aquatic Ecology and Toxicology Group at the Center for Organizational Research (Heidelberg University, licensed under No. 35-9185.64/BH). We[2] from the working group shared the work of feeding the fish twice daily, in the morning with commercial dry food (TetraMin™ flakes, Tetra, Melle, Germany) and evening with *Artemia salina* nauplii (Great Salt Lake Artemia Cysts, Sanders, Ogden, USA) *ad libitum*. The fish are kept in glass aquaria (> 1 L water per fish) at 26 ± 1 °C in a flow-through system. Standardized dilution water which is specified in chapter 3.1 or suitable drinking water with ≥ 60 % oxygen saturation was used for keeping and breeding. A continuous flow of water ensured that ammonia, nitrite and nitrate stayed below the detection limits of 0 - 5, 0.025 - 1 and 0 - 140 mg/L, respectively. The artificial daily rhythm was 14 h of light and 10 h of darkness. We[2] monitored the health of the fish daily, while water

---

[1] I was supported in the data collection by Bachelor students. Further information on the individual contributions can be found as statements at the beginning of relevant chapters as well as in detail in chapter 0.

[2] All PhD students and postdocs from the working group Aquatic Ecology and Toxicology at the University of Heidelberg.

quality was checked weekly, which included the conductivity, nitrate, nitrite, copper, pH values and water hardness.

Breeding groups consisted of a 1:1 ratio of male to female fish and were kept together in glass aquaria. One day prior to my experiments, I transferred the fish to a separate glass aquarium filled with dilution water and equipped with a collection tray, mesh tank, heater, plastic plants, and aeration stone. The tilted position of the mesh tank mimics a beach and, along with the plastic plants and the light, triggers mating at dawn of the next day at 8:00 a.m. (14:10 h). One hour later at 9:00 am, we[1] collected the eggs and filled them into glass dishes with dilution water. I routinely checked the quality and quantity of the eggs to be able to select the batch with the best characteristics. Further details on fish maintenance and breeding conditions can be found in Lammer et al. (2009a).

3.3 Fish embryo toxicity test

We[1] conducted the Fish embryo acute toxicity (FET) test according to the OECD TG 236 (OECD, 2013) with test chemical concentrations listed in Table 1. Briefly, in the mornings we[1] collected freshly laid and fertilized eggs. We[1] inspected and exposed them to their respective exposure solutions and the negative or solvent control (Tab. 2) latest at 1.5 hpf. Subsequently, we[1] transferred exposed embryos one-by-one into a pre-saturated wells of a 24-well-plate (TPP, Trasadingen, Switzerland) in 1 ml exposure solution and sealed it with self-adhesive foil (SealPlate™ by EXCEL Scientific, Dunn, Asbach, Germany). The plate was incubated at 26.0 ± 1.0 °C with a light/dark cycle of 14/10 h. We[1] renewed the exposure solutions daily (semi-static). Subsequently, we[1] documented morphological and behavioral changes according to the catalogue of von Hellfeld et al. (2020) at 24, 48, 72, 96, and 120 hpf. The normal daily developmental stages of a zebrafish embryo can be seen in Figure 6.

For the data analysis, I calculated effective concentrations of 10, 20 and 50 (EC_{10}, EC_{20}, EC_{50}) with a probit (normal sigmoid) analysis which used a linear maximum-likelihood regression with ToxRat (version 3.3, ToxRat™ Solutions, Alsdorf, Germany).
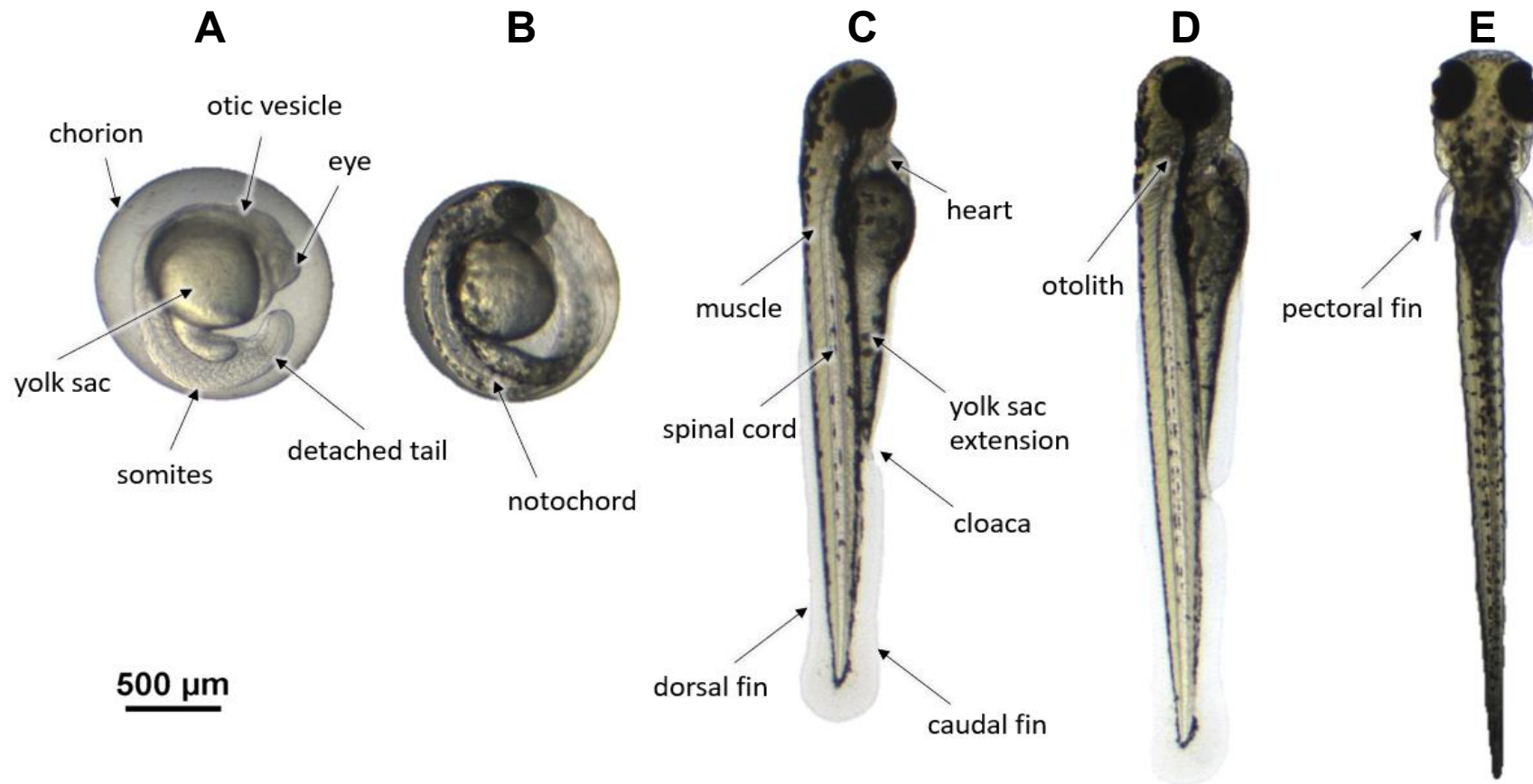
Figure 6: Normal developmental stages of a zebrafish embryo at 24 (A), 48 (B), 72 (C), 96 (D) and 120 hpf (E). Scale bar: 500 µm. The image was originally created by Katharina Zorko.

3.4 Coiling assay

Detailed experimental setup for the coiling assay was described in Zindler et al. (2019b). We[1] performed the experiment accordingly with minor modifications. Briefly, we[1] collected freshly fertilized eggs, pre-exposed and incubated them in 20 ml of respective exposure solution (Tab. 2) at 26.0 ± 1.0 °C. In the afternoon (~ 6 hpf) we[1] selected healthy developed, and stage matched embryos in the shield stage (~ 6 hpf). Afterwards, we[1] transferred five embryos per well into small Teflon rings in a 24-well-plate with 1 mL exposure solution. Rings kept embryos in the focus of the camera. We[1] placed the plate in the incubator on the recording platform with twelve installed infrared spotlights (Fig. 7). I adjusted the dark/light cycles to 14/10 h. With the Mediarecorder5 and Windows® Task Scheduler I set up an automated recording of 8 min videos (mpeg 4, 30 fps) for every hour. I set the recording time from 21 to 47 hpf. With the DanioScope 1.2 activity measurement, we[1] circled each egg manually and I analyzed the selected movements of the eggs. If one or more eggs moved out of the circled area during recording due to high activity, I excluded them from the data set for that specific time point. Additionally, I excluded videos taken immediately after renewal of the exposure solution to avoid possible deviations caused by interference from experimental handling. The output I used was "Mean burst duration" and "Burst count/minute", which I further referred to as "coil duration" (in sec) and "coiling frequency" (per min), respectively. I listed all the devices and equipment I used in Table 3 and details about the settings are included in the Appendix A (Tab. A1).
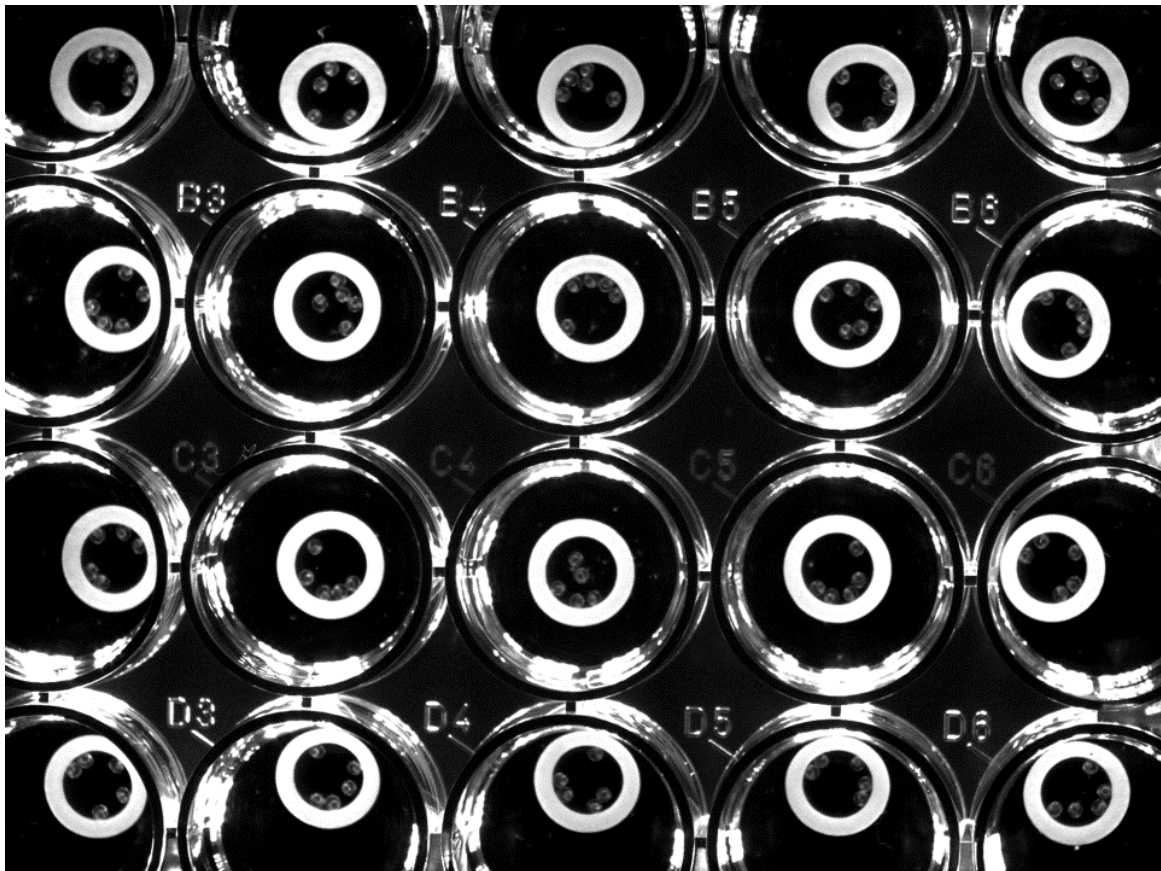
Figure 7: Representative video section of a plate prepared for the coiling assay recording. The image shows the camera view of a 24-well plate with 5 embryos and one Teflon ring each in the incubator. The rings are positioned in a way, that embryos are not able to move out of the recording field.

Table 3: Devices used for the tail coiling assay according to Zindler et al. (2019b).

Device	Specification	Supplier
Incubator	HettCube 600R	Hettich, Tuttlingen, Germany
Infrared spotlights	Knightbright 880 nm 40° 5 mm	Thomsen Elektronik, Greifenstein, Germany
Polytetrafluoroethylene rings	5.3mm	ESSKA, Hamburg, Germany
Camera	acA1920-155um USB 3.0	Basler, Ahrensburg, Germany
Lens	M7528-MP F2.8 f75mm 2/3"	Basler, Ahrensburg, Germany
Filter	RG850	Heliopan, Gräfelfing, Germany
Recording software	Mediarecorder5	Noldus, Wageningen, Netherlands
Detection software	DanioScope1.2	Noldus, Wageningen, Netherlands

4 THE DEVELOPMENTAL NEUROTOXIN NICOTINE – A PROOF-OF-CONCEPT STUDY

In this chapter, I was supported by the Bachelor student Robin Hannemann who helped me to generate the data for the structural integrity assays, namely for secondary motoneurons (4.2.3) and skeletal muscles (4.2.2). I also cooperated with Dr. Raoul Wolf to implement and improve the R script for the generalized additive modeling approach (4.2.4). All joint work is additionally marked with footnotes. If not stated otherwise, content was created by me. More information and an overview of the contribution of the authors can be found in chapter 9.1.

The content of this chapter is part of a manuscript in preparation. All planned publications can be found in chapter 9.2.

4.1 Background

Nicotine is a plant alkaloid and is mainly found in the nightshade tobacco plant of the genus *nicotiana*. The plant uses the properties of the substance as protection against herbivores. Nicotine acts on the cholinergic system and is a nicotinic acetylcholine receptor (nAChR) agonist. Under normal conditions, acetylcholine (ACh) is the neurotransmitter and neuromodulator of the highly conserved cholinergic system and is the natural and intrinsic agonist of nAChR (Picciotto et al., 2012). The whole system is involved in important processes such as memory, nervous and motor function. ACh is released into the synaptic cleft where it can bind to two different receptor types, the muscarinic and nicotinic acetylcholine receptor (mAChR and nAChR) at the post-synapse. The nomenclature is derived from the higher binding sensitivity to their respective agonist. The nAChR type is mainly found at the neuromuscular junction. When nicotine binds, the signal transmission is enhanced, the receptor is desensitized and the expression of the receptor is upregulated (Slotkin et al., 2015).

Over the years, research has shown that nicotine poses health risks not only from smoking cigarettes, which contain additional toxins, but also from the consumption of nicotine without tobacco use. Several studies and reviews have emphasized the significant mortality and morbidity rates for the development of offspring in humans (Bruin et al., 2010, England et al., 2017, Phillips et al., 2023, Slotkin et al., 2015, Turnerwarwick et al., 1992). These risks encompass a range of issues, including neurological developmental impairments, cognitive deficiencies and behavioral challenges in children (England et al., 2017, Wessels and Winterer, 2008). Preclinical studies with rodents confirmed these results (Phillips et al., 2023, Slotkin et al., 2007, Sood et al., 2012). In addition to the survival of the litter, the function and development of the brain and nervous system, the cardiovascular and respiratory systems and the function of the musculoskeletal system were at the focus of the investigations and were highly impacted (Phillips et al., 2023).

Collier and colleagues comprehensively reviewed the differences and similarities of neuronal and behavioral disturbances of human, rodents and fish after nicotine treatment and demonstrated that embryonic stages of zebrafish are well suited as model organism (Collier et al., 2023). It has been shown that adverse impacts of nicotine includes the impairment of motoneuron development (Menelaou et al., 2015, Menelaou and Svoboda, 2009, Muth-Kohne et al., 2012, Svoboda et al., 2002, Welsh et al., 2009), muscle structure (Menelaou and Svoboda, 2009, Welsh et al., 2009) and corresponding motor behavior (Borrego-Soto and Eberhart, 2022, Eddins et al., 2010, Massarsky et al., 2015, Ogungbemi et al., 2020a,

Tilton et al., 2012, von Hellfeld et al., 2022). An overview of relevant zebrafish studies with nicotine exposure can be found in Table 4. Early nicotine exposure can lead to persistent and long-lasting alterations in behavior (Borrego-Soto and Eberhart, 2022) or even result in a reduced survival rate of the offspring within the first few months only due to maternal transmission (Zhao et al., 2014). The strong evidence base for this substance makes nicotine a good candidate for a positive substance for developmental neurotoxicity.

For this reason, I used nicotine as a well-investigated developmental neurotoxicant (Tab. 4), to investigate the suitability of a generalized additive modeling approach to improve the analysis of highly variable behavioral data such as the tail coiling behavior. To strengthen my findings and to proof the concept I also investigated structural impairments, namely integrity of secondary motoneurons and skeletal muscles, which are essential for this behavior.

Table 4: Overview of experiments with nicotine treatment and its adverse impacts on motoneurons, skeletal muscle and behavior on zebrafish. In addition to the tested concentrations, the results of no-observed effect concentration (NOEC), lowest-observed effect concentration (LOEC) or effective concentrations (EC) are listed.

	Exposure window	Endpoint	Tested concentrations	NOEC	LOEC/ ECxx	Reference
Motoneurons						
Embryo	22 – 66 hpf	Secondary motoneurons morphology (42, 66, 120 hpf)	33 µM	n.d.	33 µM	Svoboda et al. (2002)
Embryo	22 – 72 hpf	Primary and secondary motoneurons morphology (72 hpf)	15, 30 µM	n.d.	15 µM	Welsh et al. (2009)
Embryo	12 – 30 hpf	Primary and secondary motoneurons morphology (72 hpf)	1, 5, 10, 15, 30 µM	5 µM	15 µM	
Embryo	22 – 72 hpf	Primary and secondary motoneurons morphology (72 hpf)	1, 5, 10, 15, 30 µM	n.d.	1 µM	Menelaou et al. (2015)
Embryo	1 – 48 hpf	Primary and secondary motoneurons morphology (48 hpf)	100, 177.5, 315, 560, 1000 µM	n.d.	EC50: PMN 336.39 µM, SMN 307.98 µM	Muth-Kohne et al. (2012)
Embryo	22 – 72 hpf	Secondary motoneurons morphology (3 dpf)	5, 15, 30 µM	n.d.	5 µM	Menelaou and Svoboda (2009)
Juvenile	22 – 72 hpf	Secondary motoneurons morphology (17 dpf)	5, 15, 30 µM	10 µM	15 µM	
Skeletal muscle						
Embryo	22 – 72 hpf	Slow muscle morphology (72 hpf)	15, 30 µM	n.d.	15 µM	Welsh et al. (2009)
Embryo	12 – 30 hpf	Slow muscle morphology (72 hpf)	1, 5, 10, 15, 30 µM	30 µM	n.d.	
Embryo	22 – 72 hpf	Slow muscle morphology (72 hpf)	1, 5, 10, 15, 30 µM	5 µM	15 µM	Menelaou et al. (2015)

Life stage	Exposure window	Endpoint	Tested concentrations	NOEC	LOEC/ ECxx	Reference
Behavior						
Embryo	4 – 120 hpf	Dark/light response (120 hpf)	1,3,10,30 µM	3 µM	10 µM	Tilton et al. (2012)
Embryo	4 – 120 hpf	Touch response	1,3,10,30 µM	1 µM	3 µM	
Embryo	2 – 24 hpf	Tail coiling (24 hpf)	2.5, 8.5 µM	n.d.	n.d.	Massarsky et al. (2015)
Embryo	2 – 96 hpf	Dark/light response (144 hpf)	2.5, 8.5 µM	n.d.	n.d.	
Embryo	2 – 48 hpf	Tail coiling (21 – 47 hpf)	1.25, 2.5, 12.5, 25 µM	n.d.	1.25 µM	
Embryo	2 – 120 hpf	Swimming assay (83 – 120 hpf)	1.25, 2.5, 12.5, 25 µM	1.25 µM	2.5 µM	von Hellfeld et al. (2022)
Embryo	20 mins	Tail coiling (24-25 hpf)	10, 20, 30, 40 µM	n.d.	EC10: 0.69 µM EC50: 0.97 µM	Ogungbemi et al. (2020b)
Juvenile	2 hpf – 5 dpf	Startle (sudden tap) response (20 weeks)	15, 25 µM	n.d.	15 µM	Eddins et al. (2010)
Adult	6 – 120 hpf	Social behavior (5-6 months)	12.5, 25, 50 µM	25 µM	50 µM	Borrego-Soto and Eberhart (2022)

n.d. – not determined

PMN – Primary Motoneuron, SMN – Secondary Motoneuron

4.2 Materials & methods

I have described the used methods such as the fish maintenance, the FET test as well as the coiling assay comprehensively in chapter 1.

4.2.1 Test chemicals and fish exposure

Stock solution of nicotine was prepared in dilution water with a final concentration of 1,000 µMAs indicated in Table 2, I set exposure concentrations for the coiling assay to 5, 10, 20, 40 µM. For the analysis of the muscle and secondary motoneuron integrity, I additionally included 80 µM.

4.2.2 Muscle integrity assessment

Birefringence approach

For the experiment, I equipped an Olympus CK40 inverted microscope (Olympus, Hamburg, Germany) with two unframed linear polarizing filters (Edmund Optics, Mainz, Germany). The first was placed between light source and object in the condenser annulus slider and the second between object and objective. The setup of the microscope with the filters and the adjustment of the embryo on the slide is shown in Figure 8.

Skeletal muscle structure was analyzed by using the birefringence properties of skeletal muscles. The method I used has been previously described by Smith et al. (2013) and Konemann et al. (2022). In short, after an exposure to nicotine we[1] anesthetized and killed 5 d old zebrafish embryos with an overdose of ice-cold tricaine. Subsequently, we[1] fixed the embryos in 4 % PFA for 8 h at 4 °C on a bench rocker (Edmund Bühler, Bodelshausen, Germany). After fixation, we[1] washed the embryos thoroughly with 0.1 % Triton X-100 in PBS, cleaned them in a 1:1 solution of glycerol and water (v/v) and finally transferred and stored them in glycerol at 4 °C. I aligned both polarizing filters at a 90° angle to eliminate light emission. I positioned the embryo on a slide between the polarizing filters on the stage of the microscope (Fig.8).

To ensure that the highest light intensity resulting from birefringence could be observed, we[1] carefully adjusted the position of the embryo. Throughout the experiment, we[1] closely monitored the process using the intensity measurement function of the NIS software (Nikon-Europe, Amstelveen, Netherlands). With these adjustments we[1] could determine the optimal alignment that allowed visualization of comparable intensity values in both the dorsal and ventral muscles. We[1] performed the imaging on the same day for each replicate using the same camera and software settings. We[1] captured images with an Imagesource camera (The Imagine Source, Bremen, Germany) and NIS Elements software using a 4 x objective. Afterwards, I uploaded the pictures in ImageJ, converted them to 8-bit and subtracted the background (rolling ball size of 50). By using Yen´s thresholding, I was able to extract the relevant muscle areas and to determine the mean light intensity which was finally normalized to the respective controls.
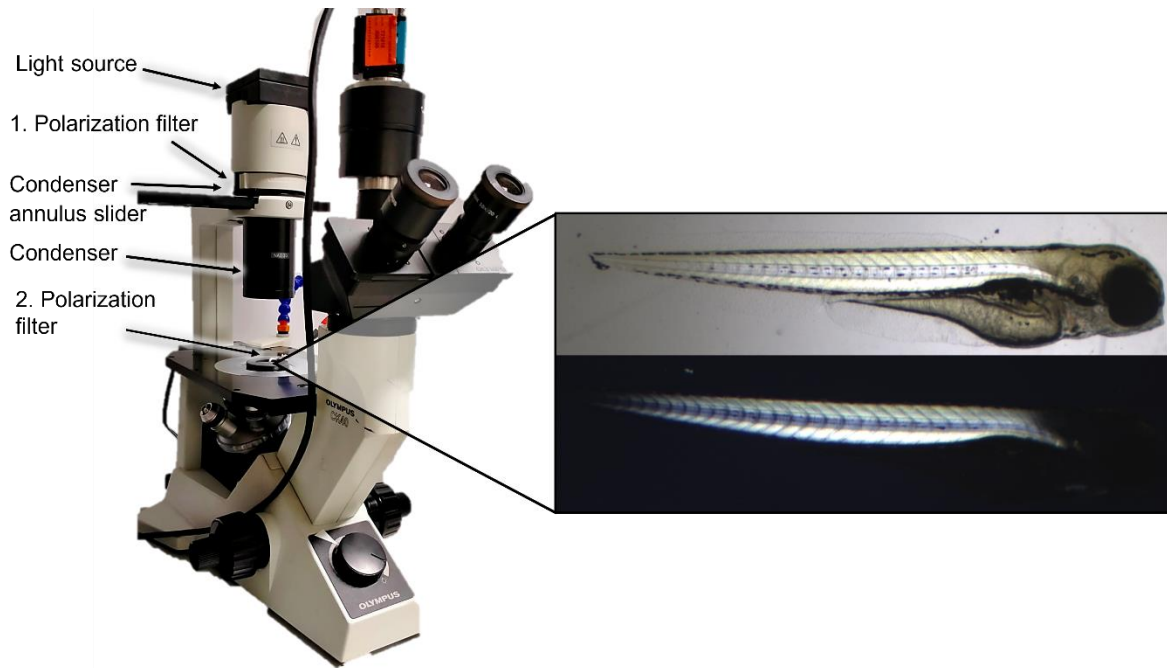
Figure 8: Microscope equipped with linear polarization filters. Shown are the positions of the two polarization filters in the microscope on the left and a magnification of a 5 d old unexposed zebrafish embryo in glycerol on the right. The upper image of the embryo shows the appearance when both filters have the same orientation. The image on the bottom demonstrates the birefringence effect with the light passing through the healthy muscles when the filters are oriented at 90°. The left part of the image with the setup of the microscope was originally created by Robin Hannemann.

4.2.3 Motoneuron integrity assessment

Immunohistochemical staining of secondary motoneurons

We[1] performed the antibody staining of secondary motoneurons according to the protocol of Konemann et al. (2022) with minor modifications. Briefly, we[1] exposed zebrafish embryos to increasing concentrations of nicotine (Tab. 2). After 3 days, we[1] terminated the experiment, placed the embryos on ice and fixed them with 4 % PFA for at least 2 h at 4 °C with agitation on a bench rocker (ibs tecnomara GmbH, Fernwald, Germany).

Thereafter, we[1] washed the embryos in 1× PBS solution for 4 × 5 min and permeabilized them sequentially in distilled water for 5 min, cold acetone (-20 °C) for 7 min, and distilled water for 5 min. After permeabilization, we[1] blocked the fish with a solution which contained 1% DMSO + 0.5 % Triton X-100 + 6% NGS in 1× PBS at RT for at least 1 h. I incubated the fixed and blocked fish with the primary antibody against DM-GRASP (Ott et al., 2001) or neuroline (Cat# zn8, 1:200; Developmental Studies Hybridoma Bank (DSHB), Iowa, USA) for 24 h at 4 °C. The next day, we[1] washed the samples thoroughly in blocking solution (10 % NGS) for 2 h and incubated them with secondary antibody (goat anti-mouse antibody Alexa fluor 568, 1:400; Thermo Fisher, Dreieich, Germany) and Hoechst 3342 (1:100; Sigma Aldrich) for an additional 24 h in the dark at 4 °C. After staining procedure, we[1] repeated the washing steps for 4 × 20 min in 1× PBS. Finally, we[1] placed the embryos laterally on a slide with Aqua-Poly/Mount (Polyscience, Cham, Germany) and covered them with a coverslip. I imaged secondary motoneurons in z-stacks in 0.5 μm increments using a Nikon eclipse 90i confocal fluorescence microscope. Images of 10 embryos per treatment, each with 3 to 4 motoneuron bundles within the yolk sac extension area, were obtained with an oil objective (40×/1.30 Oil, Nikon Plan Fluor).

I adapted the assessment of damage levels from Menelaou et al. (2015). On this basis, we[1] defined the levels of damage as follows: level 0 − no apparent damage; level 1 − one case of minor damage; level 2 has two or more cases of minor damage; level 3 − three or more cases of minor damage or one case classified as severe; and level 4 − severely damaged or complete absence of motoneurons. I classified deformations of axons as "minor damage" (Fig. 9, Level 1), whereas "severe damage" included arrest of axonal growth or excessive axonal branching (Fig. 9, Level 4). Exemplary images were taken from all replicates for the different levels and can be seen in Figure 9. In this study, I focused exclusively on examining secondary motoneurons stained with zn8 since previous literature suggests that impairments in this specific subtype of motoneuron may indicate damage in primary motoneurons (Menelaou et al., 2015; Menelaou & Svoboda, 2009). We[1] conducted the experiments three times.
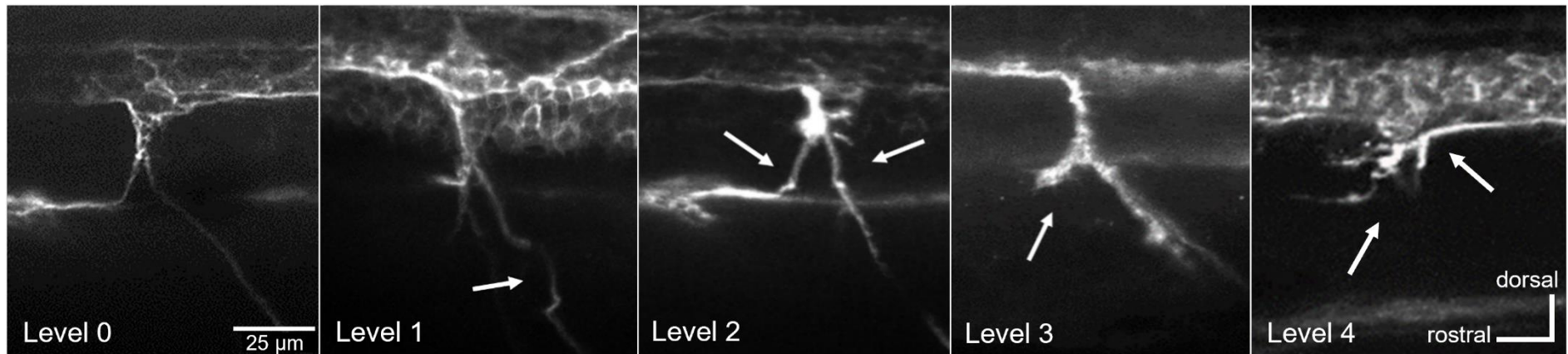
Figure 9: Semiquantitative evaluation of damage to zn8-labeled secondary motoneurons in zebrafish (*Danio rerio*) embryos. Representative images illustrate the different stages of motoneuron damage after 3 day-exposure to nicotine. The image for stage 0 shows an undamaged motoneuron bundle that has normal dorsal, rostral, and lateral projections. Level 1 represents minor damage such as deformation, level 2 shows two or more cases of minor damage, and level 3 shows three or more cases of minor damage or one case of severe damage such as growth arrest. Level 4 shows axonal growth arrest plus excessive axonal branching. Embryos were oriented with the head to the left and the dorsal side up. Scale bar: 25 µm. The microscopy images were taken by Robin Hannemann.

4.2.4 Data analysis: Generalized additive modelling approach

For all generalized additive models (GAMs) for analyzing coiling behavior, muscle and motoneuron integrity, we[3] used a restricted maximum likelihood (REML) fitting method. Additionally, a penalization of all parameters was included. We[3] analyzed the differences in the estimates of the treatment groups from the model by using a post-hoc parameter analysis with Tukey's contrasts (*i.e.,* testing all binary parameter level combinations) and Holm's multiple-testing *p*-value adjustment method.

To perform statistical analysis, we[3] used the open-source statistical software R (version 4.1.2, R Core Team, 2021) with its add-on packages *mgcv* (version 1.8-40, Wood, 2017), *multcomp* (Douma and Weedon, 2019) and *lme4* (version 1.1-33, Bates et al., 2015). We[3] created the figures using the add-on package *ggplot2* (version 3.3.6, Wickham, 2016).

I provide all R codes for the GAMs in the following test in their according sections.

Coiling assay

We[3] used a bivariate GAM to investigate the effects of the test compounds on tail coil duration and coiling frequency as part of the same model. To account for the skewed data distribution, we[3] used a log-transformation for both predictive variables, duration and frequency. We[3] used the identical parametrization for both models of the bivariate GAM: the treatment groups were implemented as fixed effect parameters. The time was treated as a non-linear smoothing parameter based on gaussian processes, as time-by-phase (dark/light phases). Moreover, we[3] treated the experimental replicates and individual groups nested within the experimental replicates as random effect smoothing parameters to account for natural occurring variance. The implemented code was used as follows:

```
nic.mv.gam <- gam(
  formula = list(
    log(duration) ~ treatment + te(time, bs = "gp", by = phase) + s(replicate, bs = "re") +
      s(group, bs = "re"),
    log(frequency) ~ treatment + te(time, bs = "gp", by = phase) + s(replicate, bs = "re") +
      s(group, bs = "re")
  ),
  family = mvn(2),
  data = nic,
  method = "REML",
  select = TRUE
)
```

Motoneuron integrity assessment

For the analysis of secondary motoneuron integrity, we[3] utilized a binomial GAM to investigate the effect of the treatments. In the model, we[3] incorporated the damage levels from 0 to 4 (Tab. 9) and express estimates of probabilities within the range of 0 to 1. Also here, we[3] included the variability resulting from individual fish, within treatment groups, and replicates as random effect smoothing. The implemented code was used as follows:

---

[3] Implementation in cooperation with Dr. Raoul Wolf from NGI, Norway.

```
d.glmer <- glmer(
  formula = cbind(grade, 4L - grade) ~ treatment + (1 | replicate / treatment / fish),
  data = d,
  family = binomial(),
  control = glmerControl(optimizer = "Nelder_Mead", calc.derivs = FALSE)
)
```

Muscle integrity assessment

For skeletal muscle integrity, we[3] used the intensity of the light as a proxy, which was automatically reported by ImageJ as the average value of the grey-scale intensity $c \in \mathbb{R}^{[0,255]}$ of an area of pixels $a \in \mathbb{N}^{+}$ determined by Yen´s thresholding. For the statistical analysis, we[3] expressed the light intensity as proportion $c_p = \frac{c}{255} \in \mathbb{R}^{[0,1]}$ and we[3] normalized the area by its arithmetic mean as $a_n = \frac{a}{\bar{a}} \in \mathbb{R}^{+}$. Since c_p was neither 0 nor 1, the variable was de facto distributed on $\mathbb{R}^{(0,1)}$ and therefore allowed for an analysis assuming a beta distribution of the data (Douma and Weedon, 2019). We[3] parameterized the used GAM with c_p as response variable, the factorized treatment as predictor variable, and the individual treatment–replicate groups nested within the replicates as random effects. We[3] implemented the replicates to incorporate the differences between replicates and to account for overdispersion of individual treatment–replicate groups, respectively. We[3] assigned weights based on a_n to account for the differences in areas as measured by ImageJ. The implemented code was used as follows:

```
data.gam <- mgcv::gam(
  formula = mean / 255 ~ treatment + s(replicate, bs = "re") + s(group, bs = "re"),
  family = mgcv::betar(),
  data = data,
  weights = area_scl,
  method = "REML",
  select = TRUE
)
```

4.3 Results

With the developmental neurotoxin nicotine, we[1] conducted two types of experiments. First, I conducted a behavioral assay, namely the tail coiling assay, and second, we[1] performed structural studies, *i.e.,* assessment of secondary motoneuron and skeletal muscle with a non-invasive birefringence method.

4.3.1 Early behavioral changes of tail movements

In this study, I analyzed a total of 7,360 observations on duration and mean frequency for all replicates spanning the time range of 21 to 47 hpf to investigate the effects of nicotine exposure on the tail coiling behavior over the course of time. I focused on these two endpoints, namely the duration and frequency of coiling movements. For the analysis, I excluded the additional parameter coiling activity due to its high correlation with frequency (0.96). I used the bivariate GAM that accounted for 50.8 % of the deviance of the raw data compared to the predicted model.

In my analysis the three phases of light (dark, light, dark) demonstrated a major influence on the pattern of the movements over time (***$p < 0.001$). Similarly, I observed that the variability between the three replicates showed significant impact on the output (***$p < 0.001$). In contrast, the variability which is naturally inherent for every individual fish had only influences on the number of coils (***$p < 0.001$) but not for the endpoint duration of the movements. I included the three light phases, replicates and individual variability in the model as smooth terms. The inclusion of these smooth terms provides a better prediction and differentiation of treatment-related effects (Tab. 6) and the random effects mentioned above (Tab. 5).

The resulting values for duration and frequency after nicotine treatment are given as predicted estimates derived from the model. Notably, I have seen two distinct patterns emerging for the two endpoints: For coil duration, there was a monotonic decrease with increasing nicotine concentrations (≥ 10 µM, ***$p < 0.001$; Fig. 10A) visible. The shortest movements I have detected was for the highest concentrations with 40 µM nicotine with only 68.8 % left of the relative duration length compared to the control. In contrast, for coiling frequency I displayed a biphasic pattern by showing a hyperactivity for 5, 10 and 20 µM nicotine treatments (***$p < 0.001$). With the most movements per min in the 5 µM treatment with approx. 160 % relative to the control. This hyperactivity was followed by a slight decrease in movements per minute at the highest nicotine group of 40 µg/L (Fig. 10B); however, this decrease finally resulted in coiling frequencies in a similar range comparable to the negative control with 93.4 %.

Table 5: Importance of smooth terms in the model for coiling behavior analysis with GAM. Chi-squared (X^2) value indicates the strength of the influence of this parameter on the model.

A – Duration

Smooth term	X^2	comments
te(time):phase1	8070.2 ***	Tensor product smooth, interaction between the time and the first dark phase (21-23 hpf)
te(time):phase2	2692.5 ***	Tensor product smooth, interaction between the time and the first light phase (24-37 hpf)
te(time):phase3	634.7 ***	Tensor product smooth, interaction between the time and the second dark phase (38-47 hpf)
s(replicate)	72738.8 ***	Smooth term for the single variable replicate (n=3)
s(group)	609.1	Smooth term for the single variable group, which is defined by the treatment groups within the replicates (3 replicates × 5 treatment groups)

A - Frequency

Smooth term	X^2	comments
te(time):phase1	577.0 ***	Tensor product smooth, interaction between the time and the first dark phase (21-23 hpf)
te(time):phase2	420.5 ***	Tensor product smooth, interaction between the time and the first light phase (24-37 hpf)
te(time):phase3	2381.4 ***	Tensor product smooth, interaction between the time and the second dark phase (38-47 hpf)
s(replicate)	2764.7 ***	Smooth term for the single variable replicate (n=3)
s(group)	126.7 **	Smooth term for the single variable group, which is defined by the treatment groups within one replicate (3 replicates × 5 treatment groups, 16 – 20 embryos per treatment and replicate)

Significance levels: ***$p < 0.001$, **$p < 0.01$

Table 6: The duration (A) and frequency (B) of the coiling behavior in zebrafish (*Danio rerio*) embryos after exposure to nicotine (n=3). Data are given as estimated values obtained from the bivariate GAM analysis relative to negative controls (%).

A – Duration of coiling behavior

	Duration estimate ± SE [a]	Duration (sec) [b]	95% CI [c]	% of control
Control	-1.26 ± 0.11	0.28	0.26; 0.35	100.0
5 µM	-1.32 ± 0.05	0.27	0.24; 0.29	94.1
10 µM	-1.52 ± 0.05	0.22	0.20; 0.24	77.3
20 µM	-1.53 ± 0.05	0.22	0.20; 0.24	76.3
40 µM	-1.64 ± 0.05	0.19	0.18; 0.21	68.8

B – Frequency of coiling behavior

	Frequency estimate ± SE [a]	Frequency (min^{-1}) [b]	95% CI [c]	% of control
Control	2.18 ± 0.19	8.81	6.11; 12.70	100.0
5 µM	2.66 ± 0.05	14.27	12.89; 15.78	161.9
10 µM	2.52 ± 0.05	12.48	11.28; 13.80	141.6
20 µM	2.45 ± 0.05	11.60	10.48; 12.83	131.7
40 µM	2.11 ± 0.05	8.23	9.11; 7.44	93.4

[a] Log-scaled estimates of duration and frequency as percent of negative controls ± SE as predicted by the GAM model

[b] Values calculated from logarithmic estimates

[c] Upper and lower limits of 95 % confidence intervals for duration and frequency
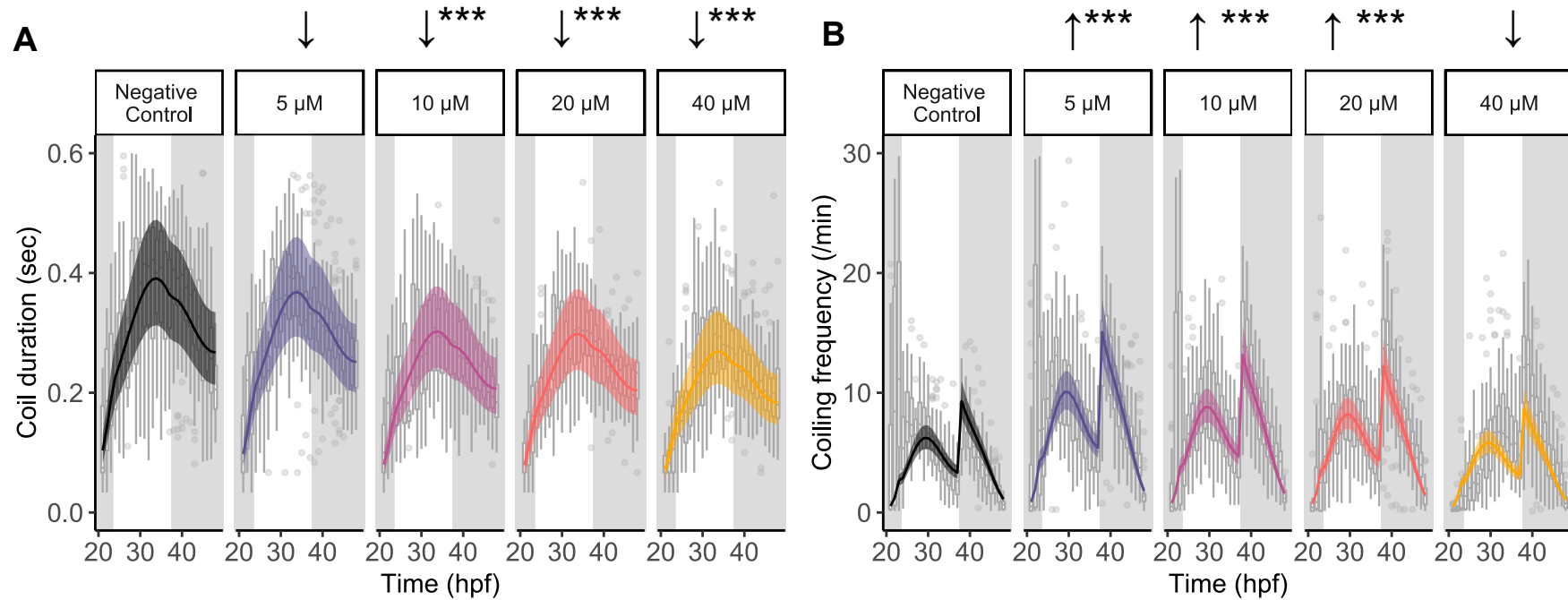
Figure 10: Coiling behavior data zebrafish (*Danio rerio*) embryos after 3 d exposure to nicotine. Coil duration (A) and coiling frequency (B) were recorded between 21 and 47 hpf. Curves illustrate the predicted course over time (hpf) as solid lines with their confidence bands (95 % CI). Boxplots represent the variability of raw data. Gray shading indicates dark phases during the experiment. Arrows refer to an increase (↑) or a decrease (↓) of activity in the respective treatment, with significant deviations from control marked with asterisks (***$p < 0.001$; Tukey´s contrast with Holm´s p-value adjustment; n=3).

4.3.2 Secondary motoneuron integrity assessment

For the evaluation of the structural damages which could be induced by nicotine, we[1] performed two different experiments: The first experiment was the assessment of secondary motoneuron integrity by using antibody labeling against neuroline which is a transmembrane protein of the secondary motoneurons. In this experiment, I decided to focus exclusively on the or zn8-positive motoneurons since previous literature has suggested and shown that damage to secondary motoneurons is an indicator of damage to primary motoneurons (Menelaou et al., 2015, Menelaou and Svoboda, 2009).

We[1] categorized deformations or excessively short axons as minor damage, while arrested or excessively branched axons were classified as severe damage. Based on the semiquantitative grading assessment, illustrated in Figure 9, we[3] used a binomial GAM to analyze the effect. The damage levels estimates were provided by the model, which can be understood as a probability, ranging from 0 to 1. By analyzing the data, we[3] used 725 individual motoneuron damage gradings from 201 individual fish in total. The analysis explained 62.7 % of the observed deviation between the raw data and the predicted model. We[3] identified that the inherent variability attributed to individual fish was highly influential, while random variation between replicates was too minor to cause a significant effect on the outcome (Tab. 7).

The data points in Figure 11A present the damage level estimates by the model of all three replicates which revealed a consistent trend: With increasing nicotine treatment, we[3] have identified a consistent increase in the mean degree of damage to motoneurons bundles. First indication of significant impairment of motoneuron structure, we[3] have seen with 20 µM nicotine (0.74; *$p<0.05$) The largest step occurred from 40 µM with 0.77 (**$p<0.01$) as damage level to 80 µM with 2.62 (***$p<0.001$). Most of the fish in this treatment group had a considerable high number of axons which showed an inhibition of growth or even a complete arrest. Taken all replicates together, we[3] detected significant differences at nicotine concentrations of 20, 40, and 80 µM (Fig. 11B). I have listed all obtained values from the model, estimate values as well as the corresponding damage levels ($\pm$ 95 % CI), in Table 8.

Table 7: Importance of smooth terms in the model for motoneuron damage grading. Chi-squared (X^2) value indicates the strength of the influence of this parameter on the model.

Smooth term	X^2	comments
s(replicate)	11.35	Smooth term for the single variable: replicate (n=3)
s(treatment)	0.00	Smooth term for the single variable: treatment group (6 treatments)
s(fish)	350.36 ***	Smooth term for the single variable: individual fish (each replicate includes 10 – 14 fish per treatment)

Significance level: ***$p < 0.001$
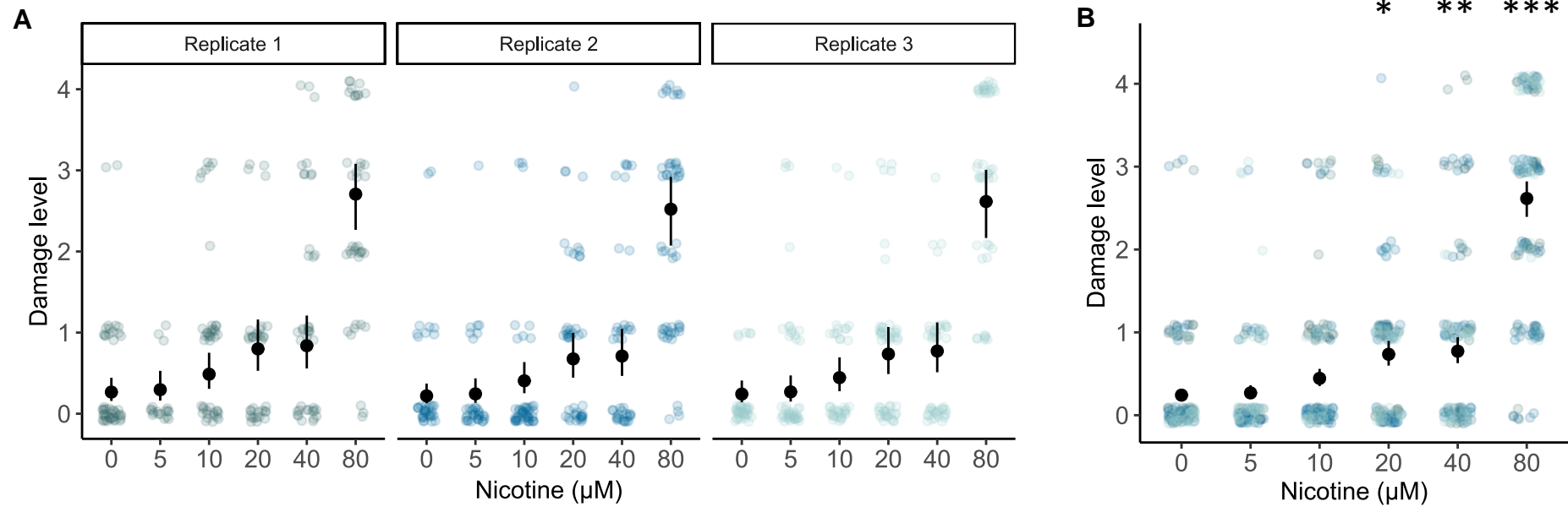
Figure 11: Semiquantitative evaluation of damage to zn8-labeled secondary motoneurons in zebrafish (*Danio rerio*) embryos after 3 d exposure to nicotine. The graph displays the three independent replicates (1-3) separately, with each data point representing the extent of damage to one motoneuron bundle (A). Each treatment group consisted of 10-14 sampled fish in each replicate. All replicates together are summarized in B. Asterisks (*$p < 0.05$, **$p < 0.01$, ***$p < 0.001$) point to significant differences between treatment and control groups (Tukey post hoc test with Holm *p*-value adjustment).

Table 8: Semiquantitative analysis of damage to secondary motoneurons of zebrafish (*Danio rerio*) embryos after 3 d exposure to nicotine as estimated with a binomial GAM (n=3).

	Damage level estimate ± SE [a]	Damage level [b]	95% CI [c]
Control	-2.98 ± 0.29	0.24	0.18; 0.32
5 µM	-2.63 ± 0.32	0.27	0.20; 0.36
10 µM	-2.08 ± 0.26	0.44	0.35; 0.56
20 µM	-1.49 ± 0.25 *	0.74	0.60; 0.90
40 µM	-1.43 ± 0.25 **	0.77	0.63; 0.94
80 µM	0.64 ± 0.24 ***	2.62	2.39; 2.82

[a]   Log data of the damage levels in control and treatments predicted by the GAM model

[b]   Damage levels: 1 = minor damage; 2 = two or more minor damages, 3 = three or more minor damages or one severe damage; 4 = two or more severe damages or character absent

[c]   Upper and lower limits of 95 % confidence intervals for damage levels

Significance level: *$p<0.05$, **$p<0.01$, ***$p<0.001$

4.3.3   Somatic muscle integrity assessment

We[1] used the birefringence properties of skeletal muscle as marker for the integrity of skeletal muscle (Fig. 12). With the beta regression GAM, we[3] were able to cover 74.2 % of the deviance of the data compared to the predicted model and it considered a total of 171 fish with their skeletal muscle. We[3] detected a significance for the impact of three replicates on the outcome, as visible in Figure 13. But we[3] saw that the muscle of fish within their treatment group was comparably affected by the respective treatment. I included all smooth terms and their impact on the outcome in Table 9.

Table 9: Importance of smooth terms in the model for muscle integrity analysis with GAM. Chi-squared (X^2) value indicates the strength of the influence of this parameter on the model.

Smooth term	X^2	comments
s(replicate)	169.47 *	Smooth term for the single variable replicate (n=3)
s(group)	72.07	Smooth term for the single variable group, which is defined by the treatment groups within one replicate (3 replicates × 6 treatment groups, 7 – 10 fish per treatment and replicate)

Significance level: *$p < 0.05$

When we[3] focus on the actual mean birefringence intensities (Tab. 10), we[3] observed a decreasing trend of intensity, which was already apparent while taking the microscopic pictures (Fig. 12A). Moreover, we[3] saw that within the third replicate, the 40 µM treatment group showed a significant difference from the other two replicates (*$p < 0.05$). Overall, among all tested concentrations, for the 40 and 80 µM treatments we[3] revealed significant differences compared to the control group (Fig. 13). In addition,

severe structural damage within the muscles can be seen as black spots in the highest treatment group of 80 µM nicotine (Fig. 12B).

Table 10: Birefringence intensity as an index of muscle integrity in zebrafish (*Danio rerio*) embryos after 3 d exposure to nicotine. Beta-distributed mean light intensity estimates are expressed in log data calculated by a GAM beta regression. Data for birefringence intensity given in grayscale values from 0 to 255 (n = 3).

	Mean light intensity estimate ± SE [a]	Mean birefringence intensity [b]	95 % CI [c]
Control	-1.16 ± 0.13	60.85	50.08; 73.10
5 µM	-1.18 ± 0.15	59.80	47.10; 74.70
10 µM	-1.19 ± 0.15	59.48	46.82; 74.34
20 µM	-1.41 ± 0.15	49.90	38.82; 63.22
40 µM	-1.70 ± 0.16 **	39.38	30.19; 50.73
80 µM	-2.04 ± 0.16 ***	29.42	22.22; 38.58

[a]   Log data of control and treatments predicted by the GAM model
[b]   Mean birefringence intensity calculated from estimates
[c]   Upper and lower limits of 95 % confidence intervals for damage levels

Significance level: **p<0.01, ***p<0.001
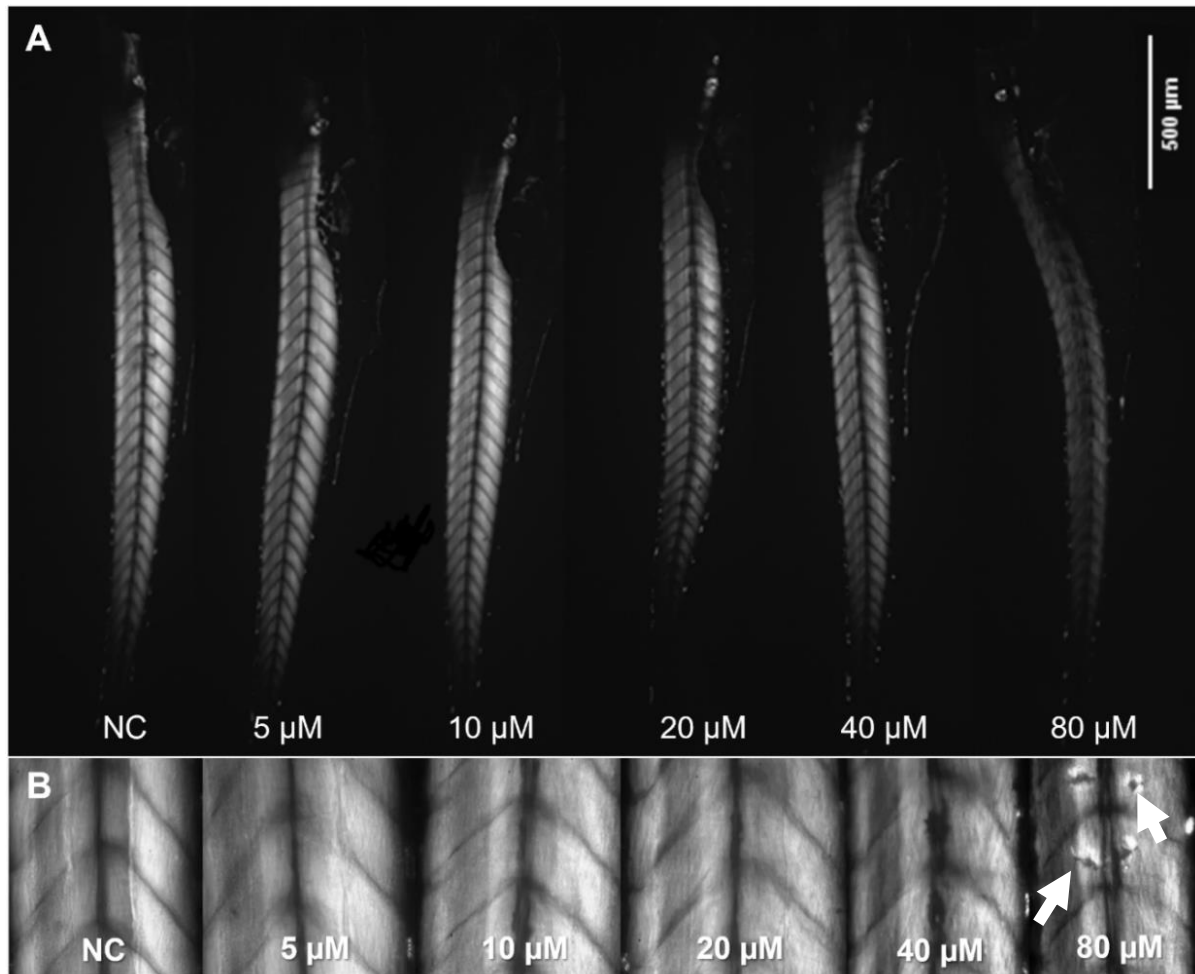
Figure 12: Birefringence of somatic muscles as a parameter of muscle integrity in 5 d old zebrafish (*Danio rerio*) embryos (orientation: head up, dorsal side left) after exposure to nicotine. (A) Micrographs with an original magnification of 20×. (B) At higher magnification (40×), the structural appearance of the muscles is less homogenous and shows an increasing number of clefts (white arrow). NC = negative control. Scale bar: 500 µm. Microscopy images were taken by Robin Hannemann.
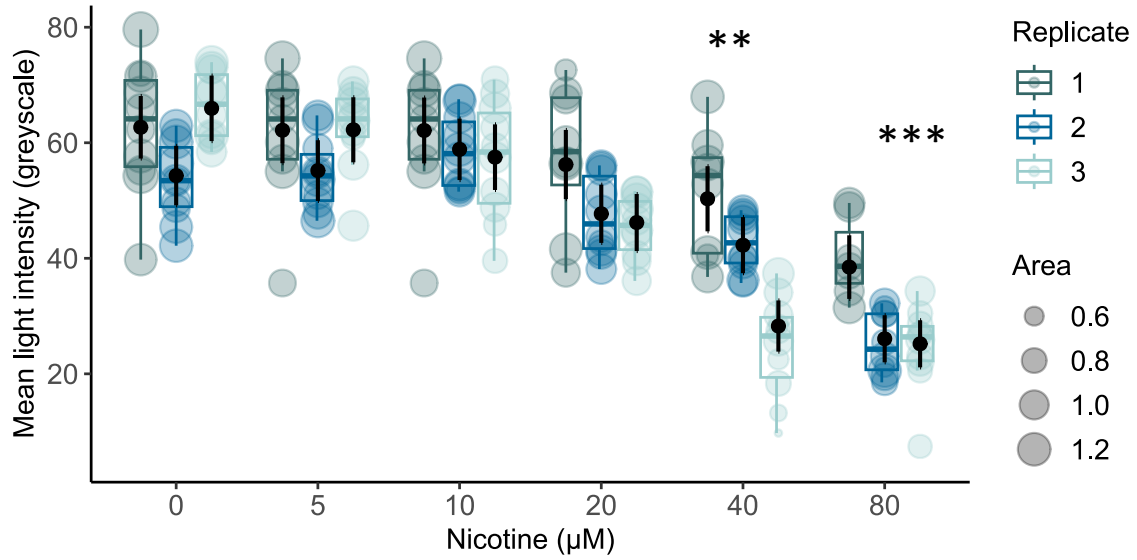
Figure 13: Mean brightness of somatic muscle birefringence as a parameter of muscle integrity in 5 d old zebrafish (Danio rerio) embryos. Boxplots and the colored dots show the mean measured grey scale values (0 – 255) of the fish over the area of their muscles. The size of the dots corresponds to the scaled area. Mean greyscale value of each replicate is predicted by the model (black dots) ± 95 % CI. The different colors indicate the independent replicates (n=3). Statistical significance between treatment groups and control: **$p < 0.01$ and ***$p < 0.001$ (Tukey´s *post-hoc* test with Holm´s *p*-value adjustment).

4.4 Discussion

I have chosen nicotine as a model compound to evaluate the suitability of a GAM approach to analyze the coiling behavioral since this compound is a well-known and good examined developmental neurotoxic compound (overview of experiments and effects of nicotine in zebrafish can be found in Tab. 4). Furthermore, to better attribute and underline the behavioral change after nicotine exposure to possible morphological causes, I included assessment of the integrity of secondary motoneurons and somatic muscles in this investigation.

4.4.1 Different approaches to analyze fish embryo behavior

Single time point measurements for tail coiling differences after chemicals expose have shown to be a rapid screening tool for neurotoxic substances (Ogungbemi et al., 2021, Selderslaghs et al., 2010, Vliet et al., 2017, Weichert et al., 2017). However, Zindler et al. (2019b) developed an assay and protocol for observing the tail coiling movements of developing zebrafish from 21 hpf until 47 hpf (at 26 °C). In the case of ethanol expose, the detectable delay in the coiling activity emphasized the need for multiple measurements of embryonic movements to avoid the risk of misinterpreting the effects of substances. If only one measurement point is selected (*e.g.* 24 hpf), one could assume a lower frequency due to the ethanol exposure compared to the control rather than an actual delay in development. Moreover, the amount of time it takes for different substances to finally pass the chorion and reach the fish embryo may vary due to their distinct physico-chemical properties (Kais et al., 2013, Pelka et al., 2017). It has been shown that lipophilic chemicals can accumulate in the yolk sac and therefore can only affect the embryo at later stages when the yolk sac is fully absorbed (Halbach et al., 2020). With several single time point measurements in a time series, the focus can be on specific temporal events such as the onset and development of movements, the peak of activity (Ogungbemi et al., 2020b, Zindler et al., 2019a, Zindler et al., 2019b) or the step change (STC) that occurs during the transition from light to dark (von Hellfeld et al., 2023, von Hellfeld et al., 2022). In this way, even delayed effects can be detected.

Instead of having a detailed and zoomed-in view on the individual time points, our[3] GAM analysis can provide an overall perspective on the data, *i.e.*, over the entire course of the coiling activity. The GAM combines various model functions and optimizes function parameters and relative weights. These weights define the degree to which each model function contributes to the overall model. Hence, GAM can describe data more flexible and is often less biased compared to a single-function approach, which is chosen based on pre-assumptions. Predicted trends of the treatments can be seen in comparison to each other, and it can therefore provide no-observed effects (NOEC) and lowest observed effects (LOECs) for the whole observation period, here from 21-47 hpf. Since we[3] included the natural inherent biological variability of every fish and every replicate into the model, these normal responses are accounted in the predicted curves. Thus, all replicates can be pooled together and can make the prediction more robust to outliers. Moreover, since we[3] incorporated the variation as random factors, the model analysis can distinguish between these non-treatment related effects and the treatment-induced effects on the activity levels of the embryos. In this way, I concluded, GAM can be used as an analysis tool for various behavioral studies, as the problem of high variability within and between replicates and also strains is a common issue (de Esch et al., 2012, Lange et al., 2013). Nevertheless, a comprehensive comparison of these different approaches – single time point analysis and modelled trend analysis – should be tested beside each other.

4.4.2   Nicotine causes short convulsive twitches of the embryo´s tail

The effects of nicotine on coiling movements have repeatedly been documented (Massarsky et al., 2015, Ogungbemi et al., 2020a, Thomas et al., 2009, von Hellfeld et al., 2022). For the frequency of the coils, data in the literature suggest that differences between hyper- or hypoactive responses of the same compound are more dependent on exposure duration and timing than on toxicant concentrations itself (Ogungbemi et al., 2019). Whereas short-term exposure stimulates effects on nAChR, which is associated with an increase of activity (Ogungbemi et al., 2020b, Thomas et al., 2009), long-term exposure produced highly variable (Ogungbemi et al., 2020a) or even opposite sedative effects, especially at high concentrations (25 µM; von Hellfeld et al., 2022). This may be the result of a desensitization of nAChR (Mudo et al., 2007, Thomas et al., 2009) or an increase of nicotine metabolization (Borrego-Soto and Eberhart, 2022).

In my present study, the frequency of tail coils follows the same general trend with a biphasic pattern: With increasing nicotine concentration, there is first a trend towards hyperactivity, which is followed by a decrease and a return to control levels at even higher concentrations up to 40 µM nicotine. For the duration of the movement, however, there is a monotonic decrease. This may be explained by increasing restriction of movement due to morphological impairments (Welsh et al., 2009) which is discuss in the following section. The duration of movements as a parameter is provided by most behavior recording systems but is often not included in the analysis. As an additional parameter, this can lead to a more versatile description of the character of the movement influenced by the substances. Using these two criteria, enables to distinguish between neurotoxic compounds with different modes of action (von Hellfeld et al., 2023, Zindler et al., 2019a). In my case study, the frequency and duration of movement together may indicate that the exposed embryos show a greater number of convulsive, i.e. shorter, movements with increasing nicotine concentration.

4.4.3   Behavioral alterations influenced by nicotine aligns with structural damage in skeletal muscle and secondary motoneurons

Our[3] analysis of somatic muscles in 5 d old zebrafish embryos *via* birefringence documented an obvious decline of light passing through the translucent trunk region. This decline in birefringence is indicative of an increasing disorganization of sarcomeres and myofiber homogeneity, since only highly ordered structures allow light to pass through the filters. Especially exposure to 80 µM nicotine revealed a particularly strong reduction of birefringence, which was accompanied by the occurrence of "dark spots", which are most likely symptoms of severe damage, which might well indicate the onset of necrotic processes. It should be anyway noted that an exposure concentration as high as 80 µM nicotine leads to an increased number of post-hatch kyphosis and lordosis, which have also been observed by von Hellfeld et al. (2022). Given such interference with severe sublethal effects, the concentration of 80 µM was only used as an experimental proof-of-concept.

Nicotine-induced changes in muscle structure have previously been demonstrated by Welsh et al. (2009) using histological transverse sections and whole-mount immunohistochemical staining of slow and fast muscle fibers of 72 hpf zebrafish embryos. Although the detail resolution of the muscle structure is not as high as for histological sections, the birefringence approach which I used in my study has the clear advantage of being fast, cheap, noninvasive, and easily quantifiable with the resulting light intensity. For these reasons, birefringence has already been used for the analysis of muscle mutants (Berger et al.,

2012, Smith et al., 2013) and neuromuscular effects following exposure to insecticides such as thiacloprid and methomyl (Konemann et al., 2022).

Muscle stimulation by nicotine is mediated by a muscle-specific nAChR isoform and can lead to paralysis, muscle degeneration and myopathy if overactivity persists (Welsh et al., 2009). Similar effects can be observed by activation with endogenous acetylcholine if it is not rapidly broken down naturally by its catabolic enzyme acetylcholinesterase (Behra et al., 2002). For muscle development, balanced neuromuscular activity patterns appears to be essential for healthy and well-organized growth (Buonanno and Fields, 1999, Kimmel et al., 1974). This principle also applies to the development and pathfinding of the corresponding motoneurons (Lefebvre et al., 2004, Menelaou et al., 2008, Zeller et al., 2002).

In the present study, nicotine exposure resulted in increasing changes in the morphology of zn8-associated motoneurons. These included in particular growth arrest or retardation, which was already reported by Svoboda et al. (2002). It is also known that this neurotoxicant impairs pathfinding processes and subsequent innervation of the muscle (Menelaou et al., 2015, Svoboda et al., 2007, Zeller et al., 2002). Nicotine disrupts the normal structure of associated secondary motoneurons (Laskowski et al., 1975, Lefebvre et al., 2004) and hyperstimulation of these neurons contributes to excitotoxicity which can lead to subsequent degeneration of muscles (Welsh et al., 2009).

Continuing studies have shown that exposure to embryonic nicotine exposure revealed also a permanent damage to morphological motoneurons and muscles in juvenile fish (Menelaou and Svoboda, 2009), impaired early predator escape response (Victoria et al., 2022), swimming ability, social behavior and finally lower survival rates in adult fish (Borrego-Soto and Eberhart, 2022).

4.4.4   Conclusions

The coiling behavior of zebrafish embryos has repeatedly been suggested as a valuable tool for the evaluation of (developmental) neurotoxicity. Typically, the frequency of coiling is the primary endpoint used to quantify movement. In my experiments and analysis, however, I noticed that the duration of movements may be an important additional endpoint to provide a more-in-depth characterization of the changes in behavior, especially when biphasic activity patterns. Moreover, my observed trend in reduction of movement duration with increasing nicotine concentrations has the potential to be an indicator of (developmental) neurotoxicity, since I could relate it to evident morphological effects indicating interference with motoneuron and muscle integrity. By using GAM for coiling time series data, I found advantages over the single time point analysis approach including flexible data description, the ability to capture biological variability and to pool replicates, which in turn increases robustness towards outliers.

5 DESNITRO-IMIDACLOPRID AS TOXIC AS NICOTINE? – A COMPARISON

In this chapter, I was supported by Dr. Caroline Bauch from Cyprotex, UK, who conducted the analytical analysis of desnitro-imidacloprid concentrations in the zebrafish embryos and exposure solutions (5.2.2). Again, Dr. Raoul Wolf and I worked together to analyze the coiling behavior data. All joint work is additionally marked with footnotes. If not stated otherwise, content was created by me. More information and an overview of the contribution of the authors can be found in chapter 9.1.

The content of this chapter is part of a manuscript in preparation. All planned publications can be found in chapter 9.2.

5.1 Background

More than 20 years ago, the first neonicotinoid pesticides were developed which are very similar to nicotine in their specific mode of action. Imidacloprid, initially approved in the U.S. in 1994, was the first and is still one of the most widely used neonicotinoid insecticides in pest control. These neonicotinoids act on the nAChRs as agonists with a higher selectivity in insect than to vertebrate receptors (Casida, 2018, Tomizawa and Casida, 2005).

Despite the higher selectivity to insect nervous systems, Kimura-Kuroda and colleagues showed overactivation of nAChR from cerebellar neurons from neonatal rats after a treatment to imidacloprid at low μM concentrations (Kimura-Kuroda et al., 2012). This developmental neurotoxic potential was underlined in rodent studies, where chronic prenatal exposure to imidacloprid caused inflammation, oxidative stress in the central nervous system as well as enduring alterations in brain functions and behavior later on (Abou-Donia et al., 2008, Burke et al., 2018, Duzguner and Erdogan, 2012).

Attention should be paid to the main metabolite, desnitro-imidacloprid, which is either formed abiotically by photodegradation, hydrolysis, chlorination or is metabolized by biota (Aregahegn et al., 2017, Koshlukova, 2006, Thompson et al., 2020). Monitoring studies in China detected the metabolite in groundwater, drinking water as well as in urine samples of adult humans, including pregnant women (Mahai et al., 2021, Mahai et al., 2022, Montiel-Leon et al., 2018, Wang et al., 2020). In *in vitro* studies, desnitro-imidacloprid proved to be a bioactivated transformation product and revealed an even higher response to mammalian receptors than its parent compound which is comparable with nicotine (Chao and Casida, 1997, Loser et al., 2021a, Tomizawa and Casida, 2000, Tomizawa and Casida, 2002). This agonistic activation may lead to impaired synaptogenesis or plasticity and could ultimately impair neuron survival (Tomizawa and Casida, 2002, Wheeler and Cooper, 2004). However, the available data for this metabolite is insufficient to evaluate its (developmental) neurotoxic for vertebrates (Thompson et al., 2020).

As a consequence of the knowledge gap in the literature considering potential impacts of desnitro-imidacloprid, my aim of this study was to investigate the toxicity of this metabolite in the widely used model organism zebrafish embryo. First, I acutely exposed the embryos with the compound during their first days of development to assess the sensitivity. After the exposure, uptake and bioaccumulation were analyzed. To address the question about the potential (developmental) neurotoxicity, I additionally observed the coiling movements of the zebrafish embryo. The gathered data was compared to the impacts of the well-known developmental neurotoxin nicotine.

5.2 Materials & methods

I have described the used methods such as the fish maintenance, the FET test as well as the coiling assay comprehensively in chapter 1.

I introduced the analysis approach with the generalized additive model in the previous chapter and more details can be found under 4.2.4.

5.2.1 Test chemicals and fish exposure

For desnitro-imidacloprid, I prepared exposure solutions for the FET test and the coiling assay in the final concentrations of 6.25, 12.5, 25, 50 and 100 µM (0.1 % DMSO). For nicotine, I chose a wide range with 6.25, 12.5, 25, 50, 100, 200 and 400 µM (0.1 % DMSO) for the FET test due to previously published data (von Hellfeld et al., 2022). For the coiling assay I prepared lower concentrations with 5, 10, 20, 40 µM (0.1 % DMSO).

5.2.2 Analytical measurements[4]

I exposed and raised the zebrafish embryos according to the FET test (3.3). For the analysis of desnitro-imidacloprid content in the exposure solutions, I provided freshly prepared solutions at 96 hpf before contact with fish and solution at 120 hpf after the exposure. Additionally, at 120 hpf I killed the embryos by rapid cooling on ice and subsequently I thoroughly washed them $3 \times$ in ice cold dilution water for 1 min each. Afterwards, I transferred the embryos into 2 ml Eppendorf tubes (Carl Roth), removed the water as far as possible and stored them at -80 °C until shipping.

The measurement of internal concentrations in the zebrafish embryo at 120 hpf as well as the amount of compound in the pre (freshly prepared) and post-exposure solutions from 96 and 120 hpf, respectively, was conducted by liquid chromatography and mass spectrometry. Briefly, 100 µl ultrapure water was added to each vial containing embryos, exposure solution or standard curve sample. After mixing, 10 µl of rosuvastatin (internal standard, IS; Sigma-Aldrich, MO, U.S.) dissolved in 50 % methanol (VWR, PA, U.S.) was added to the 100 µl sample followed by 300 µl acetonitrile (Thermo Fisher Scientific Inc., MA, U.S.). All samples were mixed and centrifugated at 13,000 rpm for 5 minutes. Supernatant of 300 µl was transferred to plates and dried with nitrogen steam at 50 °C (for approx. 30 min) until 50 µl remained in each sample. Subsequently, 100 µl ultrapure water was added and samples mixed thoroughly. Finally, plates were placed into an autosampler connected to a Sciex TripleTOF 6600 Quadruople Time-Of-Flight (QTOF) mass analyzer (AB Sciex, Singapore). For additional condition settings and information see Appendix B (Tab. B1).

---

[4] The analytical measurements of water and embryo samples were conducted by Dr. Caroline Bauch from Cyprotex, UK.

I calculated the internal concentrations c_{int} of each zebrafish embryo as shown in (1):

$$c_{int} = \frac{c \times V_{total}}{N \times V_{ZF}} \tag{1}$$

where c is the measured concentration of the sample with the sample volume V_{total} and V_{ZF} is the volume of one embryo at 120 hpf. Volume was derived from the estimates published in Simeon et al. (2020) with 3 x 10^{-7} L per embryo at 120 hpf. N represents the number of embryos analyzed.

5.3 Results

5.3.1 Fish embryo toxicity

In the FET study, I considered all replicates of both compounds, nicotine and desnitro-imidacloprid, as valid since mortality in both solvent control groups (0.1 % DMSO) stayed below 10 % throughout the experimental period (until 5 dpf). For nicotine exposure, I was able to perform a probit analysis to calculate ECs for 10, 20, and 50 % as well as NOECs and LOECs at 96 and 120 hpf (Tab. 11). However, I could not establish a concentration-response relationship for the desnitro-imidacloprid exposed groups within the concentration range used since responses stayed close to the range of the control even in highest concentration of 100 µM. The concentration-response curve of nicotine and the effects of desnitro-imidacloprid at 120 hpf are illustrated side by side in Figure 14A and B.

Table 11: Effective concentrations (EC) of the FET test of 10, 20 and 50 % at 96 and 120 hpf after exposure to nicotine and desnitro-imidacloprid. Additionally, lowest-observed effect concentration (LOEC) and no-observed effect concentration (NOEC) are listed.

Time point		Nicotine (µM)	Desnitro-Imidacloprid (µM)
	EC10	16.11	
	EC20	34.97	
96 hpf	EC50	153.98	not determined
	NOEC	100	
	LOEC	50	
	EC10	11.23	
	EC20	19.20	not determined
120 hpf	EC50	53.63	
	NOEC	50	
	LOEC	25	

During the desnitro-imidacloprid exposure experiments, I observed that the combined rate of morphological and sublethal effects, such as yolk sac and pericardial edema and slight curvature of the spine, remained below 17 % in all three replicates and stayed close to the range of the solvent control (up to 10 %). For nicotine treatment instead, I noticed a reduction in spontaneous movements (at 24

hpf), impaired heartbeat and tail development. In addition, I found that already at concentrations of ≥ 50 µM of nicotine resulted in an overall developmental delay in the embryo which became visible by late hatching. In general, both compounds, nicotine and desnitro-imidacloprid, had some effects in common, especially edema of yolk sac and pericardium and curvature of the spine. I listed all effects over the 5 days of observation in Table 12.
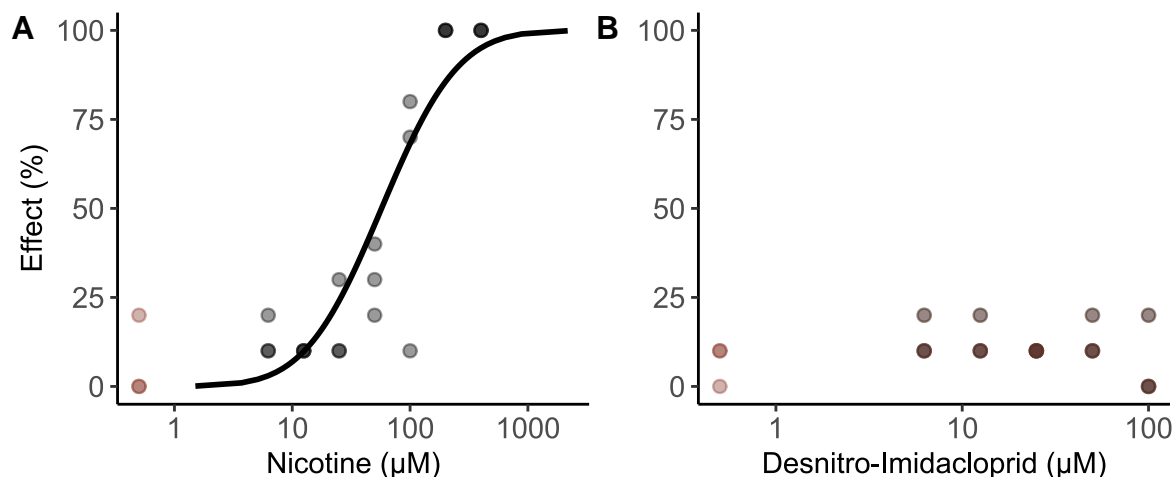
Figure 14: Concentration-response of nicotine and desnitro-imidacloprid. For a comparison between the two compounds, the effects of nicotine (A) and desnitro-imidacloprid (B), are illustrated beside each other. The concentration-response curve of nicotine is modeled by probit maximum likelihood regression. Solvent controls are indicated in red. I conducted both experimental sets in three independent replicates.

Table 12: List of sublethal endpoints at daily developmental time points for nicotine (N) and desnitro-imidacloprid (D) according to von Hellfeld et al. (2020). A grey shaded background represents endpoints that cannot be observed at the given developmental stage.

Endpoint	24 hpf	48 hpf	72 hpf	96 hpf	120 hpf
Impaired heartbeat		N	N	N	N
Altered spontaneous movement	N				
Oedema (yolk sac/pericardium)	N, D	N, D	N, D	N, D	N, D
Impaired tail development	N	N	N	N, D	N
Impaired head development	N				N, D
Delayed hatching				N	
Tremor			N		
Curvature of the spine		N	N, D	N, D	N, D
Delayed development			N	N	N

5.3.2   Internal concentration in embryos and exposure medium

The amount of desnitro-imidacloprid which was found in the bodies of the embryos increased with higher exposure concentration (Fig. Figure 17: Comparison coiling behavior over time of negative and solvent control.17A). The relationship between the waterborne exposure and the internal concentration within the embryo's bodies can be described in a linear fashion (y = 1.5 + 0.1x; R^2 = 0.85), although it visibly underestimates the internal concentration at lower concentrations such as with 6.25 µM treatment group (Fig. 17B). I have seen the highest internal concentrations measured were in the two highest nominal treatment groups (50 and 100 µM), with values of 10.49 µM and 12.21 µM, respectively. This only corresponds to an uptake of 14 % and 11 %, considering the ratio between the mean values of substance in the body and the fresh exposure solution. I calculated the highest uptake in the treatment with 25 µM with 65 % (Tab. 13).

Table 13: Measured concentrations of desnitro-imidacloprid in water and zebrafish embryos. Concentrations of the exposure solution from 96 (fresh solution) and 120 hpf (24 h later) as well as embryo internal concentrations at 120 hpf are listed as means ± SE (µM).

Nominal	Fresh solution	after 24 h	Embryo	Embryo/Water
SC	0.02 ± 0.01	0.18 ± 0.06	0.12 ± 0.06	1.07
6.25	3.59 ± 0.15	3.61 ± 0.22	1.12 ± 0.33	0.32
12.5	4.76 ± 0.10	5.01 ± 0.10	1.99 ± 0.92	0.42
25	6.13 ± 0.18	6.25 ± 0.40	3.98 ± 1.41	0.65
50	76.87 ± 6.15	70.23 ± 15.49	10.49 ± 4.10	0.13
100 [a]	112.66 ± 24.53	114.86 ± 13.23	12.21 ± 0.42	0.11

[a] duplicate
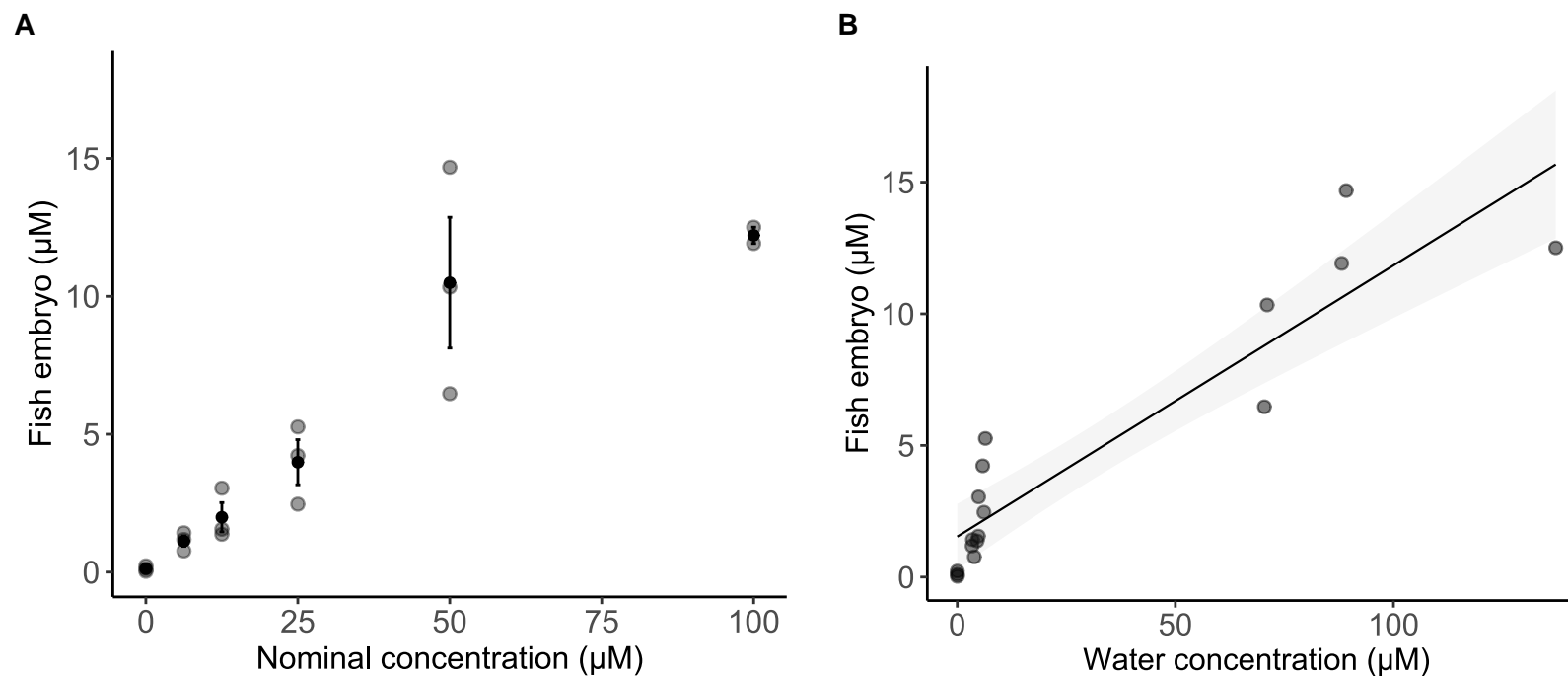
Figure 15: Desnitro-imidacloprid concentrations in fish. Internal concentrations per zebrafish embryo after semi-static exposure to the metabolite for 120 hpf in water (**A**). Means are illustrated as black dots (± SE) whereas single measurements are shown in grey. The linear correlation between the measured water concentrations and the internal concentration in the embryos is plotted in **B**. Dots show one measurement each, with the 95 % confidence band highlighted in grey. Controls are depicted as black dots. All measurements were repeated three times, except for the embryos with a nominal 100 µM desnitro-imidacloprid exposure (duplicate). Analytical work was done by Caroline Bauch[4].

5.3.3   Coiling behavior after exposure to desnitro-imidacloprid and nicotine

For the coiling experiments, I have chosen nicotine concentrations of 40, 20, 10, and 5 µM, all of which were below the LOEC and EC_{50} of 120 hpf in my FET experiment (Tab. 11). Since the neonicotinoid metabolite did not show severe effects at acute exposure, I included all concentrations from 100 to 12.5 µM. At the end the data included a total of 7445 observations for all three replicates of nicotine and two replicates with 4992 for desnitro-imidacloprid over the period from 21 to 47 hpf. In these experiments, I analyzed the two endpoints mean duration and mean frequency and excluded the data on coiling activity because of its high correlation with the data on frequency (0.97) for nicotine and 0.94 for desnitro-imidacloprid.

By looking on the smooth terms integrated in the bivariate GAM (Tab. 14), in both exposure scenarios, nicotine and desnitro-imidacloprid, not only the light phases over the course of time but also all replicates differed from each other. Moreover, the groups/wells in which the embryos were exposed to the different concentrations varied, except for the duration endpoint for desnitro-imidacloprid.

Using the bivariate GAM, I was able to explain 47.7 % of the nicotine and 53.1 % for desnitro-imidacloprid deviation of the raw data against the predicted model. I extracted and tested potential differences of the solvent control estimates from both experiments, which resulted in no significant differences for either endpoint ($p \gg 0.05$). I discuss the impact of the solvent DMSO more in detail in the following chapter 6.

When analyzing the treatment category estimates from the model, I found significant differences in duration for all nicotine exposures. At the highest exposure concentration of 40 µM, embryonic coiling duration decreased by 46 % (***$p < 0.0001$). The reductions observed at 20 µM and 10 µM exposures were close, 35 % (***$p < 0.0001$) and 32 % (***$p < 0.0001$), respectively. Even at the lowest concentration (5 µM), the model predicted only 82 % (***$p < 0.0001$) of coil duration compared to the solvent control. Looking at the frequency data over time, only 40 µM nicotine was able to significantly reduce the occurrence of coils, leaving a residual of 26 % (***$p < 0.0001$) of the control frequency. After treatment with the metabolite, I could neither detect a reduction nor an increase in coiling activity and is therefore similar to the control group. I plotted all replicates separately which can be found in Appendix B Figure B1 and B2 for nicotine and desnitro-imidacloprid, respectively.

Table 14: Impact of smooth terms in the model for the coiling analysis of nicotine and desnitro-imidacloprid (Dn-imi) treatment with DMSO as a solvent. Chi-squared (X^2) value indicates the strength of the influence of this parameter on the model.

Duration	Nicotine	Dn-imi	
Smooth term	X^2	X^2	comments
te(time):phase1	3509.1 ***	8070.2 ***	Tensor product smooth, interaction between the time and the first dark phase (21-23 hpf)
te(time):phase2	2723.8 ***	2692.5 ***	Tensor product smooth, interaction between the time and the first light phase (24-37 hpf)
te(time):phase3	154.4 ***	634.7 ***	Tensor product smooth, interaction between the time and the second dark phase (38-47 hpf)
s(replicate)	64549.3 ***	72738.8 ***	Smooth term for the single variable replicate (n=3 for nicotine and n=2 for dn-imi)
s(group)	5007.5 *	609.1	Smooth term for the single variable group, which is defined by the treatment groups within the replicates (3 nicotine or 2 dn-imi replicates × 5 treatment groups)

Frequency	Nicotine	Dn-imi	
Smooth term	X^2		comments
te(time):phase1	1219.8 ***	577.0 ***	Tensor product smooth, interaction between the time and the first dark phase (21-23 hpf)
te(time):phase2	379.1 ***	420.5 ***	Tensor product smooth, interaction between the time and the first light phase (24-37 hpf)
te(time):phase3	371.4 ***	2381.4 ***	Tensor product smooth, interaction between the time and the second dark phase (38-47 hpf)
s(replicate)	< 0.0	2764.7 ***	Smooth term for the single variable replicate (n=3 for nicotine and n=2 for dn-imi)
s(group)	5331.4 ***	126.7 **	Smooth term for the single variable group, which is defined by the treatment groups within one replicate (3 nicotine or 2 dn-imi replicates × 5 treatment groups)

Significance levels: ***$p < 0.001$, **$p < 0.01$, *$p < 0.05$

Table 15: Results of coiling analysis from nicotine and desnitro-imidacloprid treatment.
Estimates predicted from the multivariate model (± SE) for duration (A) and frequency (B) of coiling movements.

B – Duration of coiling behavior

	Treatment	Duration estimate ± SE [a]	Duration (sec) [b]	95% CI [c]
Nicotine	Solvent control	-1.18 ± 0.10	0.31	100
	5 µM	-1.38 ± 0.06 *	0.25	82
	10 µM	-1.56 ± 0.06 **	0.21	68
	20 µM	-1.61 ± 0.06 **	0.20	65
	40 µM	-1.80 ± 0.06 **	0.17	54
Desnitro-Imidacloprid	Solvent control	-1.41 ± 0.04	0.24	100
	12.5 µM	-1.36 ± 0.05	0.26	106
	25 µM	-1.45 ± 0.05	0.22	92
	50 µM	-1.47 ± 0.05	0.23	94
	100 µM	-1.41 ± 0.05	0.24	100

A – Frequency of coiling behavior

	Treatment	Frequency estimate ± SE [a]	Frequency (min⁻¹) [b]	95% CI [c]
Nicotine	Solvent control	2.16 ± 0.17	8.67	100
	5 µM	2.41 ± 0.22	11.18	129
	10 µM	2.16 ± 0.22	8.65	100
	20 µM	1.89 ± 0.22	6.65	77
	40 µM	0.81 ± 0.22 **	2.25	26
Desnitro-Imidacloprid	Solvent control	3.81 ± 0.26	45.28	100
	12.5 µM	3.92 ± 0.07	50.14	111
	25 µM	3.72 ± 0.07	41.38	91
	50 µM	3.65 ± 0.07	38.40	85
	100 µM	3.76 ± 0.07	42.78	95

[a] log-scaled control estimates and corresponding differences to the control values

[b] absolute means calculated from logarithmic estimated values predicted by the model

[c] upper and lower limits of 95% confidence intervals for duration and frequency

[d] SC = solvent control DMSO (0.01 %, v/v)

Significance codes: ***$p < 0.001$, **$p < 0.01$ Tukey *post-hoc* test with Holm *p*-value adjustment
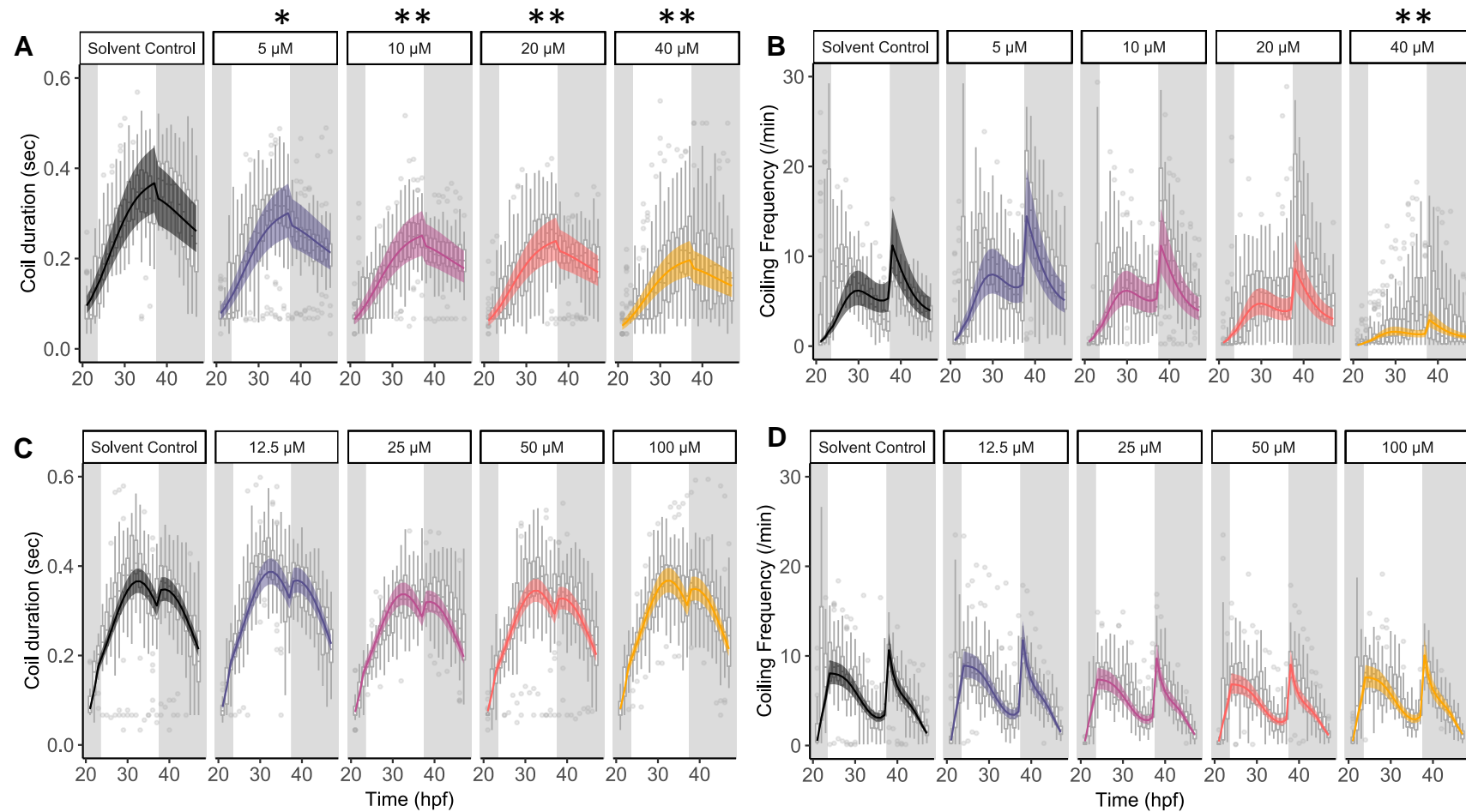
Figure 16: Coiling behavior of embryos exposed to nicotine or desnitro-imidacloprid. Duration and frequency for nicotine (**A, B**) and desnitro-imidacloprid (**C, D**) exposure between 21 and 47 hpf. The curves show the predicted trend over time for these two endpoints and are represented by lines with their confidence intervals. White box plots in the background illustrate the variability of the data. Gray shading indicates dark phases during the experiment. Asterisks * and ** indicate $p < 0.001$ and $p < 0.0001$, respectively, resulting from Tukey´s *post hoc* test with Holm´s *p*-value adjustment. I performed the nicotine and desnitro-imidacloprid experiments in three and two independent replicates, respectively.

5.4 Discussion

In the literature the metabolite of imidacloprid, desnitro-imidacloprid, has shown to have a stronger affinity for the vertebrate nAChR leading to increased toxicity in this taxonomic group (Chao and Casida, 1997, Loser et al., 2021a, Tomizawa, 2004, Tomizawa and Casida, 2003). *In vitro* studies investigated the agonistic potency of this compound and concluded that can be compared to nicotine (Chao and Casida, 1997). The irreversible binding and overactivation may lead to impaired synaptic plasticity and ultimately reduced neuron survival (Tomizawa and Casida, 2002, Wheeler and Cooper, 2004). For this reason, I investigated the potentially higher developmental neurotoxic potential to vertebrates compared to the parent compound using the developing zebrafish.

5.4.1   No severe acute toxicity of desnitro-imidacloprid at detectable levels of the compounds in the organism

To evaluate the acute toxicity of desnitro-imidacloprid in a developing organism, I used the FET test (TG No. 236; OECD, 2013) to determine concentrations where it reveals teratogenic effects. Over the experimental period of 5 days, no severe morphological effects in zebrafish embryos could be detected up to the highest used nominal exposure concentration of 100 µM desnitro-imidacloprid. In addition, no concentration-dependent response was evident and effects where comparable to control. This may be an indication for the concentrations I used for the testing were too low and/or the exposure duration was too short to affect the fish. I did not include higher concentrations, since these would exceed any realistic scenario based on a physiology-based toxicokinetic model which predicts body concentrations in humans (Loser et al., 2021a, Loser et al., 2021b).

When I looked on the parent compound imidacloprid, it neither caused acute teratogenic effects in zebrafish embryos in the same concentration range (von Hellfeld et al., 2022). This result is additionally underlined by the high lethal value (LC_{50}) of 241 mg/l of imidacloprid, which corresponds to ~ 1 mM, reported by Tisler et al. (2009). But pesticide exposure experiments revealed neurotransmitter concentration changes already at a concentration levels were no morphological effects were visible (100 µM; Tufi et al., 2016).

From the measurements of water concentrations before and after the contact with the fish, I could not see a strong degradation or transformation of the substance within 24 h, neither abiotically nor by the fish. The two highest nominal concentrations resulted in the greatest amount of compound in the embryo with 10.49 and 12.21 µM for 50 and 100 µM, respectively. However, I have compared internal to water concentrations and found a peak uptake ratio of 65 % for 25 µM exposures. Since above this treatment only lower internal concentration have been detected, this value could represent a threshold beyond which elimination of desnitro-imidacloprid is initiated or enhanced. I assume limited adsorption via the skin or further transformation into other metabolites where the products escaped target analysis should be additionally considered. Loser and colleagues have shown in *in vitro* experiments that already concentrations over 100 nM triggered signaling responses in human neurons and thereby revealed a two orders of magnitude higher potency than imidacloprid (Loser et al., 2021a).

Compared to other animals, desnitro-imidacloprid was frequently detected in the plasma of birds exposed to imidacloprid, but concentrations were generally short-lived and decreased rapidly within the first six hours after administration of the insecticide (Eng et al., 2021). Increased transformation and excretion rate was also evident in the measurements of human urine samples, where desnitro-imidacloprid concentrations were higher than imidacloprid (Mahai et al., 2022). In fish, however, little is known about the metabolism of imidacloprid, with previous toxicokinetic *ex-vivo* liver and *in vitro*

microsome studies with rainbow trout identified none (Frew et al., 2018) or only one other metabolite (5-hydroxy-imidacloprid) in their experiments (Kolanczyk et al., 2020).

But even in the case that fish are unable to metabolize imidacloprid into desnitro-imidacloprid, there is still a hazard of exposure since this compound is built by bacterial degradation and is also formed in plants (Koshlukova, 2006) which could in turn lead to waterborne or dietary exposure routes. Even though I could not detect severe morphological alterations it is important to investigate possible low but nervous system impacting concentrations.

5.4.2 No developmental neurotoxic potential detected for desnitro-imidacloprid

The first spontaneous lateral contractions of the trunk leading to tail coils, occur after the growth of primary motoneurons from the spinal cord and innervation of the developing myotome muscle cells. Signal transmission follows a simple, electrically as well as glycerin, and non-supraspinal mediated neural circuit (Brustein et al., 2003, Drapeau et al., 2002, Kimmel et al., 1995, Saint-Amant and Drapeau, 1998, Saint-Amant and Drapeau, 2001). Provided that the neurons are correctly connected, the signals are transmitted and the muscles are well-developed, these movements have a stereotypical behavioral pattern with different levels of activity over time. It can therefore serve as a sensitive test to detect even minor changes caused by (developmental) neurotoxic agents (Fritsche et al., 2015, von Hellfeld et al., 2022).

In this coiling behavior assay over a prolonged period of time (21-47 hpf), selected concentrations of desnitro-imidacloprid from 12.5 to 100 µM did not significantly alter the movements. Similarly, no strong effect on the coil behavior was detected for the parent compound imidacloprid (von Hellfeld et al., 2022). In contrast, nicotine exposure significantly reduced the length of the movements in a concentration-dependent fashion and simultaneously demonstrated decreased quantity of coils per minute.

By comparing these two responses, I conclude that desnitro-imidacloprid is not as potent as nicotine to affect neuron-muscle interaction which is important for the coiling movement in the developing zebrafish embryo.

5.4.3 Conclusion

Therefore, I conclude desnitro-imidacloprid unlike nicotine treatment, has not the ability to exhibit severe acute toxicity to the fish embryo even though substance was proven to be accumulated in the organism. Furthermore, despite the sensitive tail coiling behavior test, no significant difference to the control can be detected. This means that in these studies, at least for this complex vertebrate model, I was not able to determine a comparable developmental neurotoxic potency for this metabolite as shown in *in vitro* studies.

6   DIMETHYL SULFOXIDE – BRIEF OUTLINE OF THE USE OF THE SOLVENT DMSO IN COILING BEHAVIOR EXPERIMENTS

In this chapter, I reuse the data from chapter 4 and 5 where the contribution is stated accordingly. The analysis of the coiling activities of negative and solvent control was done in cooperation with Dr. Raoul Wolf. All joint work is additionally marked with footnotes. If not stated otherwise, content was created by me. More information and an overview of the contribution of the authors can be found in chapter 9.1.

6.1   Background

Solvents are essential if a poorly water-soluble substance has to be added to water as a test substance and a concentration above the solubility limit is selected. One widely used organic solvent is dimethyl sulfoxide (DMSO). In zebrafish embryos, DMSO is a commonly used solvent since it is not known to have lethal or developmental adverse impacts even at high concentrations (> 2 % (v/v); Hallare et al., 2006). But on the other hand, concentration levels which are accepted and used in biological assays implemented in the OECD test guidelines (≥ 0.01 %; OECD, 2013) induce heat shock proteins, which indicates an increased amount of misfolded proteins and thus indicating proteotoxic potential of this solvent (Hallare et al., 2006). Additionally, in combination with teratogenic agents like *e.g.*, methylmercury chloride, it can potentiate the lethal impacts on frog embryos (Rayburn et al., 1991). This means that if we focus on highly sensitive endpoints which also includes gene expression (Turner et al., 2012), solvents should be excluded as much as possible from the experimental exposure. Since the main focus of this work is the embryonic behavior of zebrafish, the question arises whether this is also relevant for the behavior.

Effects of DMSO on the locomotion behavior of 4 to 6 d old zebrafish embryos have been studied and lowest observed effect concentrations (LOECs) laid between 0.55 % (Christou et al., 2020) to 0.1 % (Chen et al., 2011, Huang et al., 2018). It has to be mentioned that the responses of the embryos were not uniform and showed hypo- and hypolocomotion. This variability might be explained by different age or strain of the embryos (de Esch et al., 2012). The impact of the solvent on the early tail coiling behavior has led to a non-dose-response conform lowering of burst activity (Huang et al., 2018).

In this chapter, I further investigate the impact of nicotine on the coiling behavior. However, I rather focused here on the role of the solvent DMSO. I have not performed additional experiments for this section. The original data are taken from the experiments which can be found in 4.3.1 and 5.3.3

6.2   Materials & methods

I comprehensively described the coiling assay in chapter 1 and I introduced the analysis approach with GAM in the chapter 4.2.4.. Here in this chapter, I used data from chapter 4 and 5 for further investigation with the focus on the solvent DMSO. All these materials and methods are part of the study discussed here.

6.3   Results & Discussion

In this section I want to illustrate the effects of the nicotine treatment solely and in combination with DMSO. In the following, I refer to the different experiments, the nicotine experiments with and without DMSO (4.3.1 and 5.3.3), as nicotine-water and nicotine-DMSO treatment, respectively, in order to better separate the terms.

6.3.1   Replicates are more variable than the effect of DMSO itself

The literature and my experiments indicate that DMSO is not enhancing the acute toxicity for zebrafish embryos in their embryonic developmental at the concentrations of < 1 % (Christou et al., 2020, Huang et al., 2018, von Hellfeld et al., 2022). Due to its low toxicity and its important properties to dissolve lipophilic compounds, it is sometimes used in higher concentrations as recommended by the OECD guidance document (OECD, 2000). However, sublethal alterations in behavior of zebrafish embryos are already visible in lower concentrations.

To investigate the impact of the solvent on the coiling behavior, we[3] have extracted and compared the negative control (NC), containing only artificial water, with the solvent control (SC), which contained 0.1 % DMSO (v/v), of the nicotine-water and nicotine-DMSO experiments. To this end, I plotted the coiling duration and frequency in Figure 17 A and B and depicted all replicates of the NC and the SC beside each other. With the chosen GAM approach which we[3] used for both nicotine treatment experiments before, we[3] could capture 54.4 % of the deviance of raw data for NC and SC together to the predicted model (3068 data points in total). We[3] could not detect a difference in the behavior between NC and SC, and I have to note that the data was highly variable. It was most obvious – and also visible in Figure 17 – that the replicates themselves have had the most influence on the outcome for both treatment groups.

Differences in behavior for older embryos (> 4 dpf) caused by DMSO was first detected with concentrations over 0.1 % (Chen et al., 2011, Christou et al., 2020, Huang et al., 2018). Comparing these findings with my results, I conclude that DMSO itself is also not affecting the coiling behavior of zebrafish embryos (> 21 hpf) at the given concentration of 0.1 %.
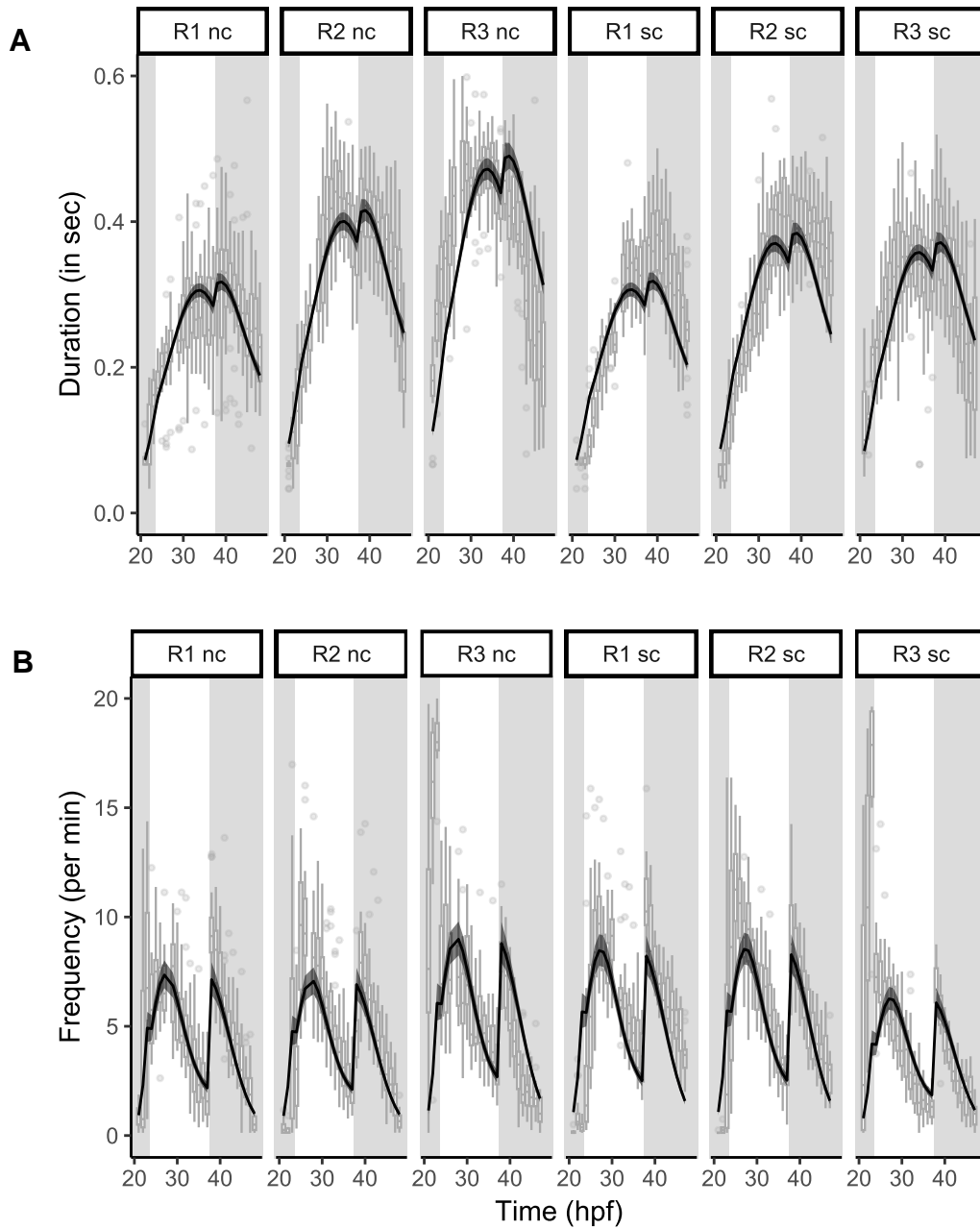
Figure 17: Comparison coiling behavior over time of negative and solvent control. For all replicates beside each other, coil duration (A) and coil frequency (B) of negative control (nc) and solvent control (sc) are represented with their fitted models as black lines and their confidence intervals (95% CI) over time (hpf). The small white box plots in the background represent the raw data. Gray shading indicates dark phases during the experiment.

Table 16: Impact of DMSO in combination with nicotine on duration and frequency of coiling behavior in zebrafish (*Danio rerio*) embryos. Outcomes of nicotine treatment without (A and C; n=3) and with the solvent DMSO (B and C; n=3) are listed beside each other. Duration and frequency values were obtained from the bivariate GAM analysis relative to negative controls (%).

A	Duration (sec)	% of control	B	Duration (sec)	% of control
NC	0.28	100.0	SC	0.31	100.0
5 µM	0.27	94.1	5 µM	0.25	80.6
10 µM	0.22	77.3	10 µM	0.21	67.7
20 µM	0.22	76.3	20 µM	0.20	64.5
40 µM	0.19	68.8	40 µM	0.17	54.8

C	Frequency (min^{-1})	% of control	D	Frequency (min^{-1})	% of control
NC	8.81	100.0	SC	8.67	100.0
5 µM	14.27	161.9	5 µM	11.18	129.0
10 µM	12.48	141.6	10 µM	8.65	99.8
20 µM	11.60	131.7	20 µM	6.65	76.7
40 µM	8.23	93.4	40 µM	2.25	26.0

6.3.2 DMSO enhanced the sublethal toxicity of nicotine

For the comparison of the impact of nicotine alone (nicotine-water) and im combination with the solvent (nicotine-DMSO), I summarized both experimental blocks in the Table 16. A comprehensive discussion for the separate experiments can be found under the sections 4.3.1 and 5.3.3. When first focusing on the duration, we[3] have found a monotonic decrease for both, with and without DMSO. In the case of the nicotine-DMSO, the reduction was more pronounced and ended at the highest exposure concentration of 40 µM with a relative reduction in movement duration of more than 45 %, while 40 µM in nicotine-water experiments showed a reduction of about 31 %. For frequency, the trends of nicotine-water and nicotine-DMSO experiment differed from each other: While the nicotine-water exposure initially led to an increase and only at the highest concentration to a decrease in coils per min, only the lowest concentration of 5 µM nicotine-DMSO led to a hyperactive count. All other concentrations had a strongly decreasing effect on the number of coils, with 26 % of the original remaining at the end. I assume that this inhibition of movements is a shift towards higher toxicity. It could be explained by a higher bioavailability of nicotine, since DMSO alters the permeability of biological membranes, as demonstrated in experiments by Kais et al. (2013).

6.3.3 Conclusion

In my observations of the coiling behavior between negative and solvent control of the different experiments, we[3] could not detect any obvious impact of DMSO in duration of the movement nor the frequency within the experimental period between 21 to 47 hpf. This could be due to the low concentrations (0.1 %) or the rather short exposure time. Nevertheless, the clearest difference in behavior can be attributed to the separate biological replicates, regardless of which control group (NC and SC) the fish embryos belonged to. However, it must be noted that the solvent in combination with toxic substances can enhance adverse effects. In my comparative experiments with nicotine, for instance, we[3] observed an increasing reduction in coil activity for the nicotine-DMSO treated embryos which exceeds the effect of nicotine-water experiments.

Going back to the question of whether DMSO is a suitable solvent for behavioral experiments with zebrafish embryos: DMSO should be excluded as far as possible from the experiments, as it can increase the toxicity of substances even at low concentrations of 0.1%. If it is nevertheless needed, concentrations of ≤ 0.01 % should be considered, as this level has been shown to have no further effects on the permeability of the zebrafish embryo chorion (Kais et al., 2013).

64

7 THE IMPACT OF ANTIDEPRESSANTS ON ZEBRAFISH EMBRYOS

In this chapter, I was supported by the Bachelor students Tim Freitag, Mona Wiesenberger, Katharina Zorko and Sophie Trender, who helped me to generate parts of the behavioral data in 7.3.2 and 7.3.3. Also here, I used the before introduced modeling approach for the coiling analysis which was implemented in cooperation with Dr. Raoul Wolf (see section 4.2.4.) All joint work is additionally marked with footnotes. If not stated otherwise, content was created by me. More information and an overview of the contribution of the authors can be found in chapter 9.1.

The content of this chapter is going to be part of a manuscript. All planned publications can be found in chapter 9.2.

7.1 Background

Depression is one of the most common mental disorders in humans, which is predominantly genetically predisposed, but can also be induced by environmental factors (Kou et al., 2022) or also be associated with certain diseases (Liu et al., 2020). According to Liu et al. (2020), the number of depressive disorders globally increased by almost 50 % between 1990 and 2017. The World Health Organization (WHO) states that depression could be the major burden of disease worldwide by 2030 (WHO, 2008). Treatment options include electroconvulsive therapy and psychotherapy such as cognitive behavioral therapy or pharmaceutical products. Most of the commonly prescribed psychotropic medications work by inhibiting the corresponding neurotransmitter transporters, receptors or enzymes of the system. The main antidepressants on the market are from the class of serotonin reuptake inhibitors (SSRIs) including fluoxetine (Prozac®) paroxetine (Paxil®) and sertraline (Zoloft®) and serotonin–norepinephrine reuptake inhibitors (SNRIs) such as venlafaxine (Gould et al., 2021).

The serotonin (5-hydroxytrptamine, 5-HT) system is involved in various physiological functions such as sleep, fear, aggression, food intake, memory as well as in the reward system and pain. Moreover, it is regulating important steps in brain development and plasticity, neurogenesis, differentiation and regeneration of neurons (Barreiro-Iglesias et al., 2015, Côté et al., 2007, Fricker et al., 2005, Gaspar et al., 2003, Lillesaar, 2011, Whitakerazmitia, 1991). Serotonin is based on the essential amino acid L-tryptophan. After release into the synaptic cleft, it binds to a G-protein coupled receptors, the serotonin receptors (HTRs). Finally, serotonin is re-transferred by transporters (serotonin transporter, SERT) back into the pre-synapse. Dopamine and norepinephrine are catecholamines and neurotransmitters which are also important neuromodulators. Tyrosine hydroxylase (TH) is the first enzyme of the catecholamine biosynthesis. It converts the amino acid tyrosine into dopamine via various enzymatic steps. Other catecholamines such as noradrenaline (also called norepinephrine) are formed from dopamine. All three neurotransmitters, serotonin, dopamine and noradrenaline have key roles in rewarding system and mood but also in locomotion (Sharples et al., 2014, Whelan et al., 2000).

SSRIs and SNRIs treatment influence the neurotransmitter concentration in the synaptic cleft by actively inhibiting reuptake by the SERT. At higher concentrations, SNRIs not only reduce the reuptake of serotonin and norepinephrine, but also impair the uptake of dopamine to a lesser extent. In humans, these pharmaceuticals are metabolized in the liver mainly by the cytochrome P450 (CYP) 2B6 and CYP2D6 enzymes (Crewe et al., 2004, Obach et al., 2005). The main metabolites of sertraline are

dimethylsertraline and norsertraline. The parent compound is excreted in the urine at a rate of less than 0.2 %, whereas 12 - 14 % is excreted in the feces (Nowakowska et al., 2020). Paroxetine has a high absorption rate with almost 98 %. Its metabolites are inactive and the half-life of the compound to be eliminated from the body is 24 h with 64 % being excreted through urine (Kowalska et al., 2021, Tang and Helmeste, 2008). In the case of venlafaxine, its metabolite, O-desmethylvenlafaxine, is also an active inhibitor. The elimination rate of the parent compound is between 5 and 11 h with the largest amount being excreted in the urine (1-10 % unchanged substance) and only 2 % is excreted in the feces (Dean, 2012).

Due to insufficient removal of these compounds by wastewater treatment, drugs such as antidepressants end up in streams, rivers and other bodies of water (Gould et al., 2021, Mezzelani et al., 2018, Wilkinson et al., 2022). In effluents, we are dealing with a quantity of antidepressants in ng/L to even low µg/L range (Mole and Brooks, 2019, Shaliutina-Kolešová et al., 2020). One exceptionally high concentrations of sertraline with 17.1 µg/L was found at a discharge point of wastewater from a psychiatric hospital in Denmark (Styrishave et al., 2011). In river water samples of Czech Republic, however, sertraline amounts were much lower with levels between 3 to 8.5 ng/L (Grabicová et al., 2020). Environmental concentrations of paroxetine ranged between highly polluted effluents at a manufacturing site in Canada with 3.4 µg/L (Kleywegt et al., 2019), and 10 ng/L in European rivers (Grabicová et al., 2020). For venlafaxine, a global review of pharmaceutical pollution of rivers worldwide by Wilkinson et al. (2022) summarized 71.9 and even 110 ng/L in European and North American rivers, respectively. Even more reported a review from 2018 with highest concentrations in effluents in Minnesota with 2.19 µg/L (Sehonova et al., 2018).

Antidepressants can accumulate in tissue samples of freshwater fish from polluted areas and ranged between 11 ng/g in muscle and a maximum concentration of 545 ng/g (wet weight) in liver for sertraline (Ramirez et al., 2009). Brooks et al. (2005) similarly found highest concentrations in liver but also in brain samples of three different fish species (*Lepomis macrochirus, Ictalurus punctatus, Pomoxis nigromaculatus*). Paroxetine concentrations, instead, were only measured below 1 ng/g (wet weight) in gizzard shad (*Dorosoma cepedianum*) and brown bullhead (*Ameiurus nebulosus*) in Hamilton Harbor in Canada (Chu and Metcalfe, 2007). Likewise were the outcomes from a long term mesocosm experiment with 1:4 effluent content where paroxetine levels of 0.35 ng/g and venlafaxine with 0.69 ng/g in liver tissue were detected (Lajeunesse et al., 2011).

The rather low concentrations of paroxetine and venlafaxine is also reflected in their bioconcentration factors (BCFs) with 290 (Nowakowska et al., 2020) and 18 L/kg (Lajeunesse et al., 2011), respectively. These values are not considered as a critical accumulation rate according to the threshold of concern for persistent, bioaccumulative and toxic substances (PBT) in the European Union (BCF >2000 L/kg, ECHA, 2017). In contrast, the calculated BCF in zebrafish embryos for sertraline were as high as 2280 L/kg and therefore show a realistic risk for increased accumulation in biota (Nowakowska et al., 2020). Although these pharmaceuticals are not seen as persistent chemicals, the constant import into water ways lead to a so-called "pseudopersistence" (Daughton, 2002).

As a consequence of the highly conserved nervous and neurotransmitter system across vertebrate classes, fish as a non-target can be impacted by water contamination of antidepressants (McDonald, 2017, Sehonova et al., 2019, Wang et al., 2023). And even though, the mostly rather low concentrations found in the aquatic environment are not considered acute toxic to fish, lower levels of antidepressant exposure haven been connected to increased stress markers, behavior changes as well as reduced reproductive success (Carty et al., 2017, Melnyk-Lamont et al., 2014, Yang et al., 2021). In connection with the "pseudopersistent" characteristic and the increasing trend of annual prescription, there is relevant need to examine the toxicity of the most commonly used antidepressants to fish.

Thus, the objective of my study was first the investigation of the acute toxic profile of the two SSRIs paroxetine and sertraline. Subsequently, low and non-acute toxic concentrations of both substances and additionally venlafaxine (SNRI) were selected to examine two different early behaviors of zebrafish embryos, namely the tail coiling behavior and the visual motor-response. These highly sensitive assays are used to evaluate the impact during development at concentrations which are close to environmentally relevant concentrations.

7.2 Materials & Methods

I comprehensively described the fish maintenance, the FET test as well as the coiling assay in chapter 1. These materials and methods are part of the study discussed here.

7.2.1 Test chemicals

As listed in Table 2, I chose acute exposure concentrations of sertraline with 0.1, 1, 10, 100, 1 000, 5 000, 10 000 µg/L (0.1 % DMSO) and for paroxetine with 0.625, 1.25, 2.5, 5, 10, 20 mg/L. The subsequent conducted behavioral assays, tail coiling assay and VMR, were performed with a final non-acute concentration of 0.01, 0.1, 1, 10, 10 µg/L (0.01 % DMSO) for sertraline, 100, 1 000, 10 000, 25 000 µg/L for venlafaxine. For paroxetine, two experimental runs for the coiling were performed with first 10, 100, 1 000, 2 000 µg/L and the second run with 0.01, 0.1, 1, 10 µg/L exposure concentration to fully describe the range in detail. The VMR assay was performed with 0.1, 1, 10, 100, 1 000 µg/L.

7.2.2 Visual motor response

Prior to the assay, we[1] pre-saturated a 96-well plate (TPP, Trasadingen, Switzerland) with exposure solutions (Tab. 2) for at least 24 hours. For this assay, we[5] raised the embryos in 50 ml exposure solution, which was renewed daily with a minimum water exchange of 90 %. On day four at 105 hpf, we[1] transferred the hatched embryos to the saturated plate with fresh solutions. Then, we[1] moved the plate with the embryos to the observation chamber (DanioVision) at least 1 hour before recording started (107-109 hpf). I adjusted the camera settings in Pylon Viewer (Basler AG, Ahrensburg, Germany) with a resolution of 1280 x 960 and a frame rate of 25 fps (mpeg 4). In the EthoVision XT16 (Noldus) software, for the detection settings the method differencing was chosen with "center-point-detection". Visual detection in the dark was enabled through an infrared-filtered lens (Kowa LM12JC1MS F1.4 f12 mm). The chosen endpoint for analyzing the swimming activity was "total distance moved". Details for used devices can be found in Table 17. Additional information for settings is included in Appendix C, Table C1.

Table 17: Listed devices for the visual motor response assay

Device	Specification	Supplier
Camera	acA1300-60 gm camera	Basler, Ahrensburg, Germany
Lens	Kowa LM12JC1MS F1.4 f12 mm	Basler, Ahrensburg, Germany
Filter	RG850	Heliopan, Gräfelfing, Germany
Observation chamber	DanioVision	Noldus, Wageningen, Netherlands
Detection software	EthoVision XT16	Noldus, Wageningen, Netherlands
Camera software	Pylon viewer	Basler, Ahrensburg, Germany

To visualize the swimming activity of the embryos, I used the open-source statistical software R (version 4.1.2, R Core Team, 2021). In addition, I used the package *dunn.test* (version 1.3.5., Dinno, 2015) for Krukal-Wallis and Dunn´s test with *post hoc p*-value adjustment (Holm) to analyze the differences between the treatment groups and the control separately for each replicate by mean of sum of total distance moved in the dark phases. I created the figures and plots by using the package *ggplot2* (version 3.3.6, Wickham, 2016).

7.3 Results

7.3.1 Fish Embryo Acute Toxicity

I considered all three replicates of the acute exposure to paroxetine and sertraline as valid since mortality in the control groups stayed below 10 % over the entire experimental period up to 120 hpf. Both concentration-response curves of sublethal and lethal effects, is illustrated in Figure 18.

Paroxetine treatment

For paroxetine, we[1] could not detect any differences in the development of embryos in the eggs in the first 48 h compared to the negative control, even at the highest concentration of 20 mg/L (Fig. 19A, B). At 72 hpf, we[1] could find the first morphological effects, most serious with the highest exposure. All affected embryos showed degradation of the caudal fin, which was evident in the early stages by a condensation of the tissue and always started at the tip of the caudal fin. Some embryos already showed extensive degradation of the caudal and dorsal fin at 72 hpf (Figure 19C). We[1] also observed a small number showing spinal curvature, reduced or absent blood flow and reduced heartbeat. Seldomly, there were deformed yolk sac or pericardial oedemata. At 96 hpf, all of the 20 mg/L treated embryos were affected. The effects included an initial or partly complete degradation of the fin seam, pericardial edema, sporadic yolk sac edema or deformities, a strongly reduced or absent blood flow and a strongly reduced, slow heartbeat. With 10 mg/L paroxetine, the most common effect we[1] found was caudal fin tip degradation. Rarer were pericardial edema, deformations of the yolk sac and a curvature of the spine as well as deformation of head, jaw, head, or eyes (Fig. 19D). At 120 hpf, 100 % of my 20 mg/L treated embryos were coagulated. At 10 mg/L, I calculated 65 % lethal and 100 % sublethal effects, including degradation of the fin seam, pericardial oedemata, incompletely consumed yolk sac (Fig. 19E), reduced or absent blood flow and reduced heartbeat. The pH values of the paroxetine exposure solutions ranged from 7.75 to 8.13 (± 0.02) from low to high concentrations.

Sertraline treatment

As early as 48 hpf, we[1] observed 100 % lethal coagulation when treated with ≥ 5 mg/L sertraline (Fig. 19F) whereas no morphological effects were apparent at the lower concentrations at 24 hpf. We[1] could see initial sublethal effects at 48 hpf, most commonly pericardial oedema, enlarged hearts, and poor cardiac contraction and blood circulation (Fig. 19G). After 72 hpf, some individuals recovered from mild cardiac effects, whereas in others the effects became more severe. At this point, we[1] first noticed the onset of fin seam degradation in 1,000 µg/L exposed fish. Over time, this effect became more pronounced and was also visible at the lower treatments at 96 hpf(Fig. 19I). On the last day, at 120 hpf, all sertraline exposed embryos were affected. Again, we[1] observed the inability to maintain an upright position which as well seen in the paroxetine experiments. At the highest concentration of 1,000 µg/L, this was observed in almost all individuals. Even at only 0.1 µg/L, this effect occurred in more than 10 % of the embryos. We[1] also noticed jaw, yolk sac and spine deformities (Fig. 19I, J). In addition, we[1] could already see signs for a retardation of body growth of the embryos with increasing sertraline concentration during the experimental documentation. By measuring the total body length from the head to the last pigmented spot of the tail at 120 hpf, I calculated a significant decrease in body length at 100 and 1000 µg/L compared to the solvent control based on statistical analysis for all three replicates (Fig. 20). Finally, we[1] measured the pH for all exposure solutions which ranged from 7.75 to 7.88 (± 0.02) for sertraline.

The experiments for the FET test with the antidepressant venlafaxine had already been completed in the working group[5]; I used the data as a baseline to estimate non-acute toxic concentrations to plan the next experiments, namely the coiling and visual-motor response experiments.
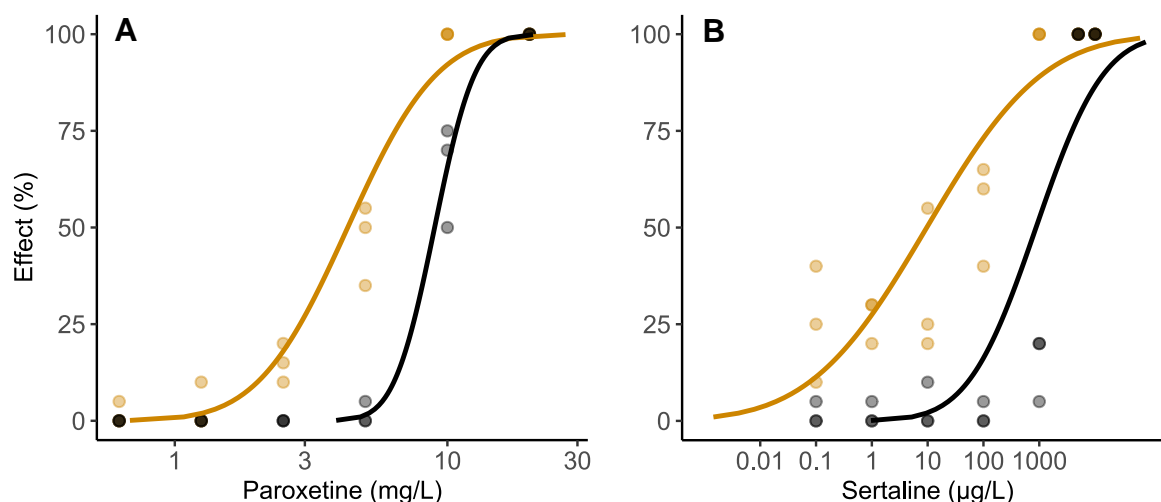
Figure 18: Acute toxicity of paroxetine and sertraline to zebrafish embryos . The semi-logarithmic plots display the sublethal (orange) and lethal (black) concentration-response relationship of the teratogenic effects of paroxetine (A) in mg/L and sertraline (B) in µg/L in zebrafish embryos at 120 hpf. Data points represent different replicates. Curves were fitted using maximum likelihood linear probit regression.

---

[5] Acute toxicity data for venlafaxine FET experiments conducted by Saskia Hagstotz, Lea Dober and Katharina Brotzmann
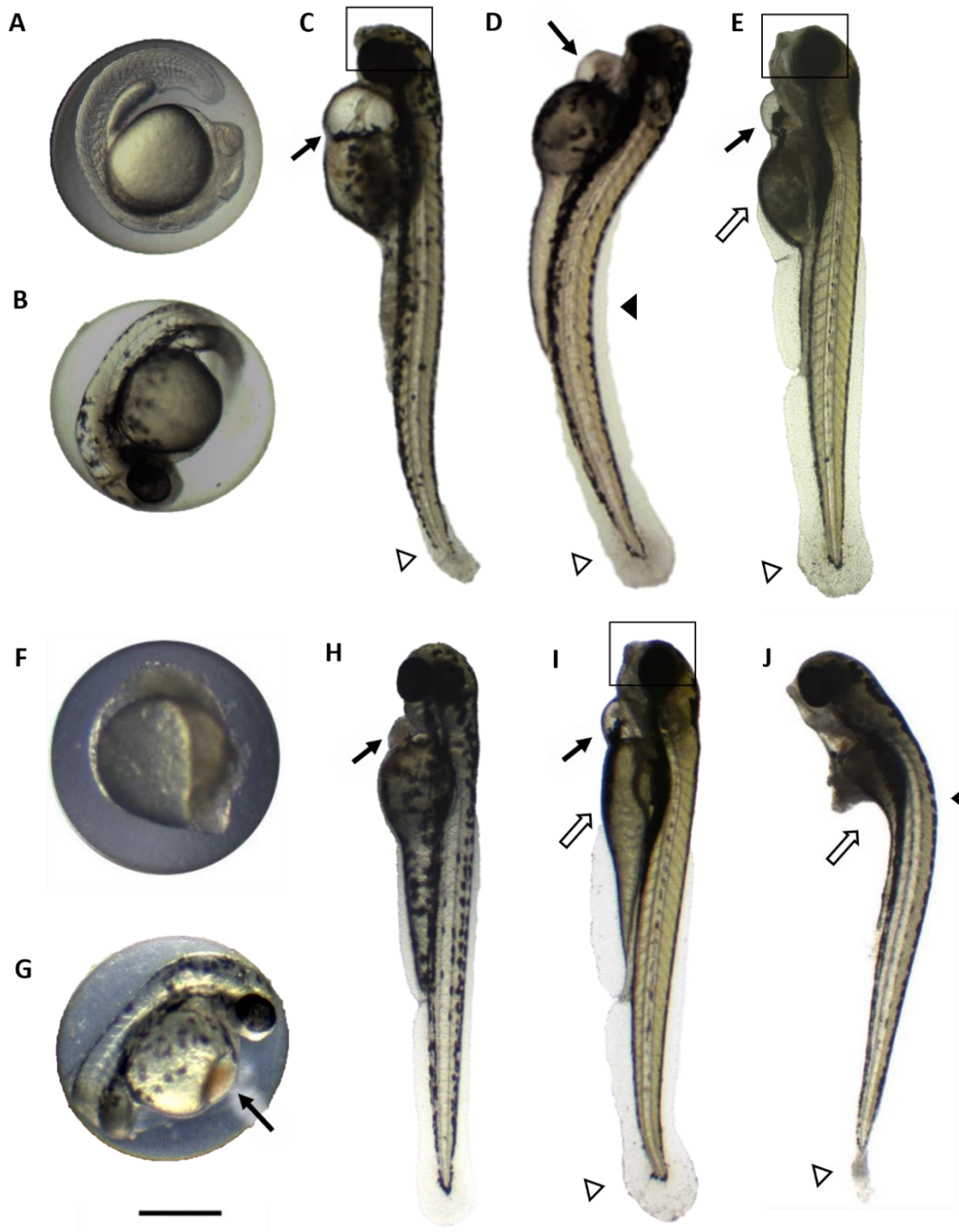
Figure 19: Morphological alterations caused by antidepressants. Shown is a selection of adverse lethal and sublethal effects that can be induced by paroxetine (A-E) and sertraline (F-J) during zebrafish embryo development at different concentrations and time points. Paroxetine treatment of 20 mg/L (A, B, C) is shown at 24, 48, and 72 hpf respectively, and 10 mg/L (D) at 96 hpf, and 1 mg/L (E) at 120 hpf. Sertraline treatment included 10 mg/L (F) at 24 hpf and 10 µg/L (G) at 48 hpf. The embryos at time 72 hpf (H), at 120 hpf (I and J) were all treated with 1 mg/L. Adverse effects are marked with different indicators: pericardial edema (black arrows), yolk sac deformation (white arrow), dorsal deformation (black arrowheads), and caudal fin seam degradation (white arrowheads). Black boxes around the heads illustrate jaw deformation. The black bar corresponds to 500 µm. Microscopic

images were taken by Katharina Zorko and Mona Wiesenberger for sertraline and paroxetine, respectively.
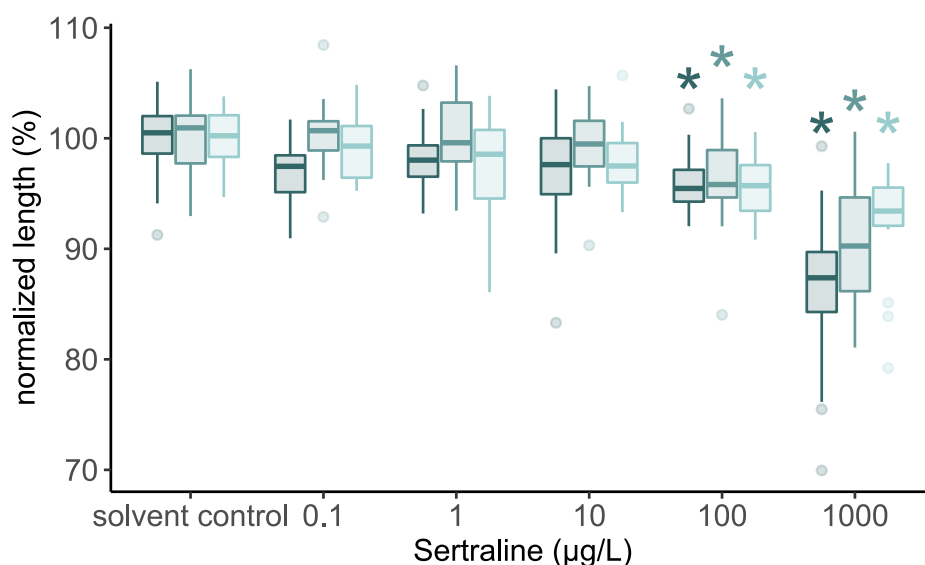
Figure 20: Body length of sertraline-exposed zebrafish embryos (5dpf). Graph shows the snout-to-tip length of three replicates (different colors) normalized to their respective control group. Boxplots illustrate median, 1st and 3rd quartile as well as upper and lower whiskers. Asterisk (*) indicates a $p < 0.05$ (Kruskal-Wallis-Dunn´s test with Holm´s p-value adjustment).

Table 18: Effective and lethal concentrations of the FET test of 10, 20 and 50 % at 96 and 120 hpf after exposure to antidepressants.

Time point		Paroxetine (mg/L)	Sertraline (µg/L)	Venlafaxine (mg/L) [a]
96 hpf	EC_{10}	4.4	0.3	0.3
	EC_{20}	5.7	2.1	2.2
	EC_{50}	9.5	118.7	205.4
	LC_{10}	11.1	172.1	402.9
	LC_{20}	13.1	345.1	537.4
	LC_{50}	17.7	1305.9	932.7
120 hpf	EC_{10}	**2.0**	**0.1**	**1.1**
	EC_{20}	2.6	0.4	7.2
	EC_{50}	3.5	9.6	281.8
	LC_{10}	6.4	51.9	379.4
	LC_{20}	7.1	136.9	482.2
	LC_{50}	9.0	875.1	762.8

[a] The data for the ECs and LCs were provided by Lea Dober and Saskia Hagstotz, respectively, under the supervision of Katharina Brotzmann.

Looking on the effective and lethal concentrations (Tab. 18), the experiments revealed that sertraline has the highest toxicity, followed by paroxetine and venlafaxine (Fig. 21). The steep effect-concentration curve of paroxetine compared to the other two substances is quite narrow (EC_{10}=2 mg/L and EC_{50}=3.5mg/L). On the other hand, venlafaxine, on the other hand, exhibited a flat and slowly increasing curve as a result displayed a wide range from EC_{10} of 1.1 mg/L and EC_{50} of 281.8 mg/L.
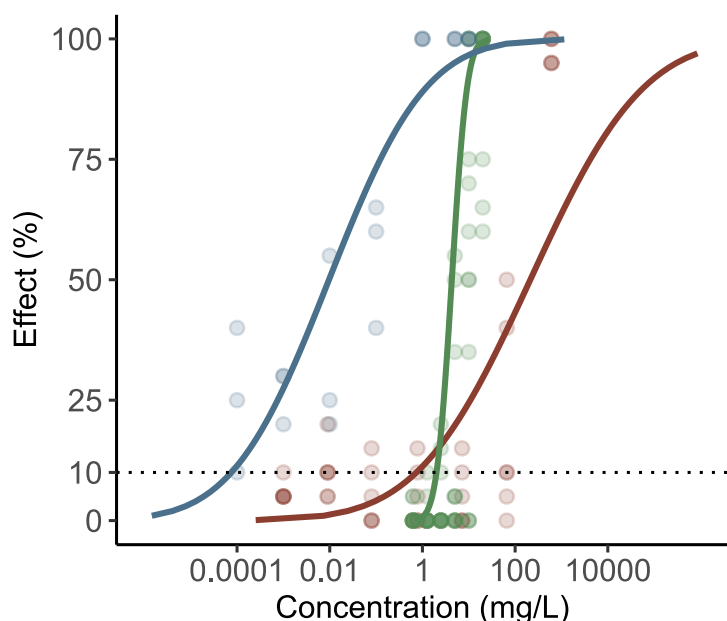
Figure 21: Fish embryo acute toxicity of the antidepressants. In this semi-logarithmic plot, the concentration-response curves of the sublethal effect of sertraline (blue), paroxetine (green), and venlafaxine (red) are shown in mg/L. The data points represent three different replicates. The dashed line indicates the effective concentration at which 10% of embryos are affected by the respective compound. Curves were fitted with probit linear maximum-likelihood regression.

.

7.3.2 Influence of antidepressants on the coiling behavior of zebrafish embryos

To reduce morphological malformation and with this the associated unspecific influences on behavior, I selected test concentrations for the behavioral assays which were adjusted around the EC_{10} value of the FET (Ogungbemi et al., 2019). An EC_{10} was first estimated for venlafaxine from previous experiments (unpublished data from our working group). Due to missing FET test results in the lower concentration ranges, a wide range of concentrations was included in the tests, namely 100 - 25, 000 µg/L. Later, an EC_{10} of 1,100 µg/L was determined and was thus within the tested concentration range (unpublished FET data from the working group). The concentrations I selected for sertraline were the lowest and was besides the FET data (EC_{10} = 0.1 µg/L) additionally based on previously publish behavior results (Chiffre et al., 2016, Faria et al., 2022, Nowakowska et al., 2020, Suryanto et al., 2021). Therefore, ranged from 0.01 - 10 µg/L. Since paroxetine treatment in our[1] experiments revealed an especially narrow effective concentration-response curve, instead of using only four treatment groups, three additional concentrations were included from 0.1 - 2,000 µg/L.

For all three substances, the light phases had an influential impact on the activity. Like in the other behavioral assays I analyzed with the GAM approach, also here revealed the single replicates a high variability and thus had a great influence on the outcome for both endpoints, frequency and duration (Tab.19). Separate replicates are illustrated in Appendix C, Figure C1-3.

Looking at the treatment effects of the antidepressants, I could not detect significant changes in the frequency of the movements for sertraline nor for venlafaxine compared with their control over the

course of time (21 - 47 hpf). At the highest exposure concentrations of sertraline (10 µg/L) and venlafaxine (25,000 µg/L) I could only detect a minor reduction of 10 % and 12 %, respectively, which was still in the range of the confidence range of the controls (Tab. 20).

In contrast, I have seen a biphasic response pattern for the frequency in the paroxetine experiments. For the exposures of 0.01 and 0.1 µg/L, activity stepwise increased and reached its peak which was about 123 % of control activity level. With further increasing concentrations, the frequency of coils decreased again and reached control levels with 100 µg/L treatment. With the two highest concentrations (1,000 and 2,000 mg/L), a reduction of coils per minutes occurred, most severely at 2,000 µg/L.

However, duration of the coiling movements revealed a much stronger response pattern compared to frequency. With this endpoint, I could also detect significant reductions of coil duration for sertraline and venlafaxine treatment. For paroxetine, I observed the same response pattern for duration as for frequency. Here, the prolonged or higher duration was not too pronounced, reaching only 106 % at 1 and 10 µg/L, but in contrast, duration was already 15% shorter at 100 µg/L compared with the control. It is noticeable that the same concentrations at which a shorter movement duration occurred were also the concentrations that I calculated as EC10 from the FET test (Tab. 18).

Table 19: Importance of smooth terms in the model for the coiling analysis of the three antidepressants.(A) Indicates the smooth terms of the endpoint duration and (B) for frequency. Chi-squared value (X^2) indicates the strength of the impact of this parameter on the model.

A - Duration	PAR	SER	VEN	
Smooth term	X^2	X^2	X^2	comments
te(time):phase1	1939.3 ***	920.9 ***	1612.0 ***	Tensor product smooth, interaction between the time and the first dark phase (21-23 hpf)
te(time):phase2	4687.1 ***	2605.5 ***	9684.1 ***	Tensor product smooth, interaction between the time and the first light phase (24-37 hpf)
te(time):phase3	5112.18 ***	1980.7 ***	1048.1 ***	Tensor product smooth, interaction between the time and the second dark phase (38-47 hpf)
s(replicate)	2673.0 ***	346.8 ***	8719.1 ***	Smooth term for the single variable replicate
s(group)	70.1	20.0	269.0 *	Smooth term for the single variable group, which is defined by the treatment groups within the replicates
B - Frequency	PAR	SER	VEN	
Smooth term	X^2	X^2	X^2	comments
te(time):phase1	5406.1 ***	1415.9 ***	1361.9 ***	Tensor product smooth, interaction between the time and the first dark phase (21-23 hpf)
te(time):phase2	4926.7 ***	1523.4 ***	818.0 ***	Tensor product smooth, interaction between the time and the first light phase (24-37 hpf)
te(time):phase3	11673.2 ***	5658.7 ***	4305.0 ***	Tensor product smooth, interaction between the time and the second dark phase (38-47 hpf)
s(replicate)	2733.1 ***	417.2 ***	1.0	Smooth term for the single variable replicate
s(group)	279.5	10.8	442.2 *	Smooth term for the single variable group, which is defined by the treatment groups within one replicate

Significance levels: ***p < 0.001, **p < 0.01, *p< 0.05

Table 20: Coiling behavior affected by antidepressants. The table provides estimate values (± SE) from the model and their resulting duration (A) and frequency (B) with 95 % confidence intervals and the activity levels compared to the control groups (%).

A – Duration of coiling behavior

	Concentration (µg/L)	Duration estimate ± SE [a]	Duration (sec) [b]	95% CI [c]	Activity level (%)
Paroxetine	control	-1.14 ± 0.03	0.32	0.31; 0.33	100
	0.01	-1.12 ± 0.02	0.33	0.32; 0.33	102
	0.1	-1.09 ± 0.02	0.34	0.33; 0.34	105
	1	-1.08 ± 0.02	0.34	0.33; 0.34	106
	10	-1.09 ± 0.01	0.34	0.33; 0.34	106
	100	-1.31 ± 0.02	0.27	0.27; 0.28	85
	1,000	-1.25 ± 0.02	0.29	0.28; 0.29	90
	2,000	-1.26 ± 0.02	0.28	0.28; 0.29	89
Sertraline	solvent control	-0.77 ± 0.06	0.46	0.44; 0.49	100
	0.01	-0.78 ± 0.01	0.46	0.45; 0.46	99
	0.1	-0.89 ± 0.01	0.41	0.40; 0.42	88
	1	-0.83 ± 0.01	0.43	0.43; 0.44	94
	10	-0.80 ± 0.01	0.45	0.44; 0.46	97
Venlafaxine	control	-0.67 ± 0.08	0.51	0.47; 0.55	100
	100	-0.70 ± 0.03	0.49	0.48; 0.51	97
	1,000	-0.90 ± 0.03	0.41	0.40; 0.42	80
	10,000	-0.83 ± 0.03	0.44	0.43; 0.45	86
	25,000	-0.80 ± 0.03	0.45	0.44, 0.46	88

B – Frequency of coiling behavior

	Concentration (µg/L)	Frequency estimate ± SE [a]	Frequency (min⁻¹) [b]	95% CI [c]	Activity level (%)
Paroxetine	control	1.33 ± 0.05	3.77	3.59; 3.95	100
	0.01	1.48 ± 0.06	4.41	4.17; 4.66	117
	0.1	1.53 ± 0.06	4.63	4.38; 4.89	123
	1	1.46 ± 0.06	4.31	4.08; 4.56	114
	10	1.43 ± 0.04	4.18	4.00; 4.36	111
	100	1.33 ± 0.06	3.77	3.57; 3.98	100
	1,000	1.15 ± 0.06	3.15	3.00; 3.32	84
	2,000	1.02 ± 0.06	2.76	2.61; 2.92	73
Sertraline	solvent control	1.22 ± 0.09	3.38	3.08; 3.72	100
	0.01	1.24 ± 0.03	3.45	3.35; 3.56	102
	0.1	1.25 ± 0.03	3.47	3.37; 3.58	103
	1	1.20 ± 0.03	3.31	3.21; 3.41	98
	10	1.14 ± 0.03	3.14	3.04; 3.23	93
Venlafaxine	control	0.57 ± 0.06	1.77	1.66; 1.88	100
	100	0.56 ± 0.07	1.75	1.63; 1.88	99
	1,000	0.58 ± 0.07	1.78	1.66; 1.91	100
	10,000	0.55 ± 0.07	1.73	1.61; 1.85	98
	25,000	0.47 ± 0.07	1.60	1.49; 1.71	90

[a] log-scaled estimates of duration and frequency of the control and the treatments (± SE) predicted by the model

[b] values calculated from logarithmic estimates

[c] upper and lower limits of 95 % confidence intervals for duration and frequency
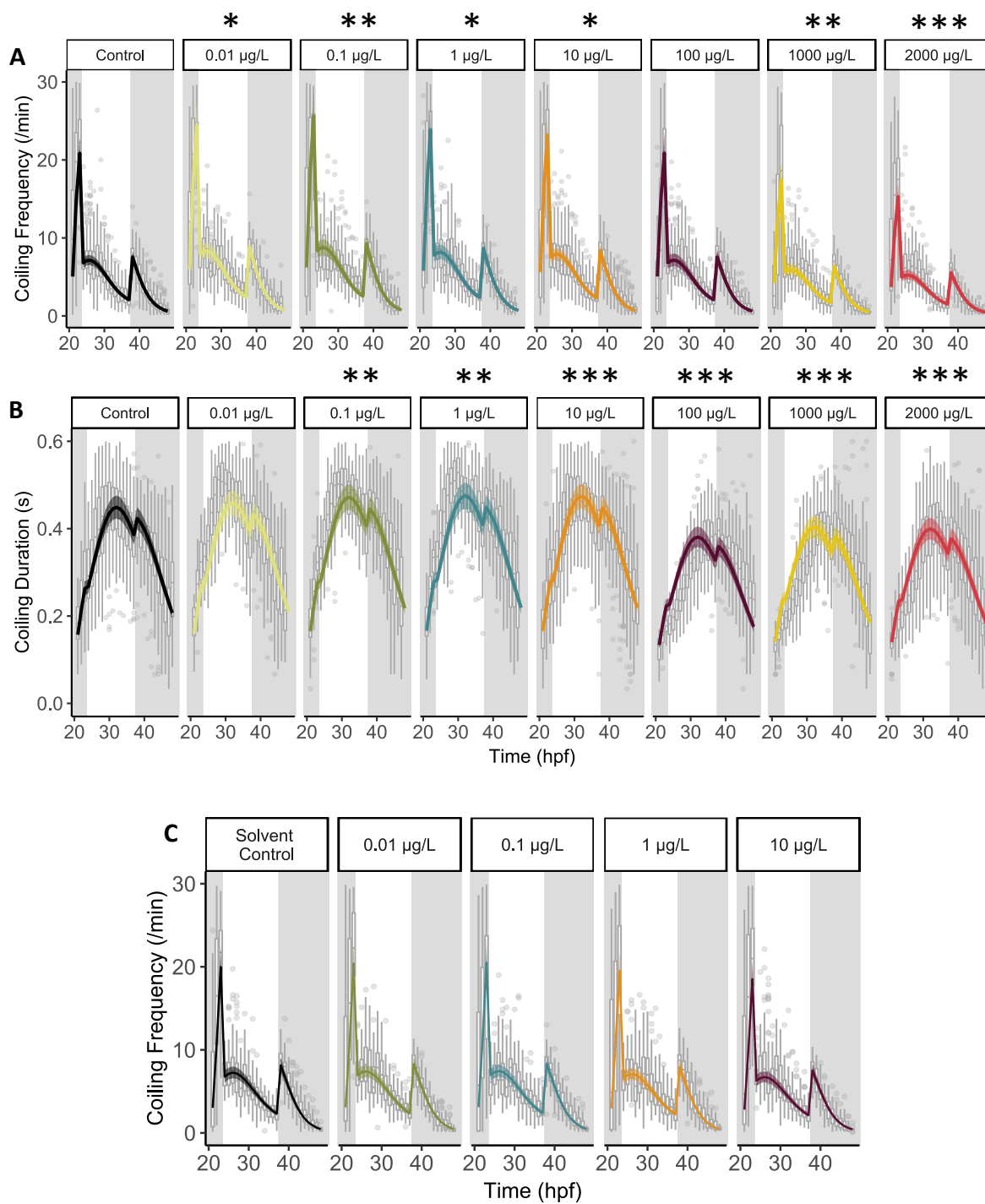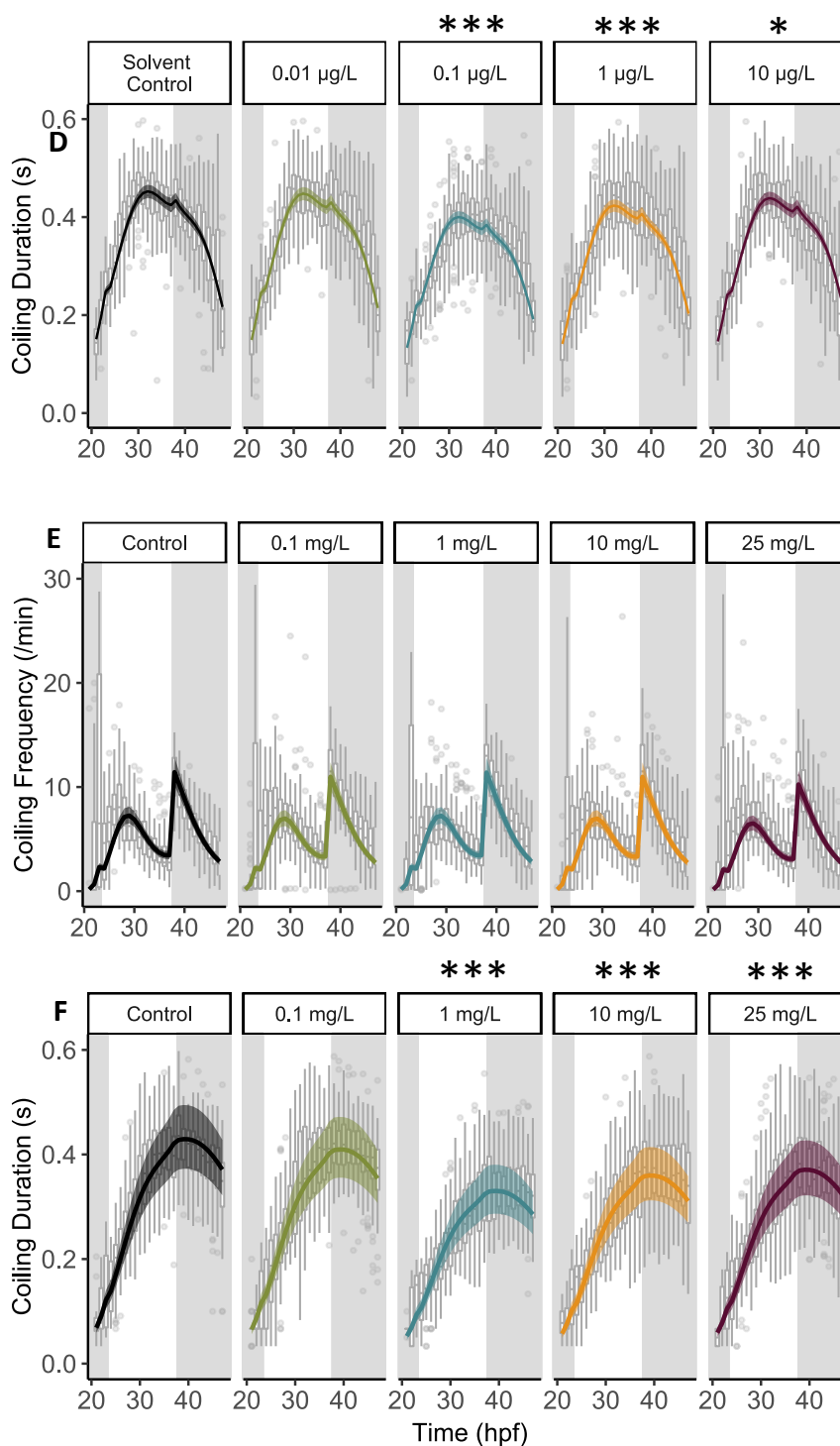
Figure 22: Coiling behavior impacted by antidepressants. The effects of the antidepressant paroxetine (**A, B**), sertraline (**C, D**) and venlafaxine (**E, F**) on the coiling behavior are presented in separated boxes in ascending concentrations based on frequency (per min) and duration (in sec). The curves depict the estimated course of behavior (within 95% confidence intervals) over the time (21- 47 hpf) as predicted by the model. Boxplots in the background show the data at each time point. The light cycle is represented by grayscale. The Tukey´s *post hoc* test with Holm´s *p*-value correction revealed significant differences between the treatment and control groups, as shown by asterisks (*$p<0.05$, **$p<0.01$, ***$p<0.001$).

7.3.3 Influence of antidepressants on the visual motor response

Test concentrations for the visual-motor response (VMR) assay were the same as in the coiling assay except for paroxetine. Because of limitation in space on the 96-well plate, I decided to exclude the lowest (0.01 µg/L) and the highest (2,000 µg/L) concentrations from the test. I performed the experiments on three different days in the evening between 8 and 10 pm for two reasons: to avoid disturbance by coworkers in the lab during normal working hours and due to the age of the embryos since the behavior response is becoming more robust with age (de Esch et al., 2012, Padilla et al., 2011).

An important part of this test is the reaction pattern in changing light conditions. In zebrafish embryos, the prototypical behavior is freezing in the light and a sudden increase in activity in the dark. I could observe this pattern in all experiments with antidepressant treatments with varying degrees of hyperactivity in the dark. As a quality control for the automated animal tracking, heatmaps were used to visualize the cumulative distance travelled by each embryo in the wells. In this way, possible errors due to errors in the software can be detected and finally excluded from the data set. I attached the heatmaps in Appendix C, Figure C4.

Different from the modelling approach, a significant alteration was defined as such when at least two out of three replicates showed a significant difference ($p < 0.05$, Kruskal-Wallis, Dunn test with Holm's p-value adjustment) to their respective control group.

Paroxetine treatment

For paroxetine, the response pattern to dark phases was higher than in the light phases. Comparable to the coiling behavior outcomes, the variation between the replicates was clearly visible. Looking at the three different biological replicates, level of activity over time (Fig. 23) as well as only in the dark phases (Fig. 26) the variation became apparent. Especially when I compared the first and second to the last replicate. On the other hand, the control embryos in the second replicate moved twice as much as the embryos from the third experiment. I have seen the lowest overall activity in the third replicate (Table 21). Additionally, the variation was relatively high over all treatment and control groups and is obviously different to the other replicates. Even after I excluded data due to irregular behavior, I could not achieve a real improvement in terms of variability. Therefore, I only excluded measurements from the analysis that showed technical errors in the software and therefore were not correctly displayed in the data set ("NA"). However, the third replicate should be considered with caution, as it was not clear if the high variability could have been caused by an overall lower fitness level of the embryos. As this replicate nevertheless corresponded to the trend of the two other replicates, I have not excluded it from the analysis. Still, a repetition of the experiment would be appropriate.

Despite these inter-replicate differences, I could see a clear pattern of behavior that is related to the treatment with paroxetine: The two lowest concentrations, 0.1 and 1 µg/L, stayed most of the time within the confidence ranges of the controls. Next, I could detect a strong reduction in movements for the higher concentrations (100 µg/L), most pronounced for the embryos which were treated with the highest concentration of 1,000 µg/L. Considering only the dark phases, this obvious reduction became also reflected by statistically significance. The sum of the distance moved within the dark phases differed equally for 100 and 1000 µg/L for all replicates from their respective controls (Fig. 26).

Sertraline treatment

The responses of the embryos of the solvent controls (0.01 % DMSO) within the sertraline experiments were comparable to the control from the paroxetine and venlafaxine VMR experiments. Also here I could see a clear inter-replicate variation with the second replicate showing the strongest response pattern to the treatments (Fig. 24B). Again, I could detect similarities between the experimental runs which were the hypoactive movement trend with increasing exposure concentrations to sertraline. This trend is most clearly in Figure 26 in the relative distance moved in all the dark phases. Compared to the other antidepressants VMR assays, I noted the strongest effect by sertraline with a reduction of movements already detectable at a treatment concentration of 0.1 µg/L (Tab. 21). I found statistically significant differences for all treatments in the second replicate. The third replicate showed lower activity patterns when embryos are treated with ≥ 0.1 µg/L. The first displayed the lowest sensitivity to the treatment and only showed differences when embryos were exposed to the highest treatment, 10 µg/L (Fig. 26).

Venlafaxine treatment

For the venlafaxine experiments, I selected much higher exposure concentrations since I missed acute toxicity data in the low ranges (EC_{10}) of the FET test. Apart from this, the baseline activity pattern is higher in comparison with the experiments with paroxetine and sertraline. This again underlines the high variability in behavior of individual fish from different breeding groups. When I focused on the dark phases over the time, a lower response is observable, which could be a habituation behavior to the stress stimuli. The treatments between 0.1 to 25 mg/L of venlafaxine led to concentration related decrease in activity. However, the second replicate showed a minor hyperactivity for the embryos which were exposed to the lowest concentrations (0.1 mg/L) and was apart from the first and the second replicate.
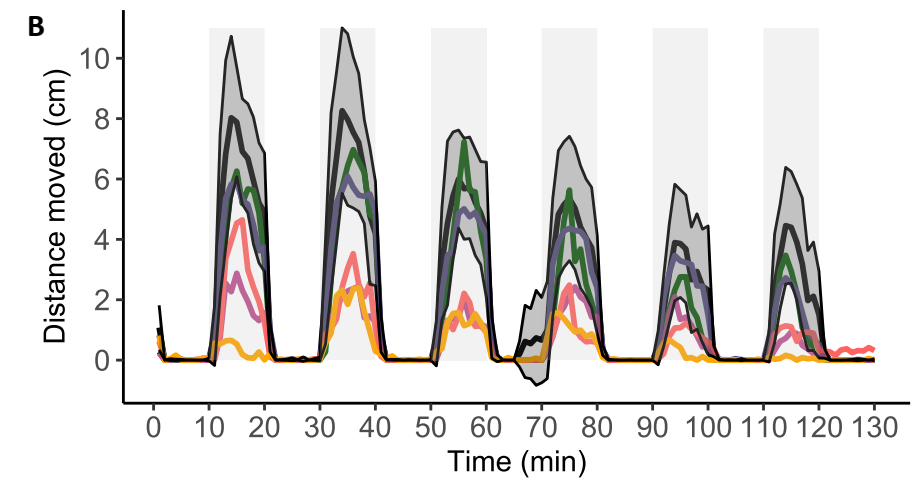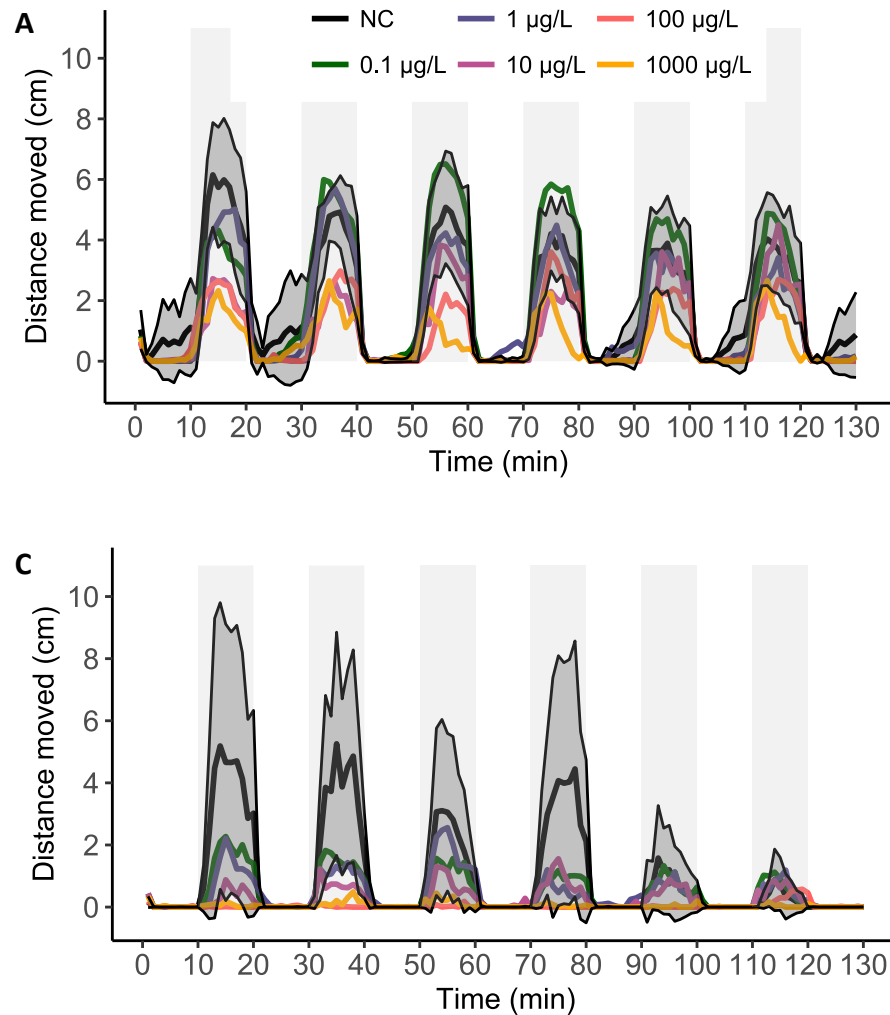
Figure 23: Distance moved over the time after paroxetine treatment. The graph shows the effects of the SSRI paroxetine on the visual-motor response of zebrafish embryos between 107 and 109 hpf. For each of the five treatments (0.1 - 1000 µg/L) and negative control, 16 embryos were placed in a 96-well plate. A, B and C illustrate three independent replicates with the control ± CI-bands. The visual stimuli are an alternating light regime of 10 min each, indicated by the grey shaded background. The embryos were exposed to the compound from < 1.5 hpf in a semi-static manner.
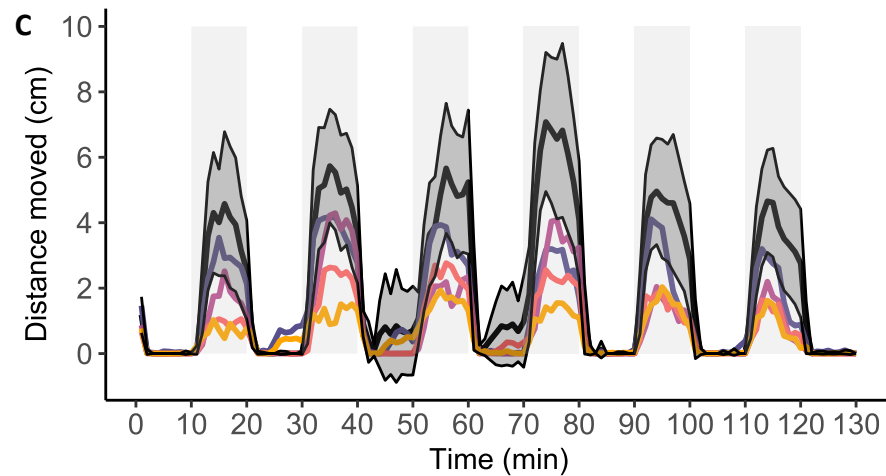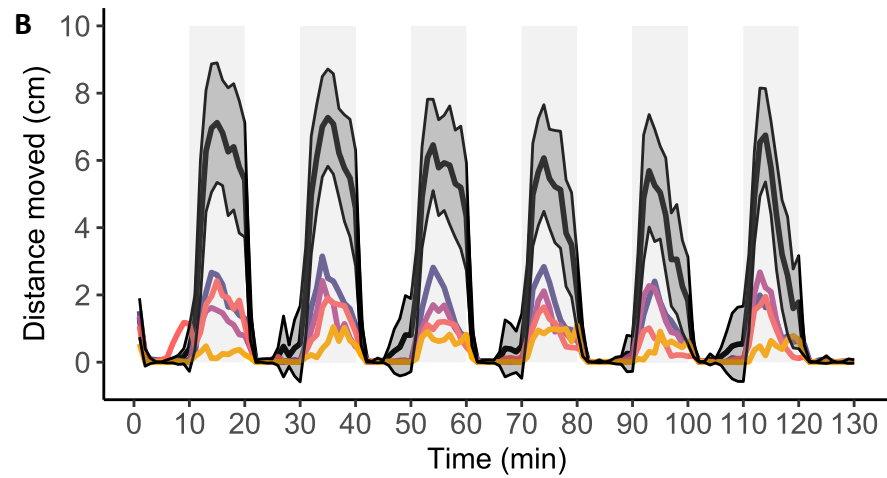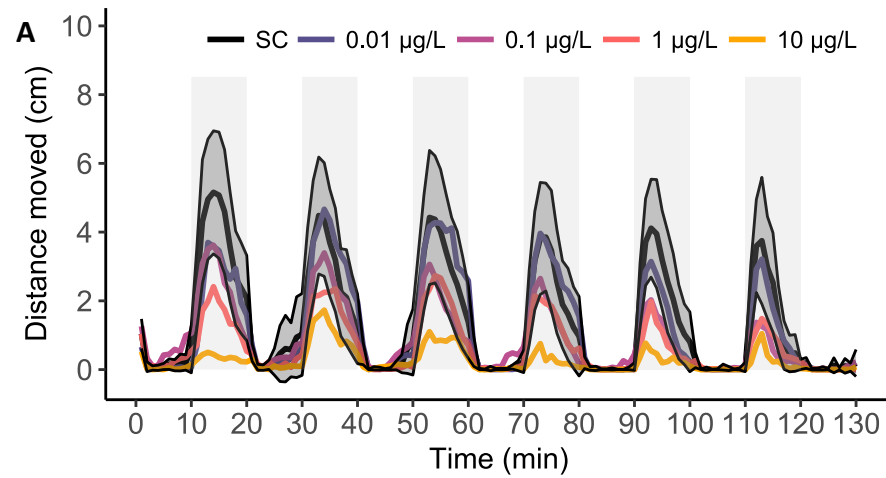
Figure 24: Distance moved over the time after sertraline treatment. The graph shows the effects of SSRI sertraline on the visual-motor response of zebrafish embryos between 107 and 109 hpf. For each of the four treatments (0.01 – 10 µg/L) and solvent control, 19 embryos were placed in a 96-well plate. A, B and C illustrate three independent replicates with the control ± CI-bands. The visual stimuli are an alternating light regime of 10 min each, indicated by the grey shaded background. The embryos were exposed to the compound from < 1.5 hpf in a semi-static manner.

A

B

C
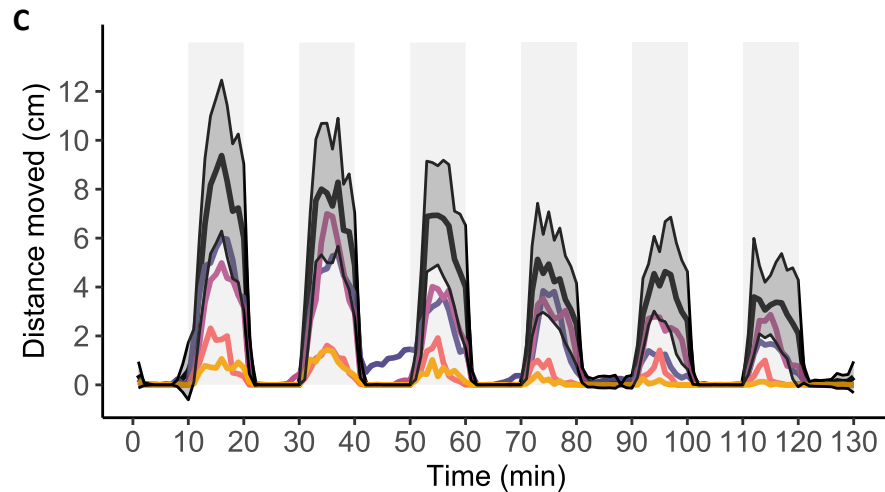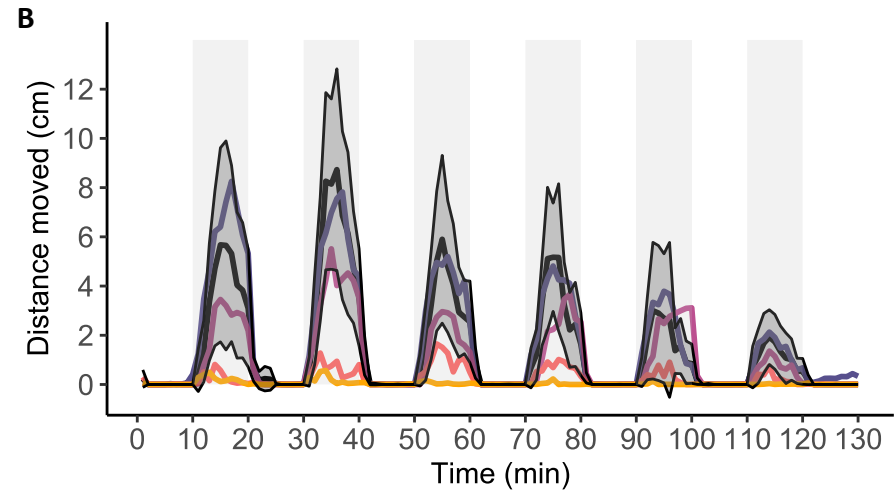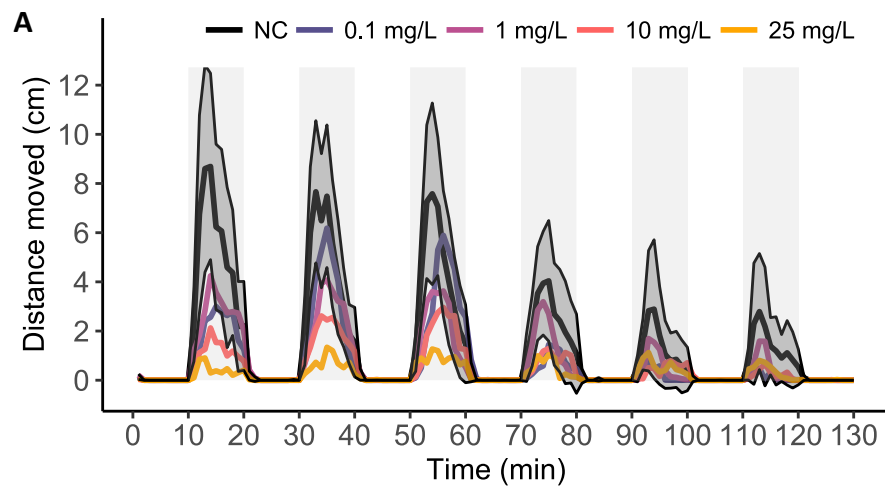
Figure 25: Distance moved over the time after venlafaxine treatment. The graph shows the effects of the SNRI venlafaxine on the visual-motor response of zebrafish embryos between 107 and 109 hpf. For each of the four treatments (0.1 - 25 mg/L) and negative control, 19 embryos were placed in a 96-well plate. A, B and C illustrate three independent replicates with the control ± CI-bands. The visual stimuli are an alternating light regime of 10 min each, indicated by the grey shaded background. The embryos were exposed to the compound from < 1.5 hpf in a semi-static manner.
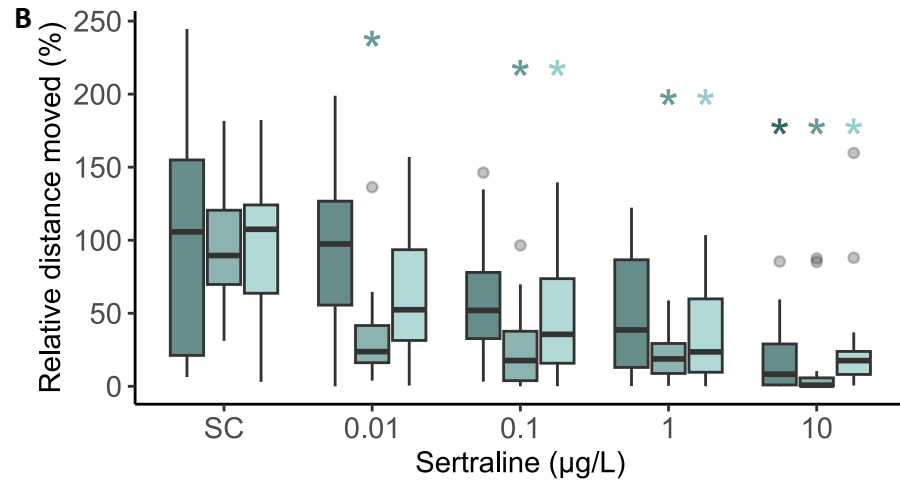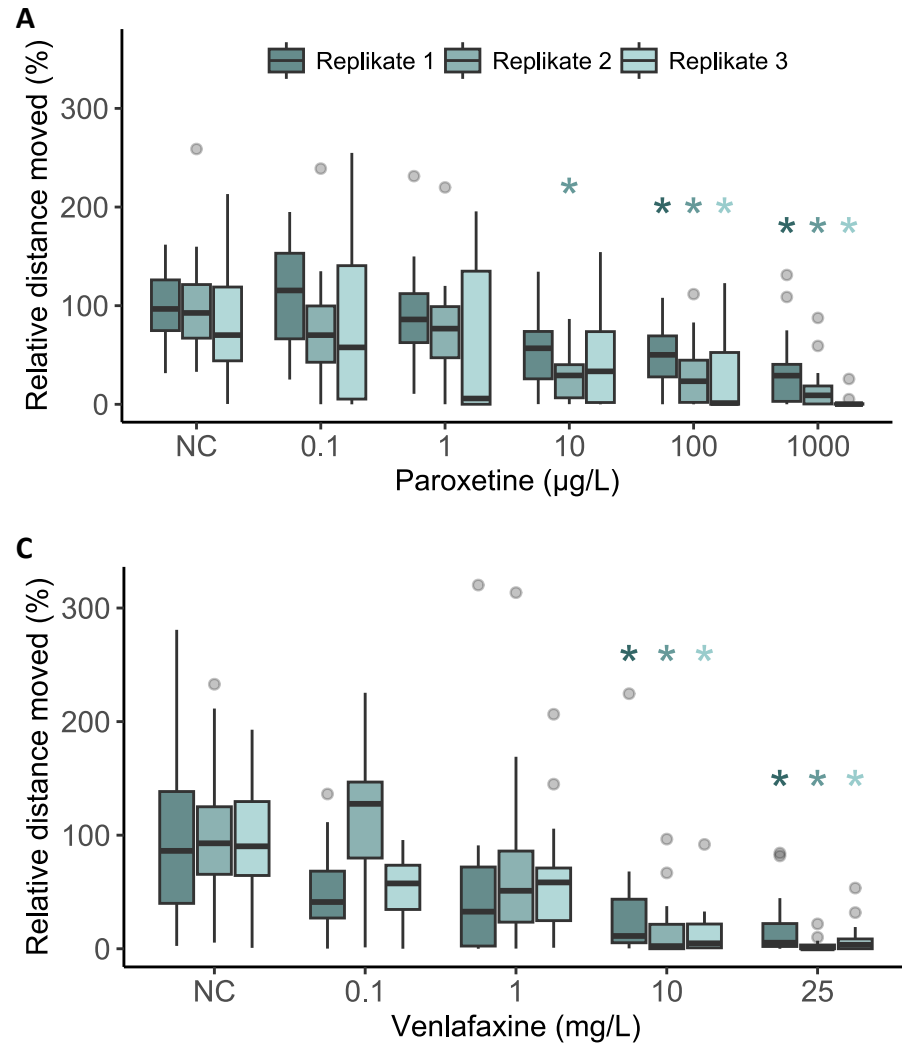
Figure 26: Relative distance moved in the dark phases after antidepressant treatment. Plots A, B and C illustrate the effects of the different drugs paroxetine, sertraline, and venlafaxine in three independent replicates each. The box plots show the median (middle line) and the upper and lower quartiles (box) with the corresponding whiskers. Outliers are marked as dots. Data were tested (Kruskal-Wallis, Dunn test with Holm's *p*-value adjustment) and significant differences are indicated by asterisks over the respective boxplot for each replicate.

Table 21: Effect on locomotion of zebrafish embryos exposed to antidepressants in the visual-motor response assay. Listed are the distance moved (%) related to the controls, and the mean of the total distance of per treatment (cm). All values are the sum of the distance moved over the dark phases.

A - Paroxetine	Relative distance moved (%)	R1	R2	R3
Control	100 (± 21.10)	213.96 (± 45.15)	257.92 (± 77.84)	139.42 (± 97.31)
0.1 µg/L	114.98 (± 27.02)	190.08 (± 58.84)	206.25 (± 68.16)	65.58 (± 40.12)
1 µg/L	88.84 (± 27.5)	246.02 (± 57.81)	189.69 (± 80.52)	58.04 (± 32.87)
10 µg/L	58.23 (± 20.44)	124.60 (± 43.73)	76.09 (± 35.76)	37.58 (± 30.58)
100 µg/L	50.94 (± 16.17)	108.98 (± 34.60)	84.79 (± 49.03)	4.51 (± 6.41)
1000 µg/L	34.14 (± 21.23)	73.05 (± 45.41)	43.84 (± 33.74)	7.13 (± 6.41)
B - Sertraline	**Relative distance moved (%)**	**R1**	**R2**	**R3**
Solvent control	100 (± 20.7)	164.23 (± 59.86)	285.82 (± 59.15)	247.73 (± 58.05)
0.01 µg/L	32.75 (± 14.71)	151.55 (± 44.64)	93.59 (± 42.05)	155.94 (± 54.78)
0.1 µg/L	26.01 (± 13.36)	95.66 (± 32.15)	74.33 (± 38.18)	112.32 (± 44.87)
1 µg/L	21.40 (± 8.01)	79.93 (± 31.04)	61.15 (± 22.89)	91.29 (± 41.30)
10 µg/L	11.12 (± 12.87)	30.70 (± 19.38)	31.75 (± 36.78)	66.97 (± 44.81)
C - Venlafaxine	**Relative distance moved (%)**	**R1**	**R2**	**R3**
Control	100 (± 17.15)	191.66 (± 70.80)	185.95 (± 61.16)	281.67 (± 67.32)
0.1 mg/L	73.68 (± 13.96)	95.03 (± 35.58)	218.11 (± 52.79)	152.52 (±34.29)
1 mg/L	59.43 (± 17.66)	98.68 (± 67.93)	127.00 (± 67.24)	98.68 (± 67.93)
10 mg/L	21.12 (± 9.56)	63.43 (± 47.46)	30.07 (± 23.49)	39.69 (± 29.93)
25 mg/L	9.56 (±4.74)	33.74 (± 23.74)	5.48 (± 4.86)	22.87 (± 18.44)

7.4 Discussion

The acute treatment of zebrafish embryo with the widely used SSRIs sertraline and paroxetine in the FET test revealed a concentration-dependent increase in mortality. Shared sublethal effects of paroxetine and sertraline were growth retardation, reduced heartbeat and blood flow, fin seam degradation and swim balance loss. Additionally, zebrafish embryos treated with paroxetine, sertraline and venlafaxine, an antidepressant from the SNRI class, revealed impaired tail movement and stress response to a light stimulus. A summary of LC, EC and LOEC values from my acute and behavioral experiments can be found in Table 22 below.

Table 22: Summarized effects from the different assays caused by paroxetine, sertraline and venlafaxine.

Assay		Paroxetine	Sertraline	Venlafaxine
FET	LC_{50} (120 hpf)	9,000 µg/L	875 µg/L	762,800 µg/L[a]
	EC_{10} (120 hpf)	2,000 µg/L	0.1 µg/L	1,100 µg/L[a]
Tail Coiling	Frequency (LOEC)	0.01 µg/L	n.a.	n.a.
	Duration (LOEC)	0.1 µg/L	0.1 µg/L	1,000 µg/L
VMR	Distance moved in the dark (LOEC)	100 µg/L	0.1 µg/L	10,000 µg/L

n.a. – not available

[a] Values for acute toxicity of venlafaxine were provided by Saskia Hagstotz and Katharina Brotzmann.

7.4.1 Acute toxicity of the serotonin reuptake inhibitors (SSRIs) paroxetine and sertraline

Given the low water solubility of sertraline, 10 µg/L have been tested in zebrafish without solvent (Nowakowska et al., 2020) and 10,000 µg/L in medaka (*Oryzias latipes*) by sonication (Chiffre et al., 2016). For my experiments, we[1] used the solvent DMSO to also reach the final concentration of 10,000 µg/L. For paroxetine no solvent was needed, and the highest concentration tested included 20,000 µg/L, which is in the same range of previously published data (Zhu et al., 2023). After 5 days of exposure, the values for acute toxicity of paroxetine (Tab. 22) was comparable to the literature (Zhu et al., 2023). For sertraline, my toxicity data for zebrafish embryos seemed to have a comparable sensitivity to treated medaka (Chiffre et al., 2016). Additionally, it has been shown that the growth of zebrafish embryos is retarded by paroxetine treatment (Zhu et al., 2023), which was similar for sertraline exposure in my experiments (Fig. 20).

Independent from the exposure concentrations, our[1] paroxetine treatment showed the first lethal and sublethal effects after hatching. Therefore, I assumed a restricted permeability by the chorion. It has been examined that the permeability of the chorion for substances is highly dependent on their size, bulkiness, lipophilicity and their ionization state as well as the developmental stage of the chorion itself (Henn and Braunbeck, 2011, Kais et al., 2013, Pelka et al., 2017). The size of paroxetine with 329 Da lays approx. 10× lower than the critical threshold described in the literature (Pelka et al., 2017) and thus I concluded it should not restrict the uptake. The ionization state is highly dependent on the pH of the water. With radioactively labeled sertraline and fluoxetine Alsop and Wilson could correlated an

increased acute toxicity in zebrafish embryos with increasing pH of the test solutions (Alsop and Wilson, 2019). They postulate that with increasing pH, a higher rate of non-ionized molecules forms. The non-ionized molecules in turn can pass biological barriers much easier than the dissociated states. Paroxetine has a pK_a of 9.51 and is a comparably weak base like the other SSRIs. I conclude that at the measured pH values between 7.75 and 8.13 (low to high exposure concentration), only a small fraction of paroxetine was in the non-ionized state which finally resulted in lower bioavailability of the compound for the embryo within the egg. In contrast, this delayed toxicity was not observed for sertraline. But I conclude, it is possible that the used solvent DMSO at a concentration of 0.1 % has enhanced the uptake since this effect has been already described before (Kais et al., 2013).

In all experiments, none of the compounds showed an apparent increase in hatching rate at 3 dpf, as described in the literature (Nowakowska et al., 2020, Yang et al., 2021, Zhu et al., 2023). Focusing on the cardiovascular system, we[1] have observed abnormalities in appearance and function, such as pericardial edema as well as enlarged heart (sertraline treatment only), weakened pumping capacity and reduced blood flow. Kent and colleagues demonstrated a link between sertraline exposure and cardiac developmental disorders in zebrafish (Kent et al., 2022). But it has to be noted that the tested concentrations were about three times higher and, in contrast to our[1] observations, the size of the heart ventricle became smaller. Also, for paroxetine we[1] could see a reduced cardiac pumping capacity of the heart combined with increased occurrence of pericardial edema. Therefore, I presume a cardiotoxic potential for sertraline and paroxetine. Zhu et al. (2023) investigated the cardiotoxic effect in zebrafish more in detail and concluded that inflammation responses might be one of the underlying mechanisms. Comparable adverse effects on the heart development were also reported for fluoxetine and citalopram, other compounds from the SSRI class (Zindler et al., 2019a) as well as for venlafaxine (Thompson et al., 2022a). Generally, for humans the developmental cardiotoxic potential of these antidepressants is known and has been described. A meta-analysis from 2013 showed that pregnant SSRI patients gave birth to children with an increased incidence of congenital heart defects (Myles et al., 2013). They concluded that paroxetine and fluoxetine are the most problematic medications from the list of SSRIs.

Another effect we[1] observed was the damaged or degrading fin seam. Many of the exposed fish were impacted in a concentration-dependent pattern (Fig. 19). Based on the before mentioned cardiotoxic impacts and associated reduced cardiac pumping capacity, I assume that the regions remote from the heart such as the caudal fin could suffered from undersupply of blood and nutrients due to insufficient circulation, which may ultimately led to the degradation of this structure. This effect was most pronounced in paroxetine treatment and became more and more visible with time and increasing concentrations.

On the fourth and fifth day post fertilization, when the fish embryos started their first swimming movements, we[1] observed a common effect for SSRIs: Most treated fish had difficulties remaining stable in an upright position and instead laid on the side. This loss of balance is in line with other findings observed in fluoxetine-treated embryos (de Farias et al., 2019). Correia et al. (2023) showed that already an exposure to low concentrations of fluoxetine ($\leq 1\ \mu g/L$) significantly delayed the inflation of the swim bladder at 168 hpf, which I assume may be one explanation for this observed behavior in our[1] experiments. Another factor being essential for balance in swimming movements is the correct development of the otoliths of the vestibular system in zebrafish embryos (Haddon and Lewis, 1996). At least for the SNRI venlafaxine, malformed, *i.e.* fused otoliths were observed after acute exposure (unpublished data of our working group). At the same time, affected fish showed loss of equilibrium. No obvious deformations of the otoliths were noted by optical inspection under a microscope in the fish which we[1] treated with paroxetine and sertraline. The underlying cause for the described loss of equilibrium should be the subject of further experiments focusing on swim bladder inflation and detailed investigation of otolith development and integrity.

7.4.2 Embryonic behavior is affected by antidepressants

The loss of balance was the first effect we[1] noticed, which can affect the behavior of the embryos. The blocking of the reuptake of serotonin, dopamine or norepinephrine back into the presynapse leads to increased extracellular levels of those neurotransmitters. Different agonistic or antagonistic serotonin receptor interaction have already been connected to physiological and behavioral changes in fish (McDonald, 2017). Accordingly, there are several experiments published which deal with behavioral alterations caused by sertraline, paroxetine and venlafaxine (Tab. 23, 24, 25).

The listed publications in the tables below mainly focus on swim and stress responses in post-hatching embryos, juvenile and adult fish. We[1] conducted a stress response assays, here a visual-motor response test (VMR), on post-hatched embryos for sertraline, paroxetine and venlafaxine. Moreover, I examined if alterations could be already detectable in the tail coil behavior. So far, information on the effects of antidepressants focusing on tail coiling movements in zebrafish embryos are, to my knowledge, only available for fluoxetine and citalopram (Bachour et al., 2020, de Oliveira et al., 2021, Zindler et al., 2019a).

Decreased stress response in zebrafish

The visual-motor response (VMR) is a startle (or stress) response to visual stimuli such as light. The stereotypical behavioral reaction of zebrafish embryos to sudden illumination is freezing of movements. Alternating dark and light phases lead to an enhanced hyperactive locomotion in dark phases (MacPhail et al., 2009). This light-seeking behavior or negative phototaxis is a normal reaction and becomes reversed in adult zebrafish (scototaxis, positive phototaxis; Kalueff et al., 2013). Fully developed eyes are not necessarily required for the perception of light stimuli, as already in early stages embryos can make a considerable contribution to visual perception due to deep brain light receptors (Easter and Nicola, 1996, Fernandes et al., 2012). The VMR, can be utilized to detect behavioral alterations in a post-hatching phase (> 3 dpf).

In the present study, for all three antidepressants we[1] tested, I could calculate and demonstrate a clear concentration-dependent decrease in activity in the dark. This behavior suggested that fish show less anxiety or fear-like behavior (MacPhail et al., 2009). For sertraline, my experiments together with the results from Faria et al. (2019), represents the lowest concentration reported to show an effect on early zebrafish behavior (Tab. 23). Similar as to what I have observed, literature showed that sertraline exposure in early life stages (starting < 5 dpf) revealed a general decrease in locomotion activity for zebrafish embryos (Huang et al., 2019, Richendrfer and Creton, 2018, Sehonova et al., 2019, Suryanto et al., 2021, Yang et al., 2021). This holds also true for our[5] paroxetine (Huang et al., 2019, Suryanto et al., 2021). Lowest detected effective concentration I determined for paroxetine for our[5] studies was 100 µg/L and is comparable to the values I have found in the literature (Tab. 24): For water-borne exposure to venlafaxine with a concentration of ≤ 100 µg/L can exhibit two different responses either increased (Henry et al., 2022, Hong et al., 2022a, Tang et al., 2021, Thompson et al., 2022b) or decreased activity (Huang et al., 2019, Sehonova et al., 2019, Suryanto et al., 2021, Tang et al., 2022, Thompson et al., 2017). I have found only two additional studies focusing on a higher concentration range which resulted in decreased swimming speed (1,000 µg/L; Hong et al., 2021b) or distanced moved (3,000 µg/L; Sehonova et al., 2019). Our[5] exposure concentrations were even higher with 25,000 µg/L for the highest concentration. My calculated outcomes – decreased distance moved – aligned with the prevailing hypoactive trend with increasing concentrations found in the literature (Tab. 25).

Table 23: Impact of sertraline on zebrafish behavior.

Substance	Stage	Exposure	Endpoint	Tested concentrations	LOEC	Effect	Reference
SSRI							
Sertraline	embryo	3 – 144 hpf	VMR[a]; 144 hpf	1,10,100 µg/L	n.a.	↓ number of movements	Huang et al. (2019)
		143 – 144 hpf	VMR[a]; 144 hpf	100 µg/L	100 µg/L	↓ number of movements	
		3 – 27 hpf	VMR[a]; 144 hpf	100 µg/L	-	-	
Sertraline	embryo	4 – 5 dpf	VMR[b], 5 dpf	1, 10, 100, 1,000 µg/L	10 µg/l	↓ distance moved	Suryanto et al. (2021)
Sertraline	embryo	1 - 144 hpf	VMR[a]; 144 hpf	0.1, 1, 10, 100, 1000 µg/L	100 µg/L	↓ distance moved	Sehonova et al. (2019)
Sertraline	embryo	4 – 182 hpf	vibrational startle response, 8 dpf	0.01, 0.1, 1, 10 µg/L	0.1 µg/L	↓ distance moved	Faria et al. (2022)
			VMR[d], 8 dpf	0.01, 0.1, 1, 10 µg/L	0.1 µg/L	↓ distance moved	
Sertraline	embryo	0 – 5 dpf	VMR[g], 5 dpf	0.01, 0.1, 1, 10 µM (3.43, 34.27, 342.69, 2426.9 µg/L*)	1 µM (342.69 µg/L)	↓ decreased swimming speed	Richendrfer and Creton (2018)
Sertraline	embryo		Dark-light preference, 4 dpf	1, 10, 100 µg/L	1 µg/L	disrupted anxiety-like behavior	Yang et al. (2021)
			VMR[b], 6 dpf		10 µg/L	↓ distance moved	
Sertraline	juvenile	5 – 140 dpf	novel tank; 90 dpf and 120 dpf	10, 100 µg/L	-	-	Venkatachalam et al. (2023)
Sertraline	juvenile	21 d	Locomotion	0.1, 1, 10, 100 µg/L	10 µg/L	↓ swimming speed	Hong et al. (2021a)
			VMR[f]		0.1 µg/L	↑ locomotion	
			social test		100 µg/L	↓ time spent in social region	
			shoaling test		0.1 µg/L	↓ distance and	
					100 µg/L	↑ distance between fish, respectively	
Sertraline	juvenile	5 – 140 dpf	novel tank; 90 dpf and 120 dpf	10, 100, 200 µg/L	100 µg/L	↓ anxiety-like behavior ↓ distance moved	Venkatachalam et al. (2023)

light:dark cycles/phases for VMR assay: (a) 5:5 min, (b) 10:10 min, (c) 5:10 min, (d) 10:15 min, (e) 4:4 min, (f) 1:1 min, (g) 15: 15 min, (h) 10: 3 min

* since not further specified, calculated with the molecular weight of sertraline hydrochloride (342.69 g/mol)

Table 24: Impact of paroxetine on zebrafish behavior.

Substance	Stage	Exposure	Endpoint	Tested concentrations	LOEC	Effect	Reference
SSRI							
Paroxetine	embryo	4 – 5 dpf	VMR[b], 5 dpf	1,000 µg/L	1,000 µg/l	↓ distance moved	Suryanto et al. (2021)
Paroxetine	embryo	3 – 144 hpf	VMR[a]; 144 hpf	1,10,100 µg/L	n.a.	↓ number of movements	Huang et al. (2019)
		143 – 144 hpf	VMR[a]; 144 hpf	100 µg/L	100 µg/L	↓ number of movements	
		3 – 27 hpf	VMR[a]; 144 hpf	100 µg/L	100 µg/L	↓ number of movements	
Paroxetine	embryo	0 – 5 dpf	Basal swimming activity, 5 dpf	40, 400 µg/L	40 µg/L	↓ distance moved	Ferreira et al. (2023)
			VMR[i], 5 dpf		40 µg/L	non-monotonic response	
Paroxetine	juvenile	21 d	locomotion	0.1, 1, 10, 100 µg/L	-	-	Hong et al. (2021a)
			VMR[f]		-	-	
			social test		-	-	
			shoaling test			↓ distance between fish	
Paroxetine	juvenile	5 – 140 dpf	novel tank; 90 dpf and 120 dpf	10, 100, 200 µg/L	10 µg/L	↓ anxiety-like behavior ↓ distance moved	Venkatachalam et al. (2023)
	adult		120-170 dpf, reproductive success		10 µg/L	↓ eggs, fertilization rate	

light:dark cycles/phases for VMR assay: (a) 5:5 min, (b) 10:10 min, (c) 5:10 min, (d) 10:15 min, (e) 4:4 min, (f) 1:1 min, (g) 15: 15 min, (h) 10: 3 min

n.a. – not available

Table 25: Impact of venlafaxine on zebrafish behavior.

Substance	Stage	Exposure	Endpoint	Tested concentrations	LOEC	Effect	Reference
SNRI							
Venlafaxine	embryo	Microinjection 1-4 cell stage	VMR[h], 5 dpf	1 and 10 ng	1 ng	↓ distance moved	Thompson et al. (2017)
Venlafaxine	embryo	Offsprings of treated parents	VMR[a], 5 dpf	1, 10, 100 µg/L	1 µg/L	↓ distance moved	Tang et al. (2022)
Venlafaxine	embryo	2 – 120 hpf	VMR[a], 5 dpf	1, 10, 100 µg/L	1 µg/L 10 µg/L	↑ distance moved ↓ distance moved	Tang et al. (2021)
Venlafaxine	embryo	4 – 5 dpf	VMR[b], 5 dpf	1,000 µg/L	1,000 µg/l	↓ distance moved	Suryanto et al. (2021)
Venlafaxine	embryo	3 – 144 hpf 143 – 144 hpf 3 – 27 hpf	VMR[a]; 144 hpf VMR[a]; 144 hpf VMR[a]; 144 hpf	1,10,100 µg/L 100 µg/L 100 µg/L	n.a. - 100 µg/L	↓ number of movements - ↑ number of movements	Huang et al. (2019)
Venlafaxine	embryo	5 – 120 hpf	spontaneous swimming; 120 hpf VMR[e]; 120 hpf thermal preference response; 120 hpf	0.22 µg/L 0.22 µg/L 0.22 µg/L	- 0.22 µg/L - 100 µg/L	- ↑ distance moved (light phases) - ↓ mating duration	Henry et al. (2022)
Venlafaxine	embryo	1 - 144 hpf	VMR[a]; 144 hpf	0.3, 3, 30, 300, 3000 µg/L	3000 µg/L	↓ distance moved	Sehonova et al. (2019)
Venlafaxine	juvenile	21 d	locomotion VMR[f] social test shoaling test	1, 10, 100, 1000 µg/L	1000 µg/L 1 µg/L 100 µg/L 0.1 µg/L	↓ swimming speed ↑ locomotion ↓ time spent in social region ↑ distance between fish	Hong et al. (2021a)
Venlafaxine	juvenile adult	Microinjection 1-4 cell stage	open-field test	1 and 10 ng	1 ng 10 ng 10 ng	↑ distance moved ↓ anxiety-like behavior ↑ distance moved (only males)	Thompson et al. (2022b)
Venlafaxine	adult	20 d	courtship test	1, 10, 100 µg/L	1 µg/L	disrupted courtship behavior	Tang et al. (2022)
Venlafaxine	adult	2 hpf – 180 dpf	reproductive behavior	0.1, 1, 10, 100 µg/L	0.1 µg/L	↑ mating interval	Hong et al. (2022a)

light:dark cycles/phases for VMR assay: (a) 5:5 min, (b) 10:10 min, (c) 5:10 min, (d) 10:15 min, (e) 4:4 min, (f) 1:1 min, (g) 15: 15 min, (h) 10: 3 min

Tail coiling behavior as a sensitive early warning system

Like the stress response to alternating light, the earliest spontaneous movements of the tail were affected by the tested antidepressants sertraline, paroxetine and venlafaxine.

Besides the commonly used endpoint frequency of coils, the duration of the movements can be a meaningful additional endpoint. In all results of the tail coiling experiments I presented in this thesis the endpoint duration was more sensitive to detect a decrease or a partly inhibition of movements. This also applies to my tests with antidepressants. This statistically significant reduction in tail movements was the first sign of a change in behavior and can also be seen at the same concentrations in the VMR assay. Therefore, the coiling assay can serve as an early warning system for neurotoxic substances.

However, the frequency of occurring movements could not distinguish treatment from control groups for sertraline and venlafaxine. Likewise, Zindler and colleagues who used the same setup, did not see changes for tested fluoxetine concentrations up to 12 mg/L (Zindler et al., 2019a). In contrast, citalopram exposure caused a significant reduction in coiling frequency although with a considerable high exposure concentration of 200 mg/L (Zindler et al., 2019a). Looking at my paroxetine treatment outcomes, all low concentrations (0.01, 0.1, 1, 10 µg/L) caused hyperactive movements. Above 100 µg/L treatment the activity decreased and showed thus a biphasic pattern along a concentration gradient.

Hyper- and hypoactive patterns have been shown to not only be affected by concentrations of the test compounds. Ogungbemi and colleagues systematically reviewed the influential experimental factors which are relevant for hyper- or hypoactivity (Ogungbemi et al., 2019). They concluded that the daytime when the behavior is measured, the time window when the embryos are exposed, and size or volume of the well are among the elements which have a significant influence on the activity level. Additionally, not only the developmental timing of exposure but also its length can make a huge difference. As seen in nicotine experiments, high concentrations (40 µM) of this neurotoxicant can have a stimulatory effect in short exposure (20 min; Ogungbemi et al., 2020a) and a sedative effect in longer exposure settings (2 d; Fig. 10).

Sensitivity of behavioral endpoints

All used experiments, the FET test, tail coiling and VMR assay, can be sensitive tools to detect changes in behavior in zebrafish embryos. Even though the FET test is primarily suitable for assessing morphological changes, it can provide valuable first indications for early behavioral changes and thus can initiate more detailed inspection with specific behavioral assays. In the two embryonic behavioral tests I used, the coiling provided mostly more sensitive outcomes compared to the results of the VMR.

For paroxetine, the increased frequency of tail movements at 0.01 µg/L is, to my knowledge, the lowest measured effective concentration for behavior in fish. A reduction in anxiety-like behavior and reproductive success caused by paroxetine was reported in adult zebrafish with a long-term exposure to 10 µg/L (Venkatachalam et al., 2023). Up to 100 µg/L impaired swimming abilities in early stages of zebrafish development (Huang et al., 2019).

For venlafaxine, instead, I was only able to detect a change in tail coiling behavior at relatively high concentrations of 1,000 µg/L. At the same concentration, a long-term exposure study by Ziegler and colleagues with brown trout larvae, revealed changes in swimming patterns, away from the bottom towards the top of the aquaria (Ziegler et al., 2021). Together with an additional stressor such as lower temperatures this behavior became already visible at 100 µg/L. They also showed that growth was also significantly reduced with this treatment. Additionally, 100 µg/L impaired circadian rhythm of male mosquitofish (*Gambusia holbrooki*) and increased mortality in fathead minnows (*Pimephales promelas*)

(Sehonova et al., 2018, Singh et al., 2022). After seven days of contact to low concentration of venlafaxine (1 µg/L) rainbow trout displayed elevated neurotransmitter concentrations in midbrain regions, increased cortisol levels in subordinate fish, reduced food intake (Melnyk-Lamont et al., 2014) and showed lowered metabolic response to stressors in the liver (Best et al., 2014).

A chronic exposure study with ≥ 1 µg/L sertraline demonstrated an induction of oxidative stress, signs of neurotoxicity by enhancing acetylcholinesterase activity as well as elevated neurotransmitter levels in the brain of zebrafish (Yang et al., 2022). So far, the LOEC I could determine (0.1 µg/L) together with the data on embryonic behavioral impairments in zebrafish published by Faria and colleagues seemed to be the lowest concentration reported in the literature for fish behavior (Faria et al., 2022). Nevertheless, at the same concentrations steroidogenic enzyme regulation can be disrupted in fathead minnow larvae (*Pimephales promelas*) (Carty et al., 2017).

These results show that behavioral tests and neurologically relevant biomarkers such as neurotransmitter levels or enzyme activities are similarly sensitive and can indicate the neurotoxic potential of the substances.

7.4.3 Do environmental concentrations of antidepressants pose a risk to fish?

Pharmaceuticals are either metabolized or excreted unchanged by humans and ultimately end up in domestic or medical wastewaters. Wastewater treatment plants (WWTPs) can only degrade or remove pharmaceuticals to a limited extent, as most medications are designed to be stable (Wang et al., 2023). Nowadays, antidepressants are considered contaminants of emerging concern (CEC) since they are increasingly being detected in the aquatic environment worldwide (Grabicová et al., 2020, Mole and Brooks, 2019, Wang et al., 2023, Wilkinson et al., 2022).

Table 26: Overview of environmentally relevant concentrations of antidepressants in water systems.

Compound	Effluent	Fresh water	fish liver (wet wt)	Reference
Sertraline	17.1 µg/L	8.5 ng/L	545 ng/g	Grabicová et al. (2020), Ramirez et al. (2009), Styrishave et al. (2011)
Paroxetine	3.4 µg/L	10 ng/L	0.35 ng/L	Grabicová et al. (2020), Kleywegt et al. (2019), Lajeunesse et al. (2011)
Venlafaxine	2.19 µg/L	110 ng/L	0.69 ng/L	Lajeunesse et al. (2011), Sehonova et al. (2018), Wilkinson et al. (2022)

For sertraline, paroxetine and venlafaxine, environmentally relevant concentrations (Tab. 26) were not considered to be within the lethal range for fish (Sehonova et al., 2018). However, according to the literature, venlafaxine water concentrations in highly contaminated environments such as effluents are in the range which are able to affect relevant behavior such as social, courtship and reproduction (Hong et al., 2021a, Hong et al., 2022b, Tang et al., 2022). Especially the metabolite of venlafaxine should be further investigated since it was detected in higher amounts in effluent compared to its parent compound (Metcalfe et al., 2010). Sertraline at environmentally relevant concentrations resulted in lower anxiety-like behavior in the fish, a lower stress response and a lower fertilization rate of eggs, which could

ultimately lead to a higher predation rate and a lower number of offspring and thus affect the fitness of the individual and even the population (Faria et al., 2022, Sehonova et al., 2018, Venkatachalam et al., 2023). Paroxetine levels in surface waters were considerably lower compared to venlafaxine. In addition, paroxetine does not have a high bioaccumulation potential, which reduces the risk to aquatic organisms (Lajeunesse et al., 2011). However, my finding of altered tail movement suggests that early stages of fish development may be affected.

Looking at my results, I conclude that the most serious risks can be associated with sertraline. The combination of high concentrations in effluents, high bioaccumulation in tissue (BCF = 2280 L/kg; Nowakowska et al., 2020), and its effect range in very low concentrations makes this antidepressant a compound of concern

7.4.4   Conclusion

Embryonic behavior tests can detect the effects of exposure to antidepressants at environmentally relevant concentrations. These tests are among the most sensitive and are on the same level as molecular biomarkers. Based on the low effective concentrations found in the literature and in my studies, I assume that the concentrations of antidepressants already present in aquatic environments worldwide, and together with the increasing trends in annual prescription rates, may pose a realistic threat to the aquatic environment.

8 OVERALL CONCLUSION AND SUITABILITY OF THE ZEBRAFISH EMBRYO BEHAVIOR FOR ASSESSING DEVELOPMENTAL NEUROTOXICITY

In my dissertation, I used embryos of the alternative model organism zebrafish to investigate potential developmental neurotoxicity of different chemicals. In the first part of my thesis, my objective was to improve the outcome of the tail coiling behavior analysis. For this purpose, I used the positive substance nicotine to implement a modeling approach. In the subsequent parts, I tested various contaminants in zebrafish embryos, focusing on embryonic behavior, and evaluated the effects to determine whether these chemicals are potentially developmentally neurotoxic.

In my experiments, the tail coiling behavior of the zebrafish embryo has proven to be highly sensitive to detect impacts by low concentrations of nicotine. Here, I showed that the GAM analysis method is suitable for behavioral evaluation because it has no rigid pre-assumptions and can describe the trend of the data flexibly. A major advantage of the approach is the possibility of pooling all replicates and incorporating the natural occurring variability of all fish. Due to the resulting large amount of data, the model is more robust against outliers, which therefore do not need to be defined nor excluded. Furthermore, with GAM I can discriminate these non-treatment related confounding factors from the significant nicotine treatment effects. At least in this proof-of-concept study, I can demonstrate that the impaired behavior at high concentrations correlates with structural defects in motoneuron and skeletal muscle which is in accordance with the literature (Welsh et al., 2009).

In the second part of my thesis, the investigated substance was the metabolite of imidacloprid, desnitro-imidacloprid. *In vitro* cell experiments revealed evidence of developmental neurotoxicity and the potency was compared with impacts of nicotine exposure (Kimura-Kuroda et al., 2012, Loser et al., 2021a). Therefore, my research question was if desnitro-imidacloprid is able to exert a similar toxic behavior in a complex developing organism. My results did not underpin the outcomes of the *in vitro* studies even though nicotine and desnitro-imidacloprid share the same mode of action. Acutely, no major impact was visible and also the sensitive coiling activity remained unaffected. Additionally, low amounts of the metabolite were detectable in the fish. Since bioaccumulation was not observed, I assume a further metabolization or excretion. The absence of effects in my findings points to the discrepancies and challenges in translating findings from cell experiments to the whole organism.

In the third part of my thesis, I investigated the developmental neurotoxic impacts of the psychoactive antidepressants sertraline, paroxetine and venlafaxine which are increasingly prevalent in the aquatic environment. After acute exposure to all three substances, I found consistent signs of cardiotoxicity and balance disturbance, which became apparent in the first swimming attempts. These first indications of behavioral toxicity were also apparent in altered coiling behavior as well as decreased swimming performance and stimuli reactions. At least for sertraline, I could detect these effects at environmentally relevant concentrations, from which I conclude that there is a realistic risk for fish in contaminated environments.

Detection of behavioral alterations, especially in developmental stages, can be alarming as they can have long-lasting and severe consequences on fitness and survival. Restricted movement has proven to impact foraging and food intake which in turn can directly be connected to reduced energy supply, growth and finally survival (de Farias et al., 2019, Little and Finger, 1990). Moreover, fish can be more vulnerable to predators as they were less able to escape quickly (Weis et al., 2001).

However, since behavior is highly sensitive, this also means that it is responsive to many different factors. This includes *i.a.* age and the differences between individuals, replicates and strains (Colwill and Creton, 2011, de Esch et al., 2012, Demin et al., 2019, Padilla et al., 2011). Besides intrinsic factors also extrinsic experimental conditions play an important role in baseline activity (Ogungbemi et al.,

2019, Zellner et al., 2011). In order to make behavioral tests replicable and to allow a better comparison of results between experiments and laboratories, it is important to minimize possible deviations by standardizing a protocol. In my opinion, GAM as a basis could complement the standardized analysis, as it can be adjusted to individual circumstances and needs.

Since the zebrafish embryo in the FET showed fewer signs of neurotoxic symptoms than the adult fish in the AFT tests, sensitive embryonic behavioral assays can bridge these limitations for this life stage. So far, proposed human cell-based *in vitro* test battery covers essential neurodevelopmental processes of a developing brain from proliferation, neuronal network formation and maturation (Masjosthusmann et al., 2020). Nevertheless, experts still doubt that cell-based test batteries are already suitable to replace *in vivo* models to adequately assess the risk for humans and the environment (Juberg et al., 2023). Therefore, the zebrafish embryo as a living organism on the one hand and an *in vitro* model from a regulatory perspective on the other can provide and complement originating test batteries to close important knowledge gaps. Within such an *in vitro* test battery, the zebrafish embryo can be especially valuable since it is able to cover both human-health and environmental related challenges associated with developmental neurotoxic substances.

9   OWN CONTRIBUTION TO DATA COLLECTION AND ANALYSIS AND OWN PUBLICATIONS

9.1   Author´s contribution statement

Unless stated otherwise, the content of this work was created entirely by me.

Under chapter 1, experiments (1.1.1 and 4.2.2) were supported by the student Robin Hannemann. In chapter 1, the students Saskia Hagstotz (3.4), Tim Freitag (3.4, 7.2.2), Mona Wiesenberger (3.3, 3.4), Katharina Zorko (3.3, 3.4), and Sophie Trender (7.2.2) supported a part of the experiments. This support included the collection of data and was always carried out with my collaboration and under my supervision. Excluded from this work was the conceptualization, planning, analysis as well as interpretation of the data which was done by me. The list of supervised bachelor theses can be found under 1.1.

For the implementation of the generalized additive model (4.2.4), I collaborated with Dr. Raoul Wolf from the Norwegian Geotechnical Institute (NGI) in Oslo, Norway, to conceptualize and improve the R code for the analysis of tail coiling behavior.

The analytical measurements (5.2.2) of desnitro-imidacloprid within zebrafish embryos was conducted by Dr. Caroline Bauch from the company Cyprotex, UK.

Joint work is labelled accordingly in the text with footnotes on the respective page and are additionally defined below.

Footnotes:

1   I was supported in the data collection by Bachelor students. Further information on the individual contributions can be found as statements at the beginning of relevant chapters as well as in detail in chapter 0.

2   All PhD students and postdocs from the working group Aquatic Ecology and Toxicology at the University of Heidelberg.

3   Implementation in cooperation with Dr. Raoul Wolf from NGI, Norway.

4   The analytical measurements of water and embryo samples were conducted by Dr. Caroline Bauch from Cyprotex, UK.

5   Acute toxicity data from venlafaxine FET experiments conducted by Saskia Hagstotz, Lea Dober and Katharina Brotzmann

9.2 Publications in preparation

In total, three manuscripts are currently under preparation.

<u>Maria Fischer</u>; Raoul Wolf, Robin Hannemann, Thomas Braunbeck (202X): **Generalized additive modeling as a tool for the analysis of the time course of tail coiling behavior in zebrafish (*Danio rerio*) embryos – a proof-of-concept study with nicotine, a known developmental neurotoxicant**

In this manuscript I will include data from chapter 4. This is going to be the data on coiling behavior, motoneuron and muscle integrity.

<u>Maria Fischer</u>; Raoul Wolf, Caroline Bauch, Thomas Braunbeck (202X): **Desnitro-imidacloprid is not as toxic as nicotine – A comparison of the tail coiling behavior in zebrafish embryos (*Danio rerio*)**

In this manuscript I will include data from chapter 5. This is going to be the data on acute toxicity, coiling behavior as well as the analytical measurements.

Maria Fischer, Katharina Brotzmann, Jorge Lejo Santiago, Soledad Norberta Muniategui Lorenzo, Thomas Braunbeck (202X): **Impact of sertraline, paroxetine and venlafaxine on the development and behavior of zebrafish (*Danio rerio*) embryo**

In this manuscript I will include data from chapter 7. This is going to be the data on acute toxicity, coiling behavior, visual-motor response as well as not yet completed analytical measurements.

9.3   Overview of supervised Bachelor theses

Saskia Hagstotz (2021/2022): **Toxizität und Teratogenität des Antidepressivums Venlafaxin im Embryo des Zebrabärblings (*Danio rerio*).** *Saskia Hagstotz was jointly supervised with Katharina Brotzmann and myself.*

Tim Freitag (2022): **Comparison of early coiling behavior and later visual motor response of zebrafish (*Danio rerio*) embryos exposed to the antidepressant venlafaxine.**

Mona Wiesenberger (2022): **An investigation into the antidepressant paroxetine using the Fish Embryo Acute Toxicity (FET) test and the coiling assay with zebrafish embryos (*Danio rerio*).**

Robin Hannemann (2023): **Evaluation of muscle and motoneuron integrity in zebrafish (*Danio rerio*) embryo after exposure to nicotine.**

Katharina Zorko (2023): **Developmental and behavioral effects of sertraline exposure in zebrafish (*Danio rerio*) embryos.**

Sophie Trender (2023): **Behavioral alterations caused by paroxetine and sertraline in zebrafish (*Danio rerio*) embryos.**

9.4 Copyright information

The following list contains copyright information about the images that were used in the introduction. A license number is provided, unless the articles, from which figures were used, are distributed under the terms of the Creative Commons Attribution License (CC BY 4.0; http://creativecommons.org/licenses/by/4.0/), which permits the use of images.

Figure 3	Mendieta-Serrano et al. (2022) – © 2022 The Authors **Slow muscles guide fast myocyte fusion to ensure robust myotome formation despite the high spatiotemporal stochasticity of fusion events** Author: Mario A. Mendieta-Serrano, Sunandan Dhar, Boon Heng Ng, Rachna Narayanan, Jorge J.Y. Lee,Hui Ting Ong, Pearlyn Jia Ying Toh, Adrian Röllin, Sudipto Roy, Timothy E. Saunders Publication: Developmental Biology Publisher: Elsevier Date: 12 September 2022 DOI 10.1016/j.devcel.2022.08.002 Open access article distributed under the terms of the Creative Commons CC-BY license (https://creativecommons.org/licenses/by/4.0/).
Figure 4	Santiago et al. (2021) © 2021 The Authors **Mechanisms of TTNtv-Related Dilated Cardiomyopathy: Insights from Zebrafish Models.** Authors: Santiago, C.F.; Huttner, I.G.; Fatkin, D. Publication: Journal for Cardiovascular Development and Disease Publisher: MDPI Date: 22. January 2021 DOI 10.3390/jcdd8020010 Open access article distributed under the terms of the Creative Commons CC-BY license (https://creativecommons.org/licenses/by/4.0/).
Figure 5	College Physics © August 22, 2016 by OpenStax Figure 13 in chapter 27.8 Polarization by the authors Paul Peter Urone and Roger Hinrichts, licensed under CC BY 4.0 (https://creativecommons.org/licenses/by/4.0/).

10 ACKNOWLEDGEMENTS

First of all, I would like to thank Prof. Dr. Thomas Braunbeck, without whom I would not have been able to start or finish this project. Your valuable insights and suggestions have contributed significantly to the development of my scientific work.

Many thanks to my second examiner, Prof. Dr. Joachim Sturve, who supervised me already during my master's degree. Jag tackar dig för ditt viktiga stöd. I would also like to thank Dr. Thomas Dickmeis as the third member of my TAC committee. Your suggestions and questions during the meetings have helped me to progress in my work. Moreover, I would like to thank Prof. Dr. Sabine Chourbaji, who agreed so quickly to be my fourth examiner. I was very happy.

To the entire Aquatic Ecology and Toxicology group, I was lucky to have you as a support. Your team spirit and intellectual exchange were really important and invaluable to me. Thanks for all the jokes and laughs outside of work. Cheers, Dr. Katharina Brotzmann, Max Rinderknecht, Dr. Patrick Heinrich, Dr. Suse Knörr, Corinna Vaßholz, Lisa Bauer, Dr. Lisa Gölz, Dr. Lisa Baumann and Dr. Nadine Kämmer. But also, thanks to Gero Hoffmann, who was always on point when his skills were needed.

Special thanks go to my Bachelor students, whom I was able to supervise. Thank you very much for your commitment. I hope you found it as interesting and exciting as I did. Many thanks to Saskia Hagstotz, Mona Wiesenberger, Tim Freitag, Robin Hannemann, Katharina Zorko and Sophie Trender.

Many thanks also to my friends, who were always happy to distract me with a bit of fun. Fabian and Tina, thanks a lot for helping me. I would especially like to thank my family. Thank you, Mama, Marc, Migge and Andy for your inexhaustible and warm-hearted support over all these years! Thanks as well, Papa. And above all, thank you, Frans, for always being there for me. That's the best support anyone could wish for! The last little thank you goes to Gigi, who has made this time easier and cheerful.

11 LITERATURE

Abou-Donia, M. B., Goldstein, L. B., Bullman, S., Tu, T., Khan, W. A., Dechkovskaia, A. M. & Abdel-Rahman, A. A. 2008. Imidacloprid induces neurobehavioral deficits and increases expression of glial fibrillary acidic protein in the motor cortex and hippocampus in offspring rats following in utero exposure. *Journal of Toxicology and Environmental Health, Part A - Current Issues,* 71**,** 119-30.

Alsop, D. & Wilson, J. Y. 2019. Waterborne pharmaceutical uptake and toxicity is modified by pH and dissolved organic carbon in zebrafish. *Aquatic Toxicology,* 210**,** 11-18.

Ames, J., Severo, E. S., Costa-Silva, D. G. D., Storck, T. R., Amaral, A. M. B. D., Miragem, A. A., Rosemberg, D. B. & Loro, V. L. 2023. Glyphosate-based herbicide (GBH) causes damage in embryo-larval stages of zebrafish. *Neurotoxicology and teratology,* 95.

Araya, C., Ward, L. C., Girdler, G. C. & Miranda, M. 2016. Coordinating cell and tissue behavior during zebrafish neural tube morphogenesis. *Developmental Dynamics,* 245**,** 197-208.

Aregahegn, K. Z., Shemesh, D., Gerber, R. B. & Finlayson-Pitts, B. J. 2017. Photochemistry of thin solid films of the neonicotinoid imidacloprid on surfaces. *Environmental Science & Technology,* 51**,** 2660-2668.

Atzei, A., Jense, I., Zwart, E. P., Legradi, J., Venhuis, B. J., Van Der Ven, L. T. M., Heusinkveld, H. J. & Hessel, E. V. S. 2021. Developmental neurotoxicity of environmentally relevant pharmaceuticals and mixtures thereof in a zebrafish embryo behavioural test. *International Journal of Environmental Research and Public Health,* 18.

Bachour, R.-L., Golovko, O., Kellner, M. & Pohl, J. 2020. Behavioral effects of citalopram, tramadol, and binary mixture in zebrafish (Danio rerio) larvae. *Chemosphere,* 238**,** 124587.

Bailey, J., Oliveri, A. & Levin, E. D. 2013. Zebrafish model systems for developmental neurobehavioral toxicology. *Birth Defects Research Part C-Embryo Today-Reviews,* 99**,** 14-23.

Bal-Price, A., Crofton, K. M., Sachana, M., Shafer, T. J., Behl, M., Forsby, A., Hargreaves, A., Landesmann, B., Lein, P. J., Louisse, J., Monnet-Tschudi, F., Paini, A., Rolaki, A., Schrattenholz, A., Suñol, C., Van Thriel, C., Whelan, M. & Fritsche, E. 2015. Putative adverse outcome pathways relevant to neurotoxicity. *Critical Reviews in Toxicology,* 45**,** 83-91.

Bal-Price, A., Pistollato, F., Sachana, M., Bopp, S. K., Munn, S. & Worth, A. 2018. Strategies to improve the regulatory assessment of developmental neurotoxicity (DNT) using methods. *Toxicology and Applied Pharmacology,* 354**,** 7-18.

Barreiro-Iglesias, A., Mysiak, K. S., Scott, A. L., Reimer, M. M., Yang, Y. J., Becker, C. G. & Becker, T. 2015. Serotonin promotes development and regeneration of spinal motor neurons in zebrafish. *Cell Reports,* 13**,** 924-932.

Basnet, R. M., Zizioli, D., Taweedet, S., Finazzi, D. & Memo, M. 2019. Zebrafish larvae as a behavioral model in neuropharmacology. *Biomedicines,* 7.

Bates, D., Machler, M., Bolker, B. M. & Walker, S. C. 2015. Fitting linear mixed-effects models using lme4. *Journal of Statistical Software,* 67**,** 1-48.

Bauer, B., Mally, A. & Liedtke, D. 2021. Zebrafish embryos and larvae as alternative animal models for toxicity testing. *International Journal of Molecular Sciences,* 22.

Behra, M., Cousin, X., Bertrand, C., Vonesch, J. L., Biellmann, D., Chatonnet, A. & Strahle, U. 2002. Acetylcholinesterase is required for neuronal and muscular development in the zebrafish embryo. *Nature Neuroscience,* 5**,** 111-8.

Belanger, S. E., Rawlings, J. M. & Carr, G. J. 2013. Use of fish embryo toxicity tests for the prediction of acute fish toxicity to chemicals. *Environmental Toxicology and Chemistry,* 32**,** 1768-1783.

Berger, J., Sztal, T. & Currie, P. D. 2012. Quantification of birefringence readily measures the level of muscle damage in zebrafish. *Biochemical and Biophysical Research Communications,* 423**,** 785-8.

Best, C., Melnyk-Lamont, N., Gesto, M. & Vijayan, M. M. 2014. Environmental levels of the antidepressant venlafaxine impact the metabolic capacity of rainbow trout. *Aquatic Toxicology,* 155**,** 190-198.

Blagden, C. S., Currie, P. D., Ingham, P. W. & Hughes, S. M. 1997. Notochord induction of zebrafish slow muscle mediated by Sonic hedgehog. *Genes & Development,* 11**,** 2163-2175.

Borrego-Soto, G. & Eberhart, J. K. 2022. Embryonic nicotine exposure disrupts adult social behavior and craniofacial development in zebrafish *Toxics,* 10.

Braunbeck, T., Kais, B., Lammer, E., Otte, J., Schneider, K., Stengel, D. & Strecker, R. 2015. The fish embryo test (FET): origin, applications, and future. *Environmental Science and Pollution Research,* 22**,** 16247-16261.

Brooks, B. W., Chambliss, C. K., Stanley, J. K., Ramirez, A., Banks, K. E., Johnson, R. D. & Lewis, R. J. 2005. Determination of select antidepressants in fish from an effluent-dominated stream. *Environmental Toxicology and Chemistry: An International Journal,* 24**,** 464-469.

Bruin, J. E., Gerstein, H. C. & Holloway, A. C. 2010. Long-term consequences of fetal and neonatal nicotine exposure: a critical review. *Toxicological Sciences,* 116**,** 364-374.

Brustein, E., Saint-Amant, L., Buss, R. R., Chong, M., Mcdearmid, J. R. & Drapeau, P. 2003. Steps during the development of the zebrafish locomotor network. *J Physiol Paris,* 97**,** 77-86.

Buonanno, A. & Fields, R. D. 1999. Gene regulation by patterned electrical activity during neural and skeletal muscle development. *Current Opinion in Neurobiology,* 9**,** 110-20.

Burke, A. P., Niibori, Y., Terayama, H., Ito, M., Pidgeon, C., Arsenault, J., Camarero, P. R., Cummins, C. L., Mateo, R., Sakabe, K. & Hampson, D. R. 2018. Mammalian susceptibility to a neonicotinoid insecticide after fetal and early postnatal exposure. *Scientific Reports,* 8**,** 16639.

Busch, W., Schmidt, S., Kühne, R., Schulze, T., Krauss, M. & Altenburger, R. 2016. Micropollutants in European rivers: A mode of action survey to support the development of effect-based tools for water monitoring. *Environmental Toxicology and Chemistry,* 35**,** 1887-1899.

Busquet, F., Strecker, R., Rawlings, J. M., Belanger, S. E., Braunbeck, T., Carr, G. J., Cenijn, P., Fochtman, P., Gourmelon, A., Huebler, N., Kleensang, A., Knoebel, M., Kussatz, C., Legler, J., Lillicrap, A., Martinez-Jeronimo, F., Polleichtner, C., Rzodeczko, H., Salinas, E., Schneider, K. E., Scholz, S., Van Den Brandhof, E. J., Van Der Ven, L. T. M., Walter-Rohde, S., Weigt, S., Witters, H. & Haider, M. 2014. OECD validation study to assess intra- and inter-laboratory reproducibility of the zebrafish embryo toxicity test for acute aquatic toxicity testing. *Regulatory Toxicology and Pharmacology,* 69**,** 496-511.

Buss, R. R. & Drapeau, P. 2000. Physiological properties of zebrafish embryonic red and white muscle fibers during early development. *Journal of Neurophysiology,* 84**,** 1545-1557.

Carty, D. R., Hala, D. & Huggett, D. B. 2017. The Effects of Sertraline on Fathead Minnow (Pimephales promelas) Growth and Steroidogenesis. *Bulletin of Environmental Contamination and Toxicology,* 98**,** 753-757.

Casida, J. E. 2018. Neonicotinoids and other insect nicotinic receptor competitive modulators: progress and prospects. *Annual Review of Entomology,* 63**,** 125-144.

Chao, S. L. & Casida, J. E. 1997. Interaction of imidacloprid metabolites and analogs with the nicotinic acetylcholine receptor of mouse brain in relation to toxicity. *Pesticide Biochemistry and Physiology,* 58**,** 77-88.

Chen, T. H., Wang, Y. H. & Wu, Y. H. 2011. Developmental exposures to ethanol or dimethylsulfoxide at low concentrations alter locomotor activity in larval zebrafish: Implications for behavioral toxicity bioassays. *Aquatic Toxicology,* 102**,** 162-166.

Chiffre, A., Clérandeau, C., Dwoinikoff, C., Le Bihanic, F., Budzinski, H., Geret, F. & Cachot, J. 2016. Psychotropic drugs in mixture alter swimming behaviour of Japanese medaka (Oryzias latipes) larvae above environmental concentrations. *Environmental Science and Pollution Research,* 23**,** 4964-4977.

Choe, C. P., Choi, S.-Y., Kee, Y., Kim, M. J., Kim, S.-H., Lee, Y., Park, H.-C. & Ro, H. 2021. Transgenic fluorescent zebrafish lines that have revolutionized biomedical research. *Laboratory Animal Research,* 37**,** 26.

Christou, M., Kavaliauskis, A., Ropstad, E. & Fraser, T. W. K. 2020. DMSO effects larval zebrafish (Danio rerio) behavior, with additive and interaction effects when combined with positive controls. *Science of the Total Environment,* 709.

Chu, S. & Metcalfe, C. D. 2007. Analysis of paroxetine, fluoxetine and norfluoxetine in fish tissues using pressurized liquid extraction, mixed mode solid phase extraction cleanup and liquid chromatography–tandem mass spectrometry. *Journal of Chromatography A,* 1163**,** 112-118.

Claudio, L., Kwa, W. C., Russell, A. L. & Wallinga, D. 2000. Testing Methods for Developmental Neurotoxicity of Environmental Chemicals. *Toxicology and Applied Pharmacology,* 164**,** 1-14.

Collier, A. D., Abdulai, A. R. & Leibowitz, S. F. 2023. Utility of the zebrafish model for studying neuronal and behavioral disturbances induced by embryonic exposure to alcohol, nicotine, and cannabis. *Cells,* 12.

Colwill, R. M. & Creton, R. 2011. Locomotor behaviors in zebrafish (Danio rerio) larvae. *Behavioural Processes,* 86**,** 222-229.

Correia, D., Bellot, M., Prats, E., Gómez-Canela, C., Moro, H., Raldúa, D., Domingues, I., Oliveira, M. & Faria, M. 2023. Impact of environmentally relevant concentrations of fluoxetine on zebrafish larvae: From gene to behavior. *Chemosphere,* 345**,** 140468.

Costa, L. G., Giordano, G., Guizzetti, M. & Vitalone, A. 2008. Neurotoxicity of pesticides: a brief review. *FBL,* 13**,** 1240-1249.

Côté, F., Fligny, C., Bayard, E., Launay, J.-M., Gershon, M. D., Mallet, J. & Vodjdani, G. 2007. Maternal serotonin is crucial for murine embryonic development. *Proceedings of the National Academy of Sciences,* 104**,** 329-334.

Crewe, H. K., Lennard, M. S., Tucker, G. T., Woods, F. R. & Haddock, R. E. 2004. The effect of selective serotonin re-uptake inhibitors on cytochrome P4502D6 (CYP2D6) activity in human liver microsomes *British Journal of Clinical Pharmacology,* 58**,** S744-S747.

D'amora, M. & Giordani, S. 2018. The utility of zebrafish as a model for screening gevelopmental neurotoxicity. *Frontiers in Neuroscience,* 12.

Daughton, C. G. 2002. Environmental stewardship and drugs as pollutants. *Lancet,* 360**,** 1035-6.

De Esch, C., Van Der Linde, H., Slieker, R., Willemsen, R., Wolterbeek, A., Woutersen, R. & De Groot, D. 2012. Locomotor activity assay in zebrafish larvae: influence of age, strain and ethanol. *Neurotoxicology and teratology,* 34**,** 425-33.

De Farias, N. O., Oliveira, R., Sousa-Moura, D., De Oliveira, R. C. S., Rodrigues, M. a. C., Andrade, T. S., Domingues, I., Camargo, N. S., Muehlmann, L. A. & Grisolia, C. K. 2019. Exposure to low concentration of fluoxetine affects development, behaviour and acetylcholinesterase activity of zebrafish embryos. *Comparative Biochemistry and Physiology Part C: Toxicology & Pharmacology,* 215**,** 1-8.

De Koning, C., Beekhuijzen, M., Tobor-Kaplon, M., De Vries-Buitenweg, S., Schoutsen, D., Leeijen, N., Van De Waart, B. & Emmen, H. 2015. Visualizing compound distribution during zebrafish embryo development: The effects of lipophilicity and DMSO. *Birth Defects Research Part B-Developmental and Reproductive Toxicology,* 104**,** 253-272.

De Oliveira, A. a. S., Brigante, T. a. V. & Oliveira, D. P. 2021. Tail coiling assay in zebrafish (Danio rerio) embryos: stage of development, promising positive control candidates, and selection of an appropriate organic solvent for screening of developmental neurotoxicity (DNT). *Water,* 13.

Dean, L. 2012. Venlafaxine therapy and CYP2D6 genotype. *In:* PRATT, V. M., SCOTT, S. A., PIRMOHAMED, M., ESQUIVEL, B., KATTMAN, B. L. & MALHEIRO, A. J. (eds.) *Medical Genetics Summaries.* Bethesda (MD).

Demin, K. A., Lakstygal, A. M., Alekseeva, P. A., Sysoev, M., De Abreu, M. S., Alpyshov, E. T., Serikuly, N., Wang, D., Wang, M., Tang, Z., Yan, D., Strekalova, T. V., Volgin, A. D., Amstislavskaya, T. G., Wang, J., Song, C. & Kalueff, A. V. 2019. The role of intraspecies variation in fish neurobehavioral and neuropharmacological phenotypes in aquatic models. *Aquatic Toxicology,* 210**,** 44-55.

Devoto, S. H., Melancon, E., Eisen, J. S. & Westerfield, M. 1996. Identification of separate slow and fast muscle precursor cells in vivo, prior to somite formation. *Development,* 122**,** 3371-3380.

Diaz-Garzon Marco, J., Fernandez-Calle, P. & Ricos, C. 2020. Models to estimate biological variation components and interpretation of serial results: strengths and limitations. *Advances in Laboratory Medicine,* 1**,** 20200063.

Din, E. 2001. German standard methods for the examination of water, waste water and sludge–subanimal testing (group T)–part 6: toxicity to fish. *Determination of the non-acute-poisonous effect of waste water to fish eggs by dilution limits***,** 38415-6.

Dinno, A. 2015. Nonparametric pairwise multiple comparisons in independent groups using Dunn's test. *Stata Journal,* 15**,** 292-300.

Douma, J. C. & Weedon, J. T. 2019. Analysing continuous proportions in ecology and evolution: A practical introduction to beta and Dirichlet regression. *Methods in Ecology and Evolution,* 10**,** 1412-1430.

Downes, G. B. & Granato, M. 2006. Supraspinal input is dispensable to generate glycine-mediated locomotive behaviors in the zebrafish embryo. *Journal of Neurobiology,* 66**,** 437-451.

Drapeau, P., Saint-Amant, L., Buss, R. R., Chong, M., Mcdearmid, J. R. & Brustein, E. 2002. Development of the locomotor network in zebrafish. *Progress in Neurobiology,* 68**,** 85-111.

Duzguner, V. & Erdogan, S. 2012. Chronic exposure to imidacloprid induces inflammation and oxidative stress in the liver & central nervous system of rats. *Pesticide Biochemistry and Physiology,* 104**,** 58-64.

Easter, S. S., Jr. & Nicola, G. N. 1996. The development of vision in the zebrafish (Danio rerio). *Developmental Biology,* 180**,** 646-63.

Echa 2017. Guidance on Information Requirements and Chemical Safety Assessment, Chapter R.11: PBT/vPvB assessment.

Echa 2018. 21 551 chemicals on EU market now registered. European Chemical Agency

Eddins, D., Cerutti, D., Williams, P., Linney, E. & Levin, E. D. 2010. Zebrafish provide a sensitive model of persisting neurobehavioral effects of developmental chlorpyrifos exposure: Comparison with nicotine and pilocarpine effects and relationship to dopamine deficits. *Neurotoxicology and teratology,* 32**,** 99-108.

Eisen, J. S. 1991a. Determination of primary motoneuron identity in developing zebrafish embryos. *Science,* 252**,** 569-572.

Eisen, J. S. 1991b. Motoneuronal development in the embryonic zebrafish. *Development***,** 141-147.

Eisen, J. S., Pike, S. H. & Romancier, B. 1990. An identified motoneuron with variable fates in embryonic zebrafish. *Journal of Neuroscience,* 10**,** 34-43.

Embry, M. R., Belanger, S. E., Braunbeck, T. A., Galay-Burgos, M., Halder, M., Hinton, D. E., Léonard, M. A., Lillicrap, A., Norberg-King, T. & Whale, G. 2010. The fish embryo toxicity test as an

animal alternative method in hazard and risk assessment and scientific research. *Aquatic Toxicology,* 97**,** 79-87.

Eng, M. L., Hao, C. Y., Watts, C., Sun, F. R. & Morrissey, C. A. 2021. Characterizing imidacloprid and metabolites in songbird blood with applications for diagnosing field exposures. *Science of the Total Environment,* 760.

Engel, A. G., Branton, D., Schotland, D. L., Fleischer, S., Dekruijff, B., Charnock, J. S., Hyde, J. S., Butterfield, D. A., Sandra, A., Howland, J. L., Glaser, M., Gonzalezros, J., Kent, C., Willner, J., Cullis, P. R., Wolf, S., Murray, A. K. & Park, J. H. 1982. Abnormalities in muscle in duchenne muscular-dystrophy - synthesis and speculation. *Advances in Experimental Medicine and Biology,* 140**,** 211-259.

England, L. J., Aagaard, K., Bloch, M., Conway, K., Cosgrove, K., Grana, R., Gould, T. J., Hatsukami, D., Jensen, F., Kandel, D., Lanphear, B., Leslie, F., Pauly, J. R., Neiderhiser, J., Rubinstein, M., Slotkin, T. A., Spindel, E., Stroud, L. & Wakschlag, L. 2017. Developmental toxicity of nicotine: A transdisciplinary synthesis and implications for emerging tobacco products. *Neuroscience and Biobehavioral Reviews,* 72**,** 176-189.

Eu 2010. Directive 2010/63/EU of the European Parliament and of the Council of 22 September 2010 on the protection of animals used for scientific purposes *Official Journal of the European Union.*

Fan, C.-Y., Cowden, J., Simmons, S. O., Padilla, S. & Ramabhadran, R. 2010. Gene expression changes in developing zebrafish as potential markers for rapid developmental neurotoxicity screening. *Neurotoxicology and teratology,* 32**,** 91-98.

Faria, M., Bedrossiantz, J., Prats, E., Rovira Garcia, X., Gomez-Canela, C., Pina, B. & Raldua, D. 2019. Deciphering the mode of action of pollutants impairing the fish larvae escape response with the vibrational startle response assay. *Science of the Total Environment,* 672**,** 121-128.

Faria, M., Bellot, M., Soto, O., Prats, E., Montemurro, N., Manjarrés, D., Gómez-Canela, C. & Raldúa, D. 2022. Developmental exposure to sertraline impaired zebrafish behavioral and neurochemical profiles. *Frontiers in Physiology,* 13.

Fernandes, A. M., Fero, K., Arrenberg, A. B., Bergeron, S. A., Driever, W. & Burgess, H. A. 2012. Deep brain photoreceptors control light-seeking behavior in zebrafish larvae. *Current Biology,* 22**,** 2042-2047.

Ferreira, C. S. S., Venâncio, C., Kille, P. & Oliveira, M. 2023. Are early and young life stages of fish affected by paroxetine? A case study with Danio rerio. *Science of the Total Environment,* 900**,** 165706.

Frew, J. A., Brown, J. T., Fitzsimmons, P. N., Hoffman, A. D., Sadilek, M., Grue, C. E. & Nichols, J. W. 2018. Toxicokinetics of the neonicotinoid insecticide imidacloprid in rainbow trout (Oncorhynchus mykiss). *Comparative Biochemistry and Physiology C-Toxicology & Pharmacology,* 205**,** 34-42.

Fricker, A. D., Rios, C., Devi, L. A. & Gomes, I. 2005. Serotonin receptor activation leads to neurite outgrowth and neuronal survival. *Molecular brain research,* 138**,** 228-235.

Fritsche, E., Alm, H., Baumann, J., Geerts, L., Håkansson, H., Masjosthusmann, S. & Witters, H. 2015. Literature review on in vitro and alternative Developmental Neurotoxicity (DNT) testing methods. *EFSA Supporting Publications,* 12**,** 778E.

Ganzen, L., Venkatraman, P., Pang, C. P., Leung, Y. F. & Zhang, M. Z. 2017. Utilizing zebrafish visual behaviors in drug screening for retinal degeneration. *International Journal of Molecular Sciences,* 18.

Gaspar, P., Cases, O. & Maroteaux, L. 2003. The developmental role of serotonin: news from mouse molecular genetics. *Nature Reviews Neuroscience,* 4**,** 1002-1012.

Gould, S. L., Winter, M. J., Norton, W. H. J. & Tyler, C. R. 2021. The potential for adverse effects in fish exposed to antidepressants in the aquatic environment. *Environmental Science & Technology,* 55**,** 16299-16312.

Grabicová, K., Grabic, R., Fedorova, G., Kolářová, J., Turek, J., Brooks, B. W. & Randák, T. 2020. Psychoactive pharmaceuticals in aquatic systems: A comparative assessment of environmental monitoring approaches for water and fish. *Environmental Pollution,* 261**,** 114150.

Grandjean, P. & Landrigan, P. J. 2006. Developmental neurotoxicity of industrial chemicals. *Lancet,* 368**,** 2167-78.

Guisan, A., Edwards, T. C. & Hastie, T. 2002. Generalized linear and generalized additive models in studies of species distributions: setting the scene. *Ecological Modelling,* 157**,** 89-100.

Haddon, C. & Lewis, J. 1996. Early ear development in the embryo of the zebrafish, Danio rerio. *Journal of Comparative Neurology,* 365**,** 113-28.

Halbach, K., Ulrich, N., Goss, K. U., Seiwert, B., Wagner, S., Scholz, S., Luckenbach, T., Bauer, C., Schweiger, N. & Reemtsma, T. 2020. Yolk sac of zebrafish embryos as backpack for chemicals? *Environmental Science and Technology,* 54**,** 10159-10169.

Hallare, A., Nagel, K., Köhler, H. R. & Triebskorn, R. 2006. Comparative embryotoxicity and proteotoxicity of three carrier solvents to zebrafish (<i>Danio rerio</i>) embryos. *Ecotoxicology and Environmental Safety,* 63**,** 378-388.

Hastie, T. & Tibshirani, R. 1986. Generalized Additive Models. *Statistical Science,* 1**,** 297-318.

Henn, K. & Braunbeck, T. 2011. Dechorionation as a tool to improve the fish embryo toxicity test (FET) with the zebrafish (Danio rerio). *Comparative Biochemistry and Physiology Part C: Toxicology & Pharmacology,* 153**,** 91-98.

Henry, J., Bai, Y. T., Kreuder, F., Saaristo, M., Kaslin, J. & Wlodkowic, D. 2022. Sensory-motor perturbations in larval zebrafish (Danio rerio) induced by exposure to low levels of neuroactive micropollutants during development. *International Journal of Molecular Sciences,* 23.

Hill, B. N., Britton, K. N., Hunter, D. L., Olin, J. K., Lowery, M., Hedge, J. M., Knapp, B. R., Jarema, K. A., Rowson, Z. & Padilla, S. 2023. Inconsistencies in variable reporting and methods in larval zebrafish behavioral assays. *Neurotoxicology and teratology,* 96.

Hirata, H., Saint-Amant, L., Downes, G. B., Cui, W. W., Zhou, W. B., Granato, M. & Kuwada, J. Y. 2005. Zebrafish bandoneon mutants display behavioral defects due to a mutation in the glycine receptor β-subunit. *Proceedings of the National Academy of Sciences of the United States of America,* 102**,** 8345-8350.

Holley, S. A. & Nüsslein-Volhard, C. 1999. 8 Somitogenesis in Zebrafish. *Current Topics in Developmental Biology,* 47**,** 247-277.

Hong, X., Chen, R., Zhang, L., Yan, L., Li, J. & Zha, J. 2022a. Low doses and lifecycle exposure of waterborne antidepressants in zebrafish model: A survey on sperm traits, reproductive behaviours, and transcriptome responses. *Science of the Total Environment,* 832**,** 155017.

Hong, X., Zhao, G., Zhou, Y., Chen, R., Li, J. & Zha, J. 2021a. Risks to aquatic environments posed by 14 pharmaceuticals as illustrated by their effects on zebrafish behaviour. *Science of the Total Environment,* 771**,** 145450.

Hong, X. S., Chen, R., Zhang, L., Yan, L., Li, J. S. & Zha, J. M. 2022b. Low doses and lifecycle exposure of waterborne antidepressants in zebrafish model: A survey on sperm traits, reproductive behaviours, and. *Science of the Total Environment,* 832.

Hong, X. S., Zhao, G. F., Zhou, Y. Q., Chen, R., Li, J. S. & Zha, J. M. 2021b. Risks to aquatic environments posed by 14 pharmaceuticals as illustrated by their effects on zebrafish behaviour. *Science of the Total Environment,* 771.

Hua, J. H., Wang, X. L., Zhu, J. P., Wang, Q. W., Zhang, W., Lei, L., Zhu, B. R., Han, J., Yang, L. H. & Zhou, B. S. 2022. Decabromodiphenyl ethane induced hyperactivity in developing zebrafish at environmentally relevant concentrations. *Ecotoxicology and Environmental Safety,* 244.

Huang, I. J., Sirotkin, H. I. & Mcelroy, A. E. 2019. Varying the exposure period and duration of neuroactive pharmaceuticals and their metabolites modulates effects on the visual motor response in zebrafish (Danio rerio) larvae. *Neurotoxicology and teratology,* 72**,** 39-48.

Huang, Y. S., Cartlidge, R., Walpitagama, M., Kaslin, J., Campana, O. & Wlodkowic, D. 2018. Unsuitable use of DMSO for assessing behavioral endpoints in aquatic model species. *Science of the Total Environment,* 615**,** 107-114.

Hutchinson, S. A. & Eisen, J. S. 2006. Islet1 and Islet2 have equivalent abilities to promote motoneuron formation and to specify motoneuron subtype identity. *Development,* 133**,** 2137-2147.

Jarque, S., Rubio-Brotons, M., Ibarra, J., Ordoñez, V., Dyballa, S., Miñana, R. & Terriente, J. 2020. Morphometric analysis of developing zebrafish embryos allows predicting teratogenicity modes of action in higher vertebrates. *Reproductive Toxicology,* 96**,** 337-348.

Johnston, I. A., Bower, N. I. & Macqueen, D. J. 2011. Growth and the regulation of myotomal muscle mass in teleost fish. *Journal of Experimental Biology,* 214**,** 1617-1628.

Johnston, I. A., Davison, W. & Goldspink, G. 1977. Energy-metabolism of carp swimming muscles. *Journal of Comparative Physiology,* 114**,** 203-216.

Joint Research Centre, Health, I. F. & Protection, C. 2014. *EURL ECVAM, recommendation on the zebrafish embryo acute toxicity test method (ZFET) for acute aquatic toxicity testing*, Publications Office.

Juberg, D. R., Fox, D. A., Forcelli, P. A., Kacew, S., Lipscomb, J. C., Saghir, S. A., Sherwin, C. M., Koenig, C. M., Hays, S. M. & Kirman, C. R. 2023. A perspective on In vitro developmental neurotoxicity test assay results: An expert panel review. *Regulatory Toxicology and Pharmacology,* 143**,** 105444.

Kais, B., Schiwy, S., Hollert, H., Keiter, S. H. & Braunbeck, T. 2017. EROD assays with the zebrafish as rapid screening tools for the detection of dioxin-like activity. *Science of the Total Environment,* 590**,** 269-280.

Kais, B., Schneider, K. E., Keiter, S., Henn, K., Ackermann, C. & Braunbeck, T. 2013. DMSO modifies the permeability of the zebrafish (Danio rerio) chorion-Implications for the fish embryo test (FET). *Aquatic Toxicology,* 140**,** 229-238.

Kalueff, A. V., Gebhardt, M., Stewart, A. M., Cachat, J. M., Brimmer, M., Chawla, J. S., Craddock, C., Kyzar, E. J., Roth, A., Landsman, S., Gaikwad, S., Robinson, K., Baatrup, E., Tierney, K., Shamchuk, A., Norton, W., Miller, N., Nicolson, T., Braubach, O., Gilman, C. P., Pittman, J., Rosemberg, D. B., Gerlai, R., Echevarria, D., Lamb, E., Neuhauss, S. C. F., Weng, W., Bally-Cuif, L., Schneider, H. & Znrc 2013. Towards a comprehensive catalog of zebrafish behavior 1.0 and beyond. *Zebrafish,* 10**,** 70-86.

Kämmer, N., Erdinger, L. & Braunbeck, T. 2022. The onset of active gill respiration in post-embryonic zebrafish (Danio rerio) larvae triggers an increased sensitivity to neurotoxic compounds. *Aquatic Toxicology,* 249**,** 106240.

Kent, M. E., Eggleston, T. M., Squires, R. S., Zimmerman, K. A., Weiss, R. M., Roghair, R. D., Lin, F., Cornell, R. A., Haskell, S. E. & Hu, B. 2022. Hypersensitivity of Zebrafish htr2b Mutant Embryos to Sertraline Indicates a Role for Serotonin Signaling in Cardiac Development. *Journal of Cardiovascular Pharmacology,* 80**,** 261-269.

Kimmel, C. B. 1993. Patterning the brain of the zebrafish embryo. *Annual review of neuroscience,* 16**,** 707-732.

Kimmel, C. B., Ballard, W. W., Kimmel, S. R., Ullmann, B. & Schilling, T. F. 1995. Stages of embryonic development of the zebrafish. *Developmental Dynamics,* 203**,** 253-310.

Kimmel, C. B., Patterson, J. & Kimmel, R. O. 1974. The development and behavioral characteristics of the startle response in the zebra fish. *Developmental Psychobiology,* 7**,** 47-60.

Kimura-Kuroda, J., Komuta, Y., Kuroda, Y., Hayashi, M. & Kawano, H. 2012. Nicotine-like effects of the neonicotinoid insecticides acetamiprid and imidacloprid on cerebellar neurons from neonatal rats. *Plos One,* 7**,** e32432.

Kleywegt, S., Payne, M., Ng, F. & Fletcher, T. 2019. Environmental loadings of active pharmaceutical ingredients from manufacturing facilities in Canada. *Science of the Total Environment,* 646**,** 257-264.

Klüver, N., König, M., Ortmann, J., Massei, R., Paschke, A., Kühne, R. & Scholz, S. 2015. Fish embryo toxicity test: Identification of compounds with weak toxicity and analysis of behavioral effects to improve prediction of acute toxicity for neurotoxic compounds. *Environmental Science & Technology,* 49**,** 7002-7011.

Kolanczyk, R. C., Tapper, M. A., Sheedy, B. R. & Serrano, J. A. 2020. In vitro metabolism of imidacloprid and acetamiprid in rainbow trout and rat. *Xenobiotica,* 50**,** 805-814.

Konemann, S., Von Wyl, M. & Vom Berg, C. 2022. Zebrafish larvae rapidly recover from locomotor effects and neuromuscular alterations induced by cholinergic insecticides. *Environmental Science & Technology*.

Koshlukova, S. 2006. Imidacloprid risk characterization document: dietary and drinking water exposure. *In:* AGENCY, D. O. P. R. C. E. P. (ed.).

Kou, Y. Y., Li, Z. H., Yang, T., Shen, X., Wang, X., Li, H. P., Zhou, K., Li, L. Y., Xia, Z. D., Zheng, X. H. & Zhao, Y. 2022. Therapeutic potential of plant iridoids in depression: a review. *Pharmaceutical Biology,* 60**,** 2167-2181.

Kowalska, M., Fijalkowski, L. & Nowaczyk, A. 2021. Assessment of paroxetine molecular interactions with selected monoamine and γ-aminobutyric acid transporters. *International Journal of Molecular Sciences,* 22.

Lacchetti, I., Cristiano, W., Di Domenico, K., Carere, M. & Mancini, L. 2022. Coiling Tail Activity in Zebrafish Embryo: A Protocol for an Early Warning System of Neurotoxic Substances. *Fresenius Environmental Bulletin,* 31**,** 8426-8433.

Ladefoged, O. & Miljöstyrelsen 1995. *Neurotoxicology: review of definitions, methodology and criteria*, Miljöstyrelsen.

Lajeunesse, A., Gagnon, C., Gagné, F., Louis, S., Čejka, P. & Sauvé, S. 2011. Distribution of antidepressants and their metabolites in brook trout exposed to municipal wastewaters before and after ozone treatment–Evidence of biological effects. *Chemosphere,* 83**,** 564-571.

Lammer, E., Carr, G. J., Wendler, K., Rawlings, J. M., Belanger, S. E. & Braunbeck, T. 2009a. Is the fish embryo toxicity test (FET) with the zebrafish (Danio rerio) a potential alternative for the fish acute toxicity test? *Comparative Biochemistry and Physiology C-Toxicology & Pharmacology,* 149**,** 196-209.

Lammer, E., Kamp, H. G., Hisgen, V., Koch, M., Reinhard, D., Salinas, E. R., Wendler, K., Zok, S. & Braunbeck, T. 2009b. Development of a flow-through system for the fish embryo toxicity test (FET) with the zebrafish. *Toxicology in Vitro,* 23**,** 1436-1442.

Lange, M., Neuzeret, F., Fabreges, B., Froc, C., Bedu, S., Bally-Cuif, L. & Norton, W. H. J. 2013. Inter-individual and inter-strain variations in zebrafish locomotor ontogeny. *Plos One,* 8.

Laskowski, M. B., Olson, W. H. & Dettbarn, W. D. 1975. Ultrastructural changes at the motor end-plant produced by an irreversible cholinesterase inhibitor. *Experimental Neurology,* 47**,** 290-306.

Lefebvre, J. L., Ono, F., Puglielli, C., Seidner, G., Franzini-Armstrong, C., Brehm, P. & Granato, M. 2004. Increased neuromuscular activity causes axonal defects and muscular degeneration. *Development,* 131**,** 2605-18.

Legradi, J. B., Di Paolo, C., Kraak, M. H. S., Van Der Geest, H. G., Schymanski, E. L., Williams, A. J., Dingemans, M. M. L., Massei, R., Brack, W., Cousin, X., Begout, M. L., Van Der Oost, R., Carion, A., Suarez-Ulloa, V., Silvestre, F., Escher, B. I., Engwall, M., Nilen, G., Keiter, S. H.,

Pollet, D., Waldmann, P., Kienle, C., Werner, I., Haigis, A. C., Knapen, D., Vergauwen, L., Spehr, M., Schulz, W., Busch, W., Leuthold, D., Scholz, S., Vom Berg, C. M., Basu, N., Murphy, C. A., Lampert, A., Kuckelkorn, J., Grummt, T. & Hollert, H. 2018. An ecotoxicological view on neurotoxicity assessment. *Environmental Sciences Europe,* 30.

Lillesaar, C. 2011. The serotonergic system in fish. *Journal of Chemical Neuroanatomy,* 41**,** 294-308.

Linney, E., Upchurch, L. & Donerly, S. 2004. Zebrafish as a neurotoxicological model. *Neurotoxicology and teratology,* 26**,** 709-718.

Little, E. E. & Finger, S. E. 1990. Swimming behavior as an indicator of sublethal toxicity in fish. *Environmental Toxicology and Chemistry,* 9**,** 13-19.

Liu, Q. Q., He, H. R., Yang, J., Feng, X. J., Zhao, F. F. & Lyu, J. 2020. Changes in the global burden of depression from 1990 to 2017: Findings from the Global Burden of Disease study. *Journal of Psychiatric Research,* 126**,** 134-140.

Loser, D., Grillberger, K., Hinojosa, M. G., Blum, J., Haufe, Y., Danker, T., Johansson, Y., Moller, C., Nicke, A., Bennekou, S. H., Gardner, I., Bauch, C., Walker, P., Forsby, A., Ecker, G. F., Kraushaar, U. & Leist, M. 2021a. Acute effects of the imidacloprid metabolite desnitro-imidacloprid on human nACh receptors relevant for neuronal signaling. *Archives of Toxicology,* 95**,** 3695-3716.

Loser, D., Hinojosa, M. G., Blum, J., Schaefer, J., Brull, M., Johansson, Y., Suciu, I., Grillberger, K., Danker, T., Moller, C., Gardner, I., Ecker, G. F., Bennekou, S. H., Forsby, A., Kraushaar, U. & Leist, M. 2021b. Functional alterations by a subgroup of neonicotinoid pesticides in human dopaminergic neurons. *Archives of Toxicology,* 95**,** 2081-2107.

Lowery, L. A. & Sive, H. 2004. Strategies of vertebrate neurulation and a re-evaluation of teleost neural tube formation. *Mechanisms of Development,* 121**,** 1189-1197.

Macphail, R. C., Brooks, J., Hunter, D. L., Padnos, B., Irons, T. D. & Padilla, S. 2009. Locomotion in larval zebrafish: Influence of time of day, lighting and ethanol. *Neurotoxicology,* 30**,** 52-58.

Mahai, G., Wan, Y., Wang, A., Xia, W., Shi, L., Wang, P., He, Z. & Xu, S. 2021. Selected transformation products of neonicotinoid insecticides (other than imidacloprid) in drinking water. *Environ Pollut,* 291**,** 118225.

Mahai, G., Wan, Y., Xia, W., Wang, A., Qian, X., Li, Y., He, Z., Li, Y. & Xu, S. 2022. Exposure assessment of neonicotinoid insecticides and their metabolites in Chinese women during pregnancy: A longitudinal study. *Science of the Total Environment,* 818**,** 151806.

Masjosthusmann, S., Blum, J., Bartmann, K., Dolde, X., Holzer, A.-K., Stürzl, L.-C., Keßel, E. H., Förster, N., Dönmez, A., Klose, J., Pahl, M., Waldmann, T., Bendt, F., Kisitu, J., Suciu, I., Hübenthal, U., Mosig, A., Leist, M. & Fritsche, E. 2020. Establishment of an a priori protocol for the implementation and interpretation of an in-vitro testing battery for the assessment of developmental neurotoxicity. *EFSA Supporting Publications,* 17**,** 1938E.

Massarsky, A., Jayasundara, N., Bailey, J. M., Oliveri, A. N., Levin, E. D., Prasad, G. L. & Di Giulio, R. T. 2015. Teratogenic, bioenergetic, and behavioral effects of exposure to total particulate matter on early development of zebrafish (Danio rerio) are not mimicked by nicotine. *Neurotoxicology and teratology,* 51**,** 77-88.

Mcdonald, M. D. 2017. An AOP analysis of selective serotonin reuptake inhibitors (SSRIs) for fish. *Comparative Biochemistry and Physiology C-Toxicology & Pharmacology,* 197**,** 19-31.

Melancon, E., Liu, D. W. C., Westerfield, M. & Eisen, J. S. 1997. Pathfinding by identified zebrafish motoneurons in the absence of muscle pioneers. *Journal of Neuroscience,* 17**,** 7796-7804.

Melnyk-Lamont, N., Best, C., Gesto, M. & Vijayan, M. M. 2014. The Antidepressant Venlafaxine Disrupts Brain Monoamine Levels and Neuroendocrine Responses to Stress in Rainbow Trout. *Environmental Science & Technology,* 48**,** 13434-13442.

Mendieta-Serrano, M. A., Dhar, S., Ng, B. H., Narayanan, R., Lee, J. J. Y., Ong, H. T., Toh, P. J. Y., Rollin, A., Roy, S. & Saunders, T. E. 2022. Slow muscles guide fast myocyte fusion to ensure robust myotome formation despite the high spatiotemporal stochasticity of fusion events. *Developmental Cell,* 57**,** 2095-+.

Menelaou, E., Husbands, E. E., Pollet, R. G., Coutts, C. A., Ali, D. W. & Svoboda, K. R. 2008. Embryonic motor activity and implications for regulating motoneuron axonal pathfinding in zebrafish. *European Journal of Neuroscience,* 28**,** 1080-1096.

Menelaou, E., Paul, L. T., Perera, S. N. & Svoboda, K. R. 2015. Motoneuron axon pathfinding errors in zebrafish: Differential effects related to concentration and timing of nicotine exposure. *Toxicology and Applied Pharmacology,* 284**,** 65-78.

Menelaou, E. & Svoboda, K. R. 2009. Secondary motoneurons in juvenile and adult zebrafish: axonal pathfinding errors caused by embryonic nicotine exposure. *Journal of Comparative Neurology,* 512**,** 305-322.

Metcalfe, C. D., Chu, S. G., Judt, C., Li, H. X., Oakes, K. D., Servos, M. R. & Andrews, D. M. 2010. Antidepressants and their metabolites in municipal wastewater, and downstream exposure in an urban watershed. *Environmental Toxicology and Chemistry,* 29**,** 79-89.

Mezzelani, M., Gorbi, S. & Regoli, F. 2018. Pharmaceuticals in the aquatic environments: Evidence of emerged threat and future challenges for marine organisms. *Marine Environmental Research,* 140**,** 41-60.

Mole, R. A. & Brooks, B. W. 2019. Global scanning of selective serotonin reuptake inhibitors: occurrence, wastewater treatment and hazards in aquatic systems. *Environmental Pollution,* 250**,** 1019-1031.

Montiel-Leon, J. M., Duy, S. V., Munoz, G., Amyot, M. & Sauve, S. 2018. Evaluation of on-line concentration coupled to liquid chromatography tandem mass spectrometry for the quantification of neonicotinoids and fipronil in surface water and tap water. *Analytical and Bioanalytical Chemistry,* 410**,** 2765-2779.

Morrice, J. R., Gregory-Evans, C. Y. & Shaw, C. A. 2018. Modeling environmentally-induced motor neuron degeneration in zebrafish. *Scientific Reports,* 8.

Mudo, G., Belluardo, N. & Fuxe, K. 2007. Nicotinic receptor agonists as neuroprotective/neurotrophic drugs. Progress in molecular mechanisms. *Journal of Neural Transmission,* 114**,** 135-147.

Mundo, A. I., Muldoon, T. J. & Tipton, J. R. 2022. Generalized additive models to analyze nonlinear trends in biomedical longitudinal data using R: Beyond repeated measures ANOVA and linear mixed models. *Statistics in Medicine,* 41**,** 4266-4283.

Muth-Kohne, E., Wichmann, A., Delov, V. & Fenske, M. 2012. The classification of motor neuron defects in the zebrafish embryo toxicity test (ZFET) as an animal alternative approach to assess developmental neurotoxicity. *Neurotoxicology and teratology,* 34**,** 413-424.

Myers, P. Z., Eisen, J. S. & Westerfield, M. 1986. Development and axonal outgrowth of identified motoneurons in the zebrafish. *Journal of Neuroscience,* 6**,** 2278-2289.

Myles, N., Newall, H., Ward, H. & Large, M. 2013. Systematic meta-analysis of individual selective serotonin reuptake inhibitor medications and congenital malformations. *Australian and New Zealand Journal of Psychiatry,* 47**,** 1002-1012.

Nishimura, Y., Inoue, A., Sasagawa, S., Koiwa, J., Kawaguchi, K., Kawase, R., Maruyama, T., Kim, S. & Tanaka, T. 2016. Using zebrafish in systems toxicology for developmental toxicity testing. *Congenital Anomalies,* 56**,** 18-27.

Nishimura, Y., Murakami, S., Ashikawa, Y., Sasagawa, S., Umemoto, N., Shimada, Y. & Tanaka, T. 2015. Zebrafish as a systems toxicology model for developmental neurotoxicity testing. *Congenital Anomalies,* 55**,** 1-16.

Nowakowska, K., Giebultowicz, J., Kamaszewski, M., Adamski, A., Szudrowicz, H., Ostaszewska, T., Solarska-Dzieciolowska, U., Nalecz-Jawecki, G., Wroczynski, P. & Drobniewska, A. 2020. Acute exposure of zebrafish (Danio rerio) larvae to environmental concentrations of selected antidepressants: Bioaccumulation, physiological and histological changes. *Comparative Biochemistry and Physiology C-Toxicology & Pharmacology,* 229.

Obach, R. S., Cox, L. M. & Tremaine, L. M. 2005. Sertraline is metabolized by multiple cytochrome P450 enzymes, monoamine oxidases, and glucuronyl transferases in human: An in vitro study. *Drug Metabolism and Disposition,* 33**,** 262-270.

Oecd 2000. Guidance document on aquatic toxicity testing of difficult substances and mixtures. Author Paris

Oecd 2007. Test No. 426: Developmental Neurotoxicity Study, Guidelines for the Testing of Chemicals, Section 4: Health Effects. *OECD Guidelines for the Testing of Chemicals.*10.1787/9789264067394-en

Oecd 2013. Test No. 236: Fish Embryo Acute Toxicity (FET) Test. *OECD Guidelines for the Testing of Chemicals.*10.1787/9789264203709-en

Oecd 2018. Test No. 443: Extended One-Generation Reproductive Toxicity Study *OECD Guidelines for the Testing of Chemicals.*10.1787/9789264185371-en

Oecd 2019. Test No. 203: Fish, Acute Toxicity Test, OECD Guidelines for the Testing of Chemicals, Section 2: Effects on Biotic Systems. *OECD Guidelines for the Testing of Chemicals.*10.1787/9789264069961-en

Ogungbemi, A., Leuthold, D., Scholz, S. & Kuster, E. 2019. Hypo- or hyperactivity of zebrafish embryos provoked by neuroactive substances: a review on how experimental parameters impact the predictability of behavior changes. *Environmental Sciences Europe,* 31.

Ogungbemi, A. O., Massei, R., Altenburger, R., Scholz, S. & Kuster, E. 2021. Assessing combined effects for mixtures of dimilar and fissimilar acting neuroactive dubstances on zebrafish rmbryo movement. *Toxics,* 9.

Ogungbemi, A. O., Teixido, E., Massei, R., Scholz, S. & Kuster, E. 2020a. Optimization of the spontaneous tail coiling test for fast assessment of neurotoxic effects in the zebrafish embryo using an automated workflow in KNIME(R). *Neurotoxicology and teratology,* 81**,** 106918.

Ogungbemi, A. O., Teixido, E., Massei, R., Scholz, S. & Kuster, E. 2020b. Optimization of the spontaneous tail coiling test for fast assessment of neurotoxic effects in the zebrafish embryo using an automated workflow in KNIME(R). *Neurotoxicol Teratol,* 81**,** 106918.

Ott, H., Diekmann, H., Stuermer, C. a. O. & Bastmeyer, M. 2001. Function of neurolin (DM-GRASP/SC-1) in guidance of motor axons during zebrafish development. *Developmental Biology,* 235**,** 86-97.

Padilla, S., Hunter, D. L., Padnos, B., Frady, S. & Macphail, R. C. 2011. Assessing locomotor activity in larval zebrafish: Influence of extrinsic and intrinsic variables. *Neurotoxicology and teratology,* 33**,** 624-630.

Papan, C. & Campos-Ortega, J. A. 1994. On the formation of the neural keel and neural tube in the zebrafishDanio (Brachydanio) rerio. *Rouxs Archives of Developmental Biology* 203**,** 178-186.

Pedersen, E. J., Miller, D. L., Simpson, G. L. & Ross, N. 2019. Hierarchical generalized additive models in ecology: an introduction with mgcv. *Peerj,* 7.

Pelka, K. E., Henn, K., Keck, A., Sapel, B. & Braunbeck, T. 2017. Size does matter - Determination of the critical molecular size for the uptake of chemicals across the chorion of zebrafish (Danio rerio) embryos. *Aquatic Toxicology,* 185**,** 1-10.

Phillips, L., Thomson, R., Coleman-Haynes, T., Cooper, S., Naughton, F., Mcdaid, L., Emery, J. & Coleman, T. 2023. Developing a taxonomy to describe offspring outcomes in studies involving

pregnant mammals' exposure to non-tobacco nicotine: A systematic scoping review. *Plos One,* 18.

Picciotto, M. R., Higley, M. J. & Mineur, Y. S. 2012. Acetylcholine as a neuromodulator: cholinergic signaling shapes nervous system function and behavior. *Neuron,* 76**,** 116-129.

Ramirez, A. J., Brain, R. A., Usenko, S., Mottaleb, M. A., O'donnell, J. G., Stahl, L. L., Wathen, J. B., Snyder, B. D., Pitt, J. L. & Perez-Hurtado, P. 2009. Occurrence of pharmaceuticals and personal care products in fish: results of a national pilot study in the United States. *Environmental Toxicology and Chemistry,* 28**,** 2587-2597.

Ravindra, K., Rattan, P., Mor, S. & Aggarwal, A. N. 2019. Generalized additive models: Building evidence of air pollution, climate change and human health. *Environment International,* 132.

Rayburn, J. R., Deyoung, D. J., Bantle, J. A., Fort, D. J. & Mcnew, R. 1991. Altered developmental toxicity caused by 3 carrier solvents. *Journal of Applied Toxicology,* 11**,** 253-260.

Rice, D. & Barone, S., Jr. 2000. Critical periods of vulnerability for the developing nervous system: evidence from humans and animal models. *Environ Health Perspect,* 108 Suppl 3**,** 511-33.

Richendrfer, H. & Creton, R. 2018. Cluster analysis profiling of behaviors in zebrafish larvae treated with antidepressants and pesticides. *Neurotoxicology and teratology,* 69**,** 54-62.

Russell, W. M. S. & Burch, R. L. 1959. *The principles of humane experimental technique*, Methuen.

Sachana, M., Shafer, T. J. & Terron, A. 2021. Toward a better testing paradigm for developmental neurotoxicity: OECD efforts and regulatory considerations. *Biology (Basel),* 10.

Saint-Amant, L. & Drapeau, P. 1998. Time course of the development of motor behaviors in the zebrafish embryo. *Journal of Neuroscience,* 37**,** 622-32.

Saint-Amant, L. & Drapeau, P. 2001. Synchronization of an embryonic network of identified spinal interneurons solely by electrical coupling. *Neuron,* 31**,** 1035-1046.

Santiago, C. F., Huttner, I. G. & Fatkin, D. 2021. Mechanisms of TTNtv-related dilated cardiomyopathy: insights from zebrafish models. *Journal of Cardiovascular Development and Disease,* 8**,** 10.

Schmitz, B., Papan, C. & Camposortega, J. A. 1993. Neurulation in the anterior trunk region of the zebrafish Brachydanio-Rerio. *Rouxs Archives of Developmental Biology,* 202**,** 250-259.

Sehonova, P., Hodkovicova, N., Urbanova, M., Orn, S., Blahova, J., Svobodova, Z., Faldyna, M., Chloupek, P., Briedikova, K. & Carlsson, G. 2019. Effects of antidepressants with different modes of action on early life stages of fish and amphibians. *Environmental Pollution,* 254.

Sehonova, P., Svobodova, Z., Dolezelova, P., Vosmerova, P. & Faggio, C. 2018. Effects of waterborne antidepressants on non-target animals living in the aquatic environment: A review. *Science of the Total Environment,* 631-632**,** 789-794.

Selderslaghs, I. W. T., Hooyberghs, J., De Coen, W. & Witters, H. E. 2010. Locomotor activity in zebrafish embryos: A new method to assess developmental neurotoxicity. *Neurotoxicology and teratology,* 32**,** 460-471.

Shahid, M., Takamiya, M., Stegmaier, J., Middel, V., Gradl, M., Kluver, N., Mikut, R., Dickmeis, T., Scholz, S., Rastegar, S., Yang, L. & Strahle, U. 2016. Zebrafish biosensor for toxicant induced muscle hyperactivity. *Scientific Reports,* 6**,** 23768.

Shaliutina-Kolešová, A., Shaliutina, O. & Nian, R. 2020. The effects of environmental antidepressants on macroinvertebrates: a mini review. *Water and Environment Journal,* 34**,** 153-159.

Sharples, S. A., Koblinger, K., Humphreys, J. M. & Whelan, P. J. 2014. Dopamine: a parallel pathway for the modulation of spinal locomotor networks. *Frontiers in Neural Circuits,* 8.

Simeon, S., Brotzmann, K., Fisher, C., Gardner, I., Silvester, S., Maclennan, R., Walker, P., Braunbeck, T. & Bois, F. Y. 2020. Development of a generic zebrafish embryo PBPK model and application to the developmental toxicity assessment of valproic acid analogs (vol 93, pg 219, 2020). *Reproductive Toxicology,* 98**,** 300-303.

Singh, A., Saidulu, D., Gupta, A. K. & Kubsad, V. 2022. Occurrence and fate of antidepressants in the aquatic environment: Insights into toxicological effects on the aquatic life, analytical methods, and removal techniques. *Journal of Environmental Chemical Engineering,* 10**,** 109012.

Sloman, K. A. & Mcneil, P. L. 2012. Using physiology and behaviour to understand the responses of fish early life stages to toxicants. *Journal of Fish Biology,* 81**,** 2175-2198.

Slotkin, T. A., Ryde, I. T., Tate, C. A. & Seidler, F. J. 2007. Lasting effects of nicotine treatment and withdrawal on serotonergic systems and cell signaling in rat brain regions: Separate or sequential exposure during fetal development and adulthood. *Brain Research Bulletin,* 73**,** 259-272.

Slotkin, T. A., Skavicus, S., Card, J., Stadler, A., Levin, E. D. & Seidler, F. J. 2015. Developmental Neurotoxicity of Tobacco Smoke Directed Toward Cholinergic and Serotonergic Systems: More Than Just Nicotine. *Toxicological Sciences,* 147**,** 178-189.

Smith, L. L., Beggs, A. H. & Gupta, V. A. 2013. Analysis of skeletal muscle defects in larval zebrafish by birefringence and touch-evoke escape response assays. *Journal of Visualized Experiments***,** e50925.

Sobanska, M., Scholz, S., Nyman, A. M., Cesnaitis, R., Alonso, S. G., Klüver, N., Kühne, R., Tyle, H., De Knecht, J., Dang, Z. C., Lundbergh, I., Carlon, C. & De Coen, W. 2018. Applicability of the fish embryo acute toxicity (FET) test (OECD 236) in the regulatory context of Registration, Evaluation, Authorisation, and Restriction of Chemicals (REACH). *Environmental Toxicology and Chemistry,* 37**,** 657-670.

Sood, P. K., Sharma, S. & Nehru, B. 2012. Consequences of nicotine exposure during different phases of rat brain development. *Brain & Development,* 34**,** 591-600.

Stehr, C. M., Linbo, T. L., Incardona, J. P. & Scholz, N. L. 2006. The developmental neurotoxicity of fipronil: Notochord degeneration and locomotor defects in zebrafish embryos and larvae. *Toxicological Sciences,* 92**,** 270-278.

Strähle, U. & Blader, P. 1994. Early neurogenesis in the zebrafish embryo. *Faseb Journal,* 8**,** 692-698.

Strähle, U., Scholz, S., Geisler, R., Greiner, P., Hollert, H., Rastegar, S., Schumacher, A., Selderslaghs, I., Weiss, C., Witters, H. & Braunbeck, T. 2012. Zebrafish embryos as an alternative to animal experiments-A commentary on the definition of the onset of protected life stages in animal welfare regulations. *Reproductive Toxicology,* 33**,** 128-132.

Styrishave, B., Halling-Sørensen, B. & Ingerslev, F. 2011. Environmental risk assessment of three selective serotonin reuptake inhibitors in the aquatic environment: A case study including a cocktail scenario. *Environmental Toxicology and Chemistry,* 30**,** 254-261.

Suryanto, M. E., Audira, G., Uapipatanakul, B., Hussain, A., Saputra, F., Siregar, P., Chen, K. H. & Hsiao, C. D. 2021. Antidepressant screening demonstrated non-monotonic responses to amitriptyline, amoxapine and sertraline in locomotor activity assay in larval zebrafish. *Cells,* 10.

Svoboda, K. R., Vijayaraghavan, S. & Tanguay, R. L. 2002. Nicotinic receptors mediate changes in spinal motoneuron development and axonal pathfinding in embryonic zebrafish exposed to nicotine. *Journal of Neuroscience,* 22**,** 10731-10741.

Svoboda, K. R., Vijayaraghavan, S. & Tanguay, R. L. 2007. Nicotinic receptors mediate changes in spinal motoneuron development and axonal pathfinding in embryonic zebrafish exposed to nicotine (vol 22, pg 10731, 2002). *Journal of Neuroscience,* 27**,** 3356-3356.

Sylvain, N. J., Brewster, D. L. & Ali, D. W. 2010. Zebrafish embryos exposed to alcohol undergo abnormal development of motor neurons and muscle fibers. *Neurotoxicology and teratology,* 32**,** 472-480.

Tang, S. W. & Helmeste, D. 2008. Paroxetine. *Expert Opinion on Pharmacotherapy,* 9**,** 787-794.

Tang, Y. Q., Fan, Z., Yang, M. Y., Zhang, S. Z., Li, M. J., Fang, Y. C., Li, J. & Feng, X. Z. 2022. Low concentrations of the antidepressant venlafaxine affect courtship behaviour and alter serotonin and dopamine systems in zebrafish (Danio rerio). *Aquatic Toxicology,* 244.

Tang, Y. Q., Mi, P., Li, M. J., Zhang, S. Z., Li, J. & Feng, X. Z. 2021. Environmental level of the antidepressant venlafaxine induces behavioral disorders through cortisol in zebrafish larvae (Danio rerio). *Neurotoxicology and teratology,* 83.

Thomas, L. T., Welsh, L., Galvez, F. & Svoboda, K. R. 2009. Acute nicotine exposure and modulation of a spinal motor circuit in embryonic zebrafish. *Toxicology and Applied Pharmacology,* 239**,** 1-12.

Thompson, D. A., Lehmler, H. J., Kolpin, D. W., Hladik, M. L., Vargo, J. D., Schilling, K. E., Lefevre, G. H., Peeples, T. L., Poch, M. C., Laduca, L. E., Cwiertny, D. M. & Field, R. W. 2020. A critical review on the potential impacts of neonicotinoid insecticide use: current knowledge of environmental fate, toxicity, and implications for human health. *Environmental Science-Processes & Impacts,* 22**,** 1315-1346.

Thompson, W. A., Arnold, V. I. & Vijayan, M. M. 2017. Venlafaxine in Embryos Stimulates Neurogenesis and Disrupts Larval Behavior in Zebrafish. *Environmental Science & Technology,* 51**,** 12889-12897.

Thompson, W. A., Shvartsburd, Z. & Vijayan, M. M. 2022a. The antidepressant venlafaxine perturbs cardiac development and function in larval zebrafish. *Aquatic Toxicology,* 242.

Thompson, W. A., Shvartsburd, Z. & Vijayan, M. M. 2022b. Sex-Specific and Long-Term Impacts of Early-Life Venlafaxine Exposure in Zebrafish. *Biology-Basel,* 11.

Tilson, H. A., Macphail, R. C. & Crofton, K. M. 1995. Defining neurotoxicity in a decision-making context. *Neurotoxicology,* 16**,** 363-375.

Tilton, S. C., Tal, T. L., Scroggins, S. M., Franzosa, J. A., Peterson, E. S., Tanguay, R. L. & Waters, K. M. 2012. Bioinformatics resource manager v2.3: an integrated software environment for systems biology with microRNA and cross-species analysis tools. *Bmc Bioinformatics,* 13.

Tisler, T., Jemec, A., Mozetic, B. & Trebse, P. 2009. Hazard identification of imidacloprid to aquatic environment. *Chemosphere,* 76**,** 907-914.

Tomizawa, M. 2004. Neonicotinoids and derivatives: Effects in mammalian cells and mice. *Journal of Pesticide Science,* 29**,** 177-183.

Tomizawa, M. & Casida, J. E. 2000. Imidacloprid, thiacloprid, and their imine derivatives up-regulate the alpha 4 beta 2 nicotinic acetylcholine receptor in M10 cells. *Toxicology and Applied Pharmacology,* 169**,** 114-120.

Tomizawa, M. & Casida, J. E. 2002. Desnitro-imidacloprid activates the extracellular signal-regulated kinase cascade via the nicotinic receptor and intracellular calcium mobilization in N1E-115 cells. *Toxicology and Applied Pharmacology,* 184**,** 180-186.

Tomizawa, M. & Casida, J. E. 2003. Selective toxicity of neonicotinoids attributable to specificity of insect and mammalian nicotinic receptors. *Annual Review of Entomology,* 48**,** 339-64.

Tomizawa, M. & Casida, J. E. 2005. Neonicotinoid insecticide toxicology: mechanisms of selective action. *Annual Review of Pharmacology and Toxicology,* 45**,** 247-68.

Tufi, S., Leonards, P., Lamoree, M., De Boer, J., Legler, J. & Legradi, J. 2016. Changes in neurotransmitter profiles during early zebrafish development and after pesticide exposure. *Environmental Science & Technology,* 50**,** 3222-3230.

Turner, C., Sawle, A., Fenske, M. & Cossinsy, A. 2012. Implications of the solvent vehicles dimethylformamide and dimethylsulfoxide for establishing transcriptomic endpoints in the zebrafish embryo toxicity test. *Environmental Toxicology and Chemistry,* 31**,** 593-604.

Turnerwarwick, M., Clarke, S. W., Woodcock, A. A., Bewley, B. R., Catford, J. C., Channer, K. S., Charlton, A., Couriel, J. M., Dunmore, J., Gillies, P. A., Mcneill, A. D., Rees, P. J., Reid, D. J.,

Simpson, D., Stewartbrown, S. L., Warner, J. O., Watkeys, J. E. M. & Harvey, F. a. H. 1992. Smoking and the young - Summary of a report of a working party of the Royal-College-of-Physicians. *Journal of the Royal College of Physicians of London,* 26**,** 352-356.

Venkatachalam, A. B., Levesque, B., Achenbach, J. C., Pappas, J. J. & Ellis, L. D. 2023. Long and short duration exposures to the selective serotonin reuptake inhibitors (SSRIs) fluoxetine, paroxetine and sertraline at environmentally relevant concentrations lead to adverse effects on zebrafish behaviour and reproduction. *Toxics,* 11**,** 151.

Victoria, S., Hein, M., Harrahy, E. & King-Heiden, T. C. 2022. Potency matters: Impacts of embryonic exposure to nAChR agonists thiamethoxam and nicotine on hatching success, growth, and neurobehavior in larval zebrafish. *Journal of Toxicology and Environmental Health-Part a-Current Issues,* 85**,** 767-782.

Vliet, S. M., Ho, T. C. & Volz, D. C. 2017. Behavioral screening of the LOPAC(1280) library in zebrafish embryos. *Toxicology and Applied Pharmacology,* 329**,** 241-248.

Von Hellfeld, R., Brotzmann, K., Baumann, L., Strecker, R. & Braunbeck, T. 2020. Adverse effects in the fish embryo acute toxicity (FET) test: a catalogue of unspecific morphological changes versus more specific effects in zebrafish (Danio rerio) embryos. *Environmental Sciences Europe,* 32**,** 18.

Von Hellfeld, R., Gade, C., Baumann, L., Leist, M. & Braunbeck, T. 2023. The sensitivity of the zebrafish embryo coiling assay for the detection of neurotoxicity by compounds with diverse modes of action. *Environmental Science and Pollution Research.*

Von Hellfeld, R., Ovcharova, V., Bevan, S., Lazaridi, M. A., Bauch, C., Walker, P., Bennekou, S. H., Forsby, A. & Braunbeck, T. 2022. Zebrafish embryo neonicotinoid developmental neurotoxicity in the FET test and behavioral assays. *Altex-Alternatives to Animal Experimentation,* 39**,** 367-387.

Wang, A., Mahai, G., Wan, Y., Yang, Z., He, Z., Xu, S. & Xia, W. 2020. Assessment of imidacloprid related exposure using imidacloprid-olefin and desnitro-imidacloprid: Neonicotinoid insecticides in human urine in Wuhan, China. *Environment International,* 141**,** 105785.

Wang, W., Zhang, J., Hu, M., Liu, X., Sun, T. & Zhang, H. 2023. Antidepressants in wastewater treatment plants: Occurrence, transformation and acute toxicity evaluation. *Science of the Total Environment,* 903**,** 166120.

Weichert, F. G., Floeter, C., Meza Artmann, A. S. & Kammann, U. 2017. Assessing the ecotoxicity of potentially neurotoxic substances - Evaluation of a behavioural parameter in the embryogenesis of Danio rerio. *Chemosphere,* 186**,** 43-50.

Weis, J. S., Smith, G., Zhou, T., Santiago-Bass, C. & Weis, P. 2001. Effects of contaminants on behavior: biochemical mechanisms and ecological consequences: Killifish from a contaminated site are slow to capture prey and escape predators; altered neurotransmitters and thyroid may be responsible for this behavior, which may produce population changes in the fish and their major prey, the grass shrimp. *BioScience,* 51**,** 209-217.

Welsh, L., Tanguay, R. L. & Svoboda, K. R. 2009. Uncoupling nicotine mediated motoneuron axonal pathfinding errors and muscle degeneration in zebrafish. *Toxicology and Applied Pharmacology,* 237**,** 29-40.

Wessels, C. & Winterer, G. 2008. Brain development: nicotine-dependent morphological and functional changes of the central nervous system. *Neuroforum,* 14**,** 199-204.

Westerfield, M., Mcmurray, J. V. & Eisen, J. S. 1986. Identified motoneurons and their innervation of axial muscles in the zebrafish. *Journal of Neuroscience,* 6**,** 2267-77.

Wheeler, D. & Cooper, E. 2004. Weak synaptic activity induces ongoing signaling to the nucleus that is enhanced by BDNF and suppressed by low-levels of nicotine. *Molecular and Cellular Neuroscience,* 26**,** 50-62.

Whelan, P., Bonnot, A. & O'donovan, M. J. 2000. Properties of rhythmic activity generated by the isolated spinal cord of the neonatal mouse. *Journal of Neurophysiology,* 84**,** 2821-33.

Whitakerazmitia, P. M. 1991. Role of serotonin and other neurotransmitter receptors in brain-development - basis for developmental pharmacology. *Pharmacological Reviews,* 43**,** 553-561.

Who 2008. The global burden of disease : 2004 update. A response to the need for comprehensive, consistent and comparable information on diseases and injuries at global and regional level.**,** 146.

Wickham, H. 2016. Data Analysis. *ggplot2: Elegant Graphics for Data Analysis.* Cham: Springer International Publishing.

Wilkinson, J. L., Boxall, A. B. A., Kolpin, D. W., Leung, K. M. Y., Lai, R. W. S., Galban-Malagon, C., Adell, A. D., Mondon, J., Metian, M., Marchant, R. A., Bouzas-Monroy, A., Cuni-Sanchez, A., Coors, A., Carriquiriborde, P., Rojo, M., Gordon, C., Cara, M., Moermond, M., Luarte, T., Petrosyan, V., et al. 2022. Pharmaceutical pollution of the world's rivers. *Proceedings of the National Academy of Sciences of the United States of America,* 119.

Wilson, P. A. & Hemmati, B., A. 1997. Vertebrate neural induction: Inducers, inhibitors, and a new synthesis. *Neuron,* 18**,** 699-710.

Yang, H., Gu, X., Chen, H., Zeng, Q., Mao, Z., Jin, M., Li, H., Ge, Y., Zha, J. & Martyniuk, C. J. 2022. Transcriptome profiling reveals toxicity mechanisms following sertraline exposure in the brain of juvenile zebrafish (Danio rerio). *Ecotoxicology and Environmental Safety,* 242**,** 113936.

Yang, H., Liang, X., Zhao, Y., Gu, X., Mao, Z., Zeng, Q., Chen, H. & Martyniuk, C. J. 2021. Molecular and behavioral responses of zebrafish embryos/larvae after sertraline exposure. *Ecotoxicology and Environmental Safety,* 208**,** 111700.

Zeller, J., Schneider, V., Malayaman, S., Higashijima, S., Okamoto, H., Gui, J. F., Lin, S. & Granato, M. 2002. Migration of zebrafish spinal motor nerves into the periphery requires multiple myotome-derived cues. *Developmental Biology,* 252**,** 241-256.

Zellner, D., Padnos, B., Hunter, D. L., Macphail, R. C. & Padilla, S. 2011. Rearing conditions differentially affect the locomotor behavior of larval zebrafish, but not their response to valproate-induced developmental neurotoxicity. *Neurotoxicology and teratology,* 33**,** 674-679.

Zhang, K., Liang, J. H., Brun, N. R., Zhao, Y. B. & Werdich, A. A. 2021. Rapid zebrafish behavioral profiling assay accelerates the identification of environmental neurodevelopmental toxicants. *Environmental Science & Technology,* 55**,** 1919-1929.

Zhang, X. L. & Hartmann, P. 2023. How to calculate sample size in animal and human studies. *Frontiers in Medicine,* 10.

Zhao, S. F., Cui, W. Y., Cao, J. R., Luo, C., Fan, L. J. & Li, M. D. 2014. Impact of maternal nicotine exposure on expression of myelin-related genes in zebrafish larvae. *Zebrafish,* 11**,** 10-16.

Zhu, Y. H., Song, F. F., Gu, J., Wu, L. L., Wu, W. Z. & Ji, G. X. 2023. Paroxetine induced larva zebrafish cardiotoxicity through inflammation response. *Ecotoxicology and Environmental Safety,* 260.

Ziegler, M., Banet, M., Bauer, R., Köhler, H. R., Stepinski, S., Tisler, S., Huhn, C., Zwiener, C. & Triebskorn, R. 2021. Behavioral and Developmental Changes in Brown Trout After Exposure to the Antidepressant Venlafaxine. *Frontiers in Environmental Science,* 8.

Zindler, F., Beedgen, F., Brandt, D., Steiner, M., Stengel, D., Baumann, L. & Braunbeck, T. 2019a. Analysis of tail coiling activity of zebrafish (Danio rerio) embryos allows for the differentiation of neurotoxicants with different modes of action. *Ecotoxicology and Environmental Safety,* 186**,** 109754.

Zindler, F., Beedgen, F. & Braunbeck, T. 2019b. Time-course of coiling activity in zebrafish (Danio rerio) embryos exposed to ethanol as an endpoint for developmental neurotoxicity (DNT) - Hidden potential and underestimated challenges. *Chemosphere,* 235**,** 12-20.

APPENDIX A

Coiling assay

Recording and detection setttings

Table A1: Recording and activity measurement settings for the coiling experiments in pylon viewer and Danio Scope.

Pylon viewer:

Image Format Control	
Resolution	1600 x1200
Center X	Yes
Center Y	Yes
Pixel Format	Mono 8
Analog Control	
Gain Auto	Off
Gain Selector	All
Gain	1
Black Level Selector	All
Black Level	0
Gamma	1
Digital Shift	4
Acquisition Control	
Exposure Time [µs]	5000
Frame Rate [Hz]	30

Danio Scope 1.2:

Activity settings	
Onset [a]	Rep. 1: 8%, Rep. 2: 6%, Rep. 3: 9%
Offset	1%
Min. inter peaks interval	300 ms
Min. peak duration	0 ms

[a] *Threshold for onset of activity defined by visual inspection. Deviations of the individual replicates due to slightly different light arrangements in the incubator for the independent experiments.*
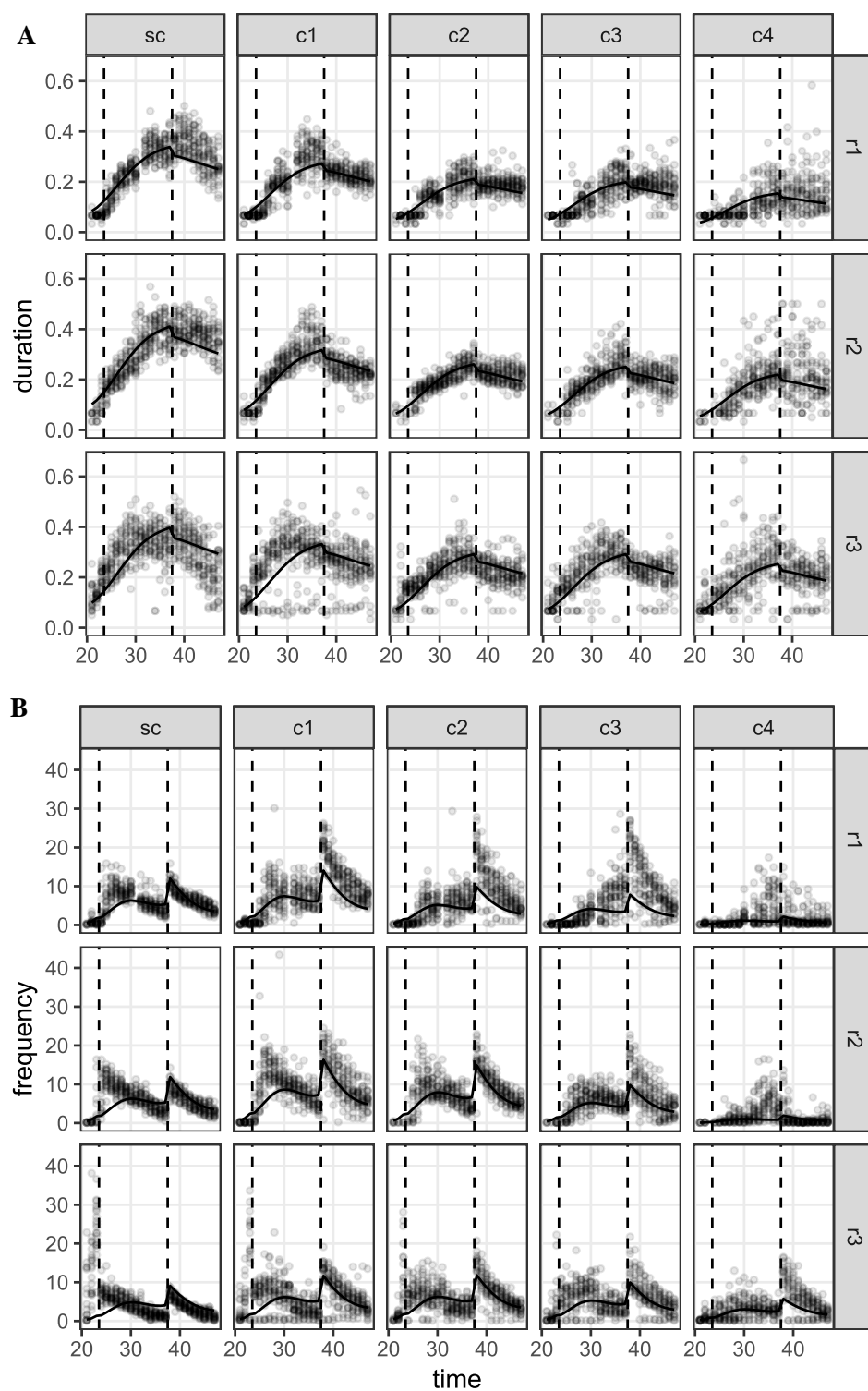
Generalized additive modelling

Nicotine treatment
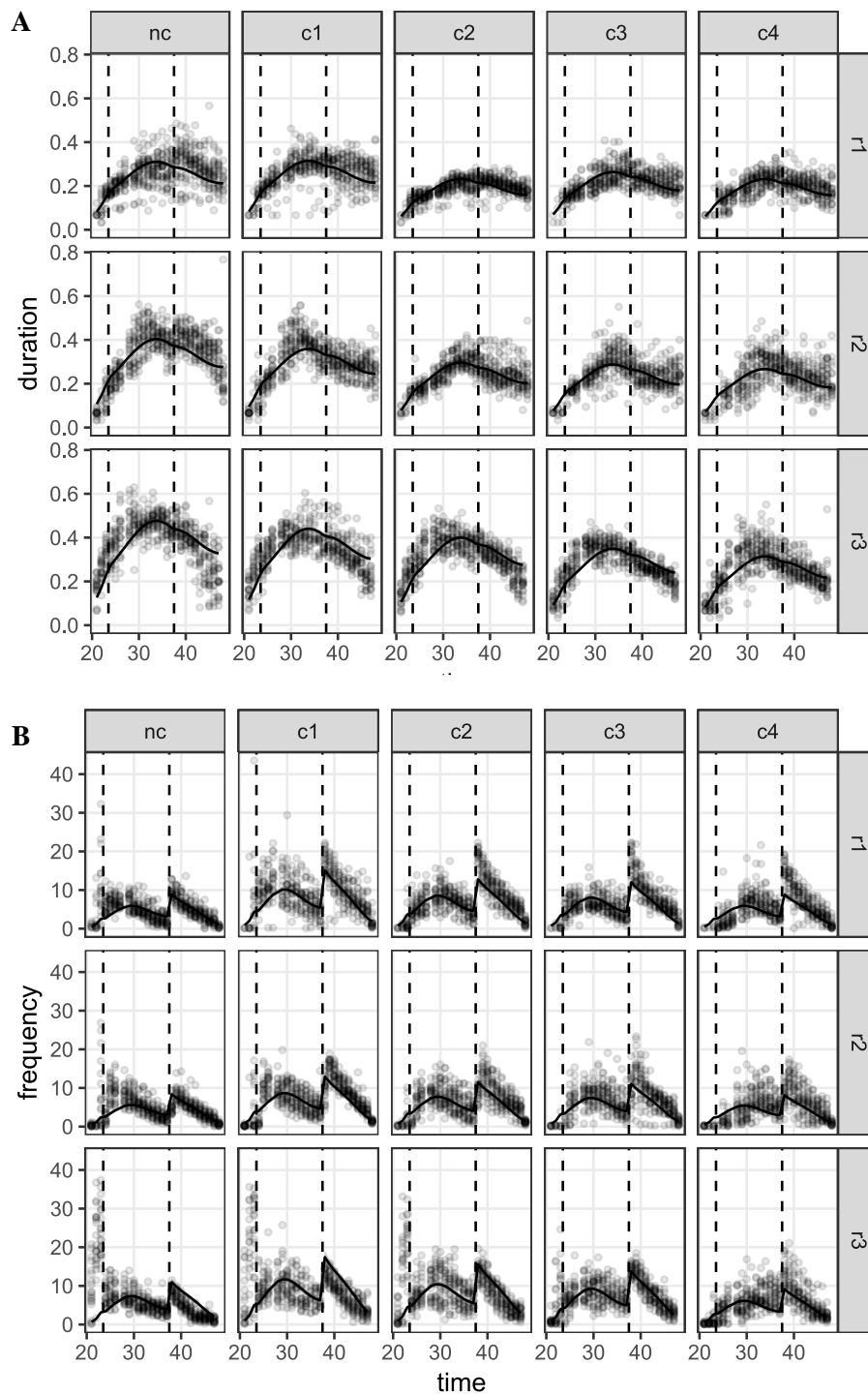
Figure A1: Coiling behavior analysis of the nicotine treatment experiment. The graphs illustrate the duration (A) and the frequency (B) of the coils of the zebrafish embryos between 21-47 hpf. Curves are predicted and fitted by the model. The columns depict the different treatments with negative control (nc), 5 µM (c1), 10 µM (c2), 20 µM (c3) and 40 µM (c4) nicotine exposure. The three rows show all three replicates (r1-3) separately.

Skeletal muscle integrity assessment

Linear polarizing filters

Table A2: Specification of linear polarizing filters provided by Edmund Optics

Extinction ratio	100:1
Thickness	2 mm
Wavelength range	400 – 700 nm
Surface Quality	80-50
Tolerance size	+0.0/-0.2 mm
Tolerance thickness	± 0.2 mm
Parallelism	< 3 arc minutes
Substrate	Polymer film on B270
Transmission	Single: ~ 30 %
Polarization efficiency (%)	95 %
Surface flatness (P-V)	4 - 6 λ
Material	Dichroic Polarizing Film on Glass
Faze	Protective bevel as needed
Edges	Cut
Working temperature	-15 to +70 °C

Measurement adjustments in the software
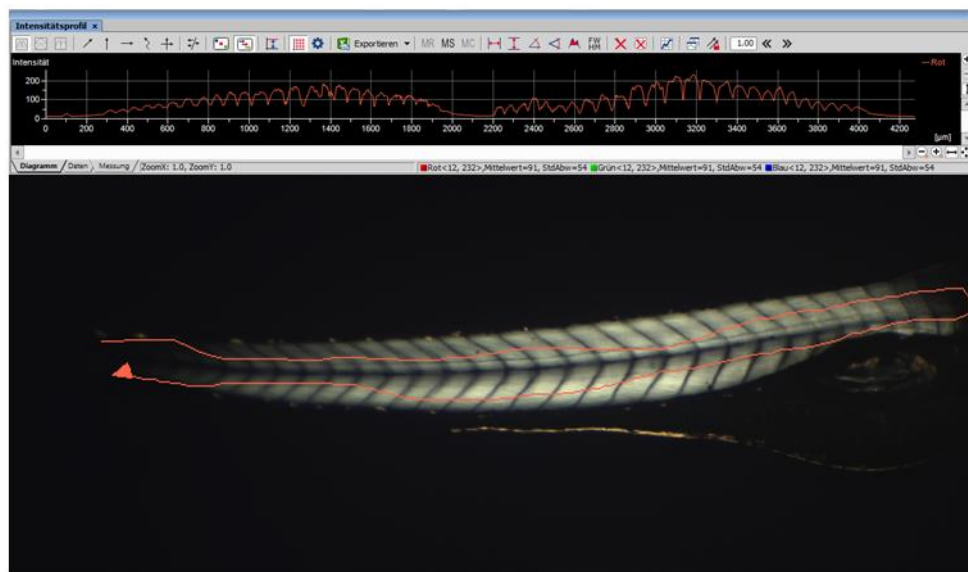
Figure A2: Placing the zebrafish embryo using intensity measurement of dorsal and ventral somite muscles of the NIS software.

APPENDIX B

Internal concentration measurements of zebrafish embryo

Table B1: Mass spectrometric (A) and chromatography conditions (B).

(A) Mass Spectrometric Conditions	
Ion Spray Voltage (V)	-4500
Temperature (°C)	50
Gas 1 (psi)	50
Gas 2 (psi)	50
Curtain Gas (psi)	40
CAD Gas (arb)	N/A
Detection	Hi Res
Mass detection range (amu)	50 - 800
Accumulation time (ms)	250

(B) Chromatography Conditions	
Column	Phenomenex Kinetex XB-C18 2.6µm 2.1x50mm
Column Temperature (°C)	60
Mobile Phase A	0.01% Formic acid (aq)
Mobile Phase B	MeOH

Time (min)	Flow Rate (µL/min)	% A	% B
0.00	800	98	2
1.50	800	5	95
1.90	800	5	95
2.00	800	98	2
2.50	800	98	2

Nicotine and desnitro-imidacloprid coiling analysis

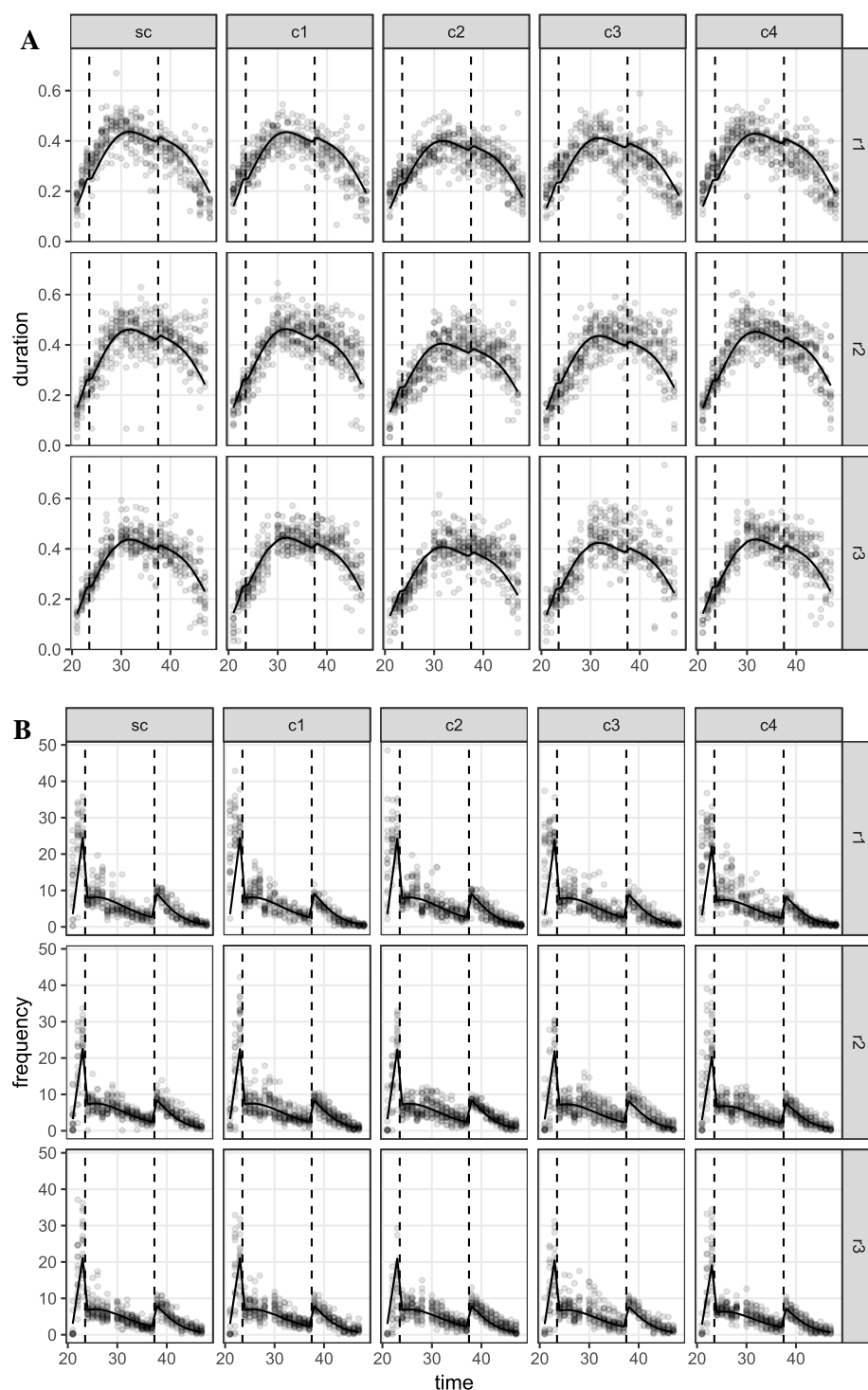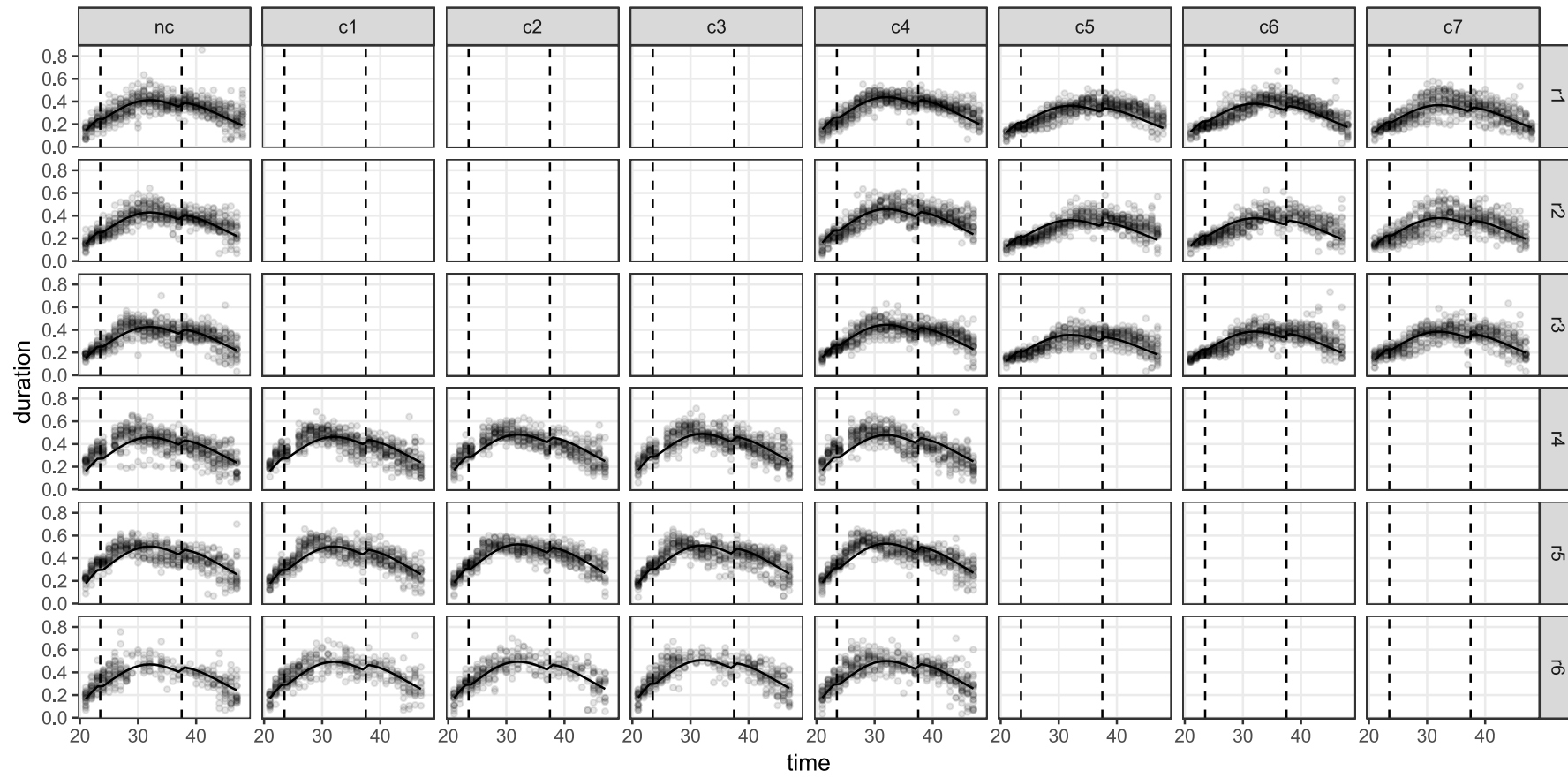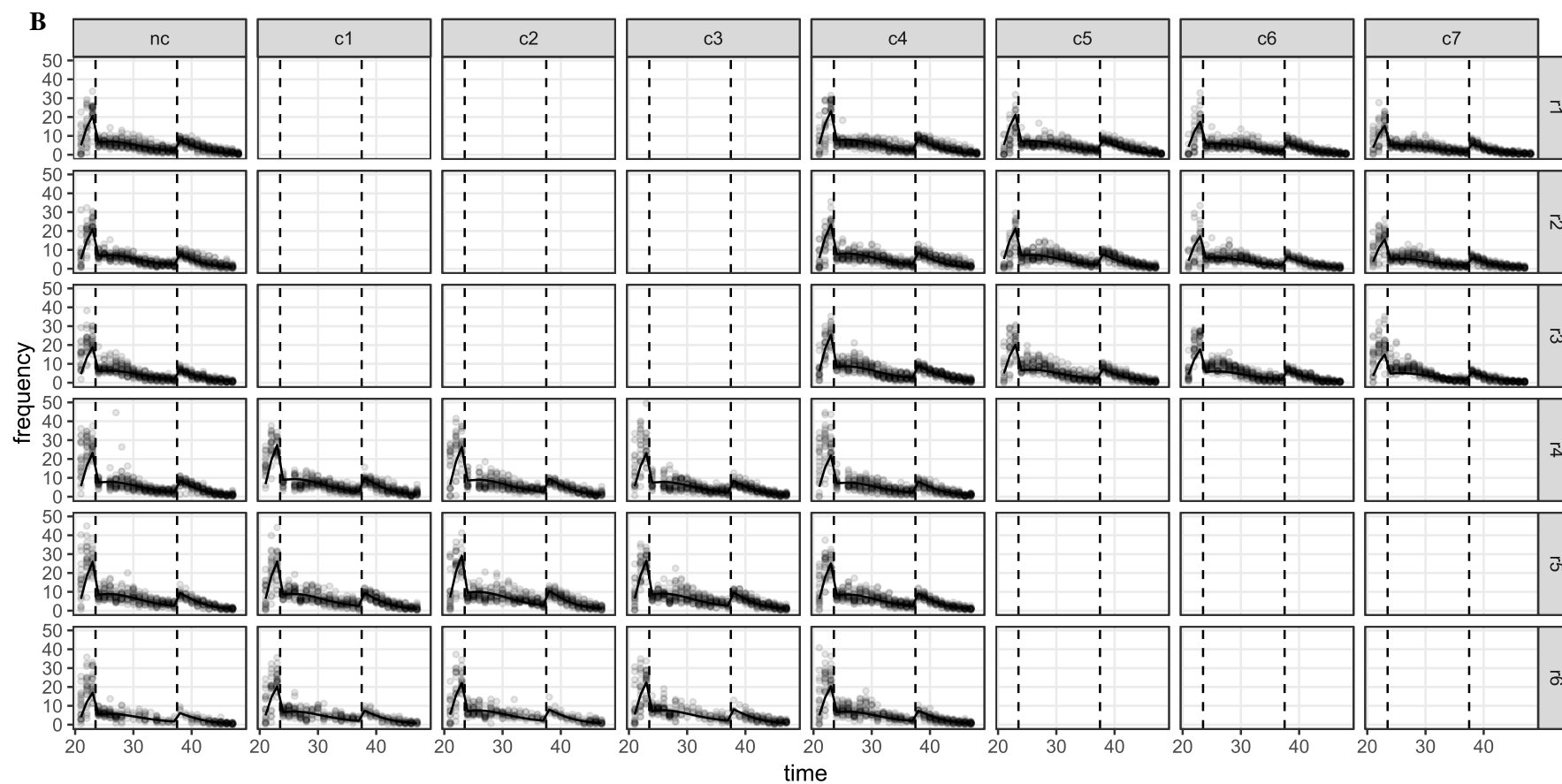

Figure B1: Coiling behavior analysis of the nicotine (+DMSO) treatment experiment. The graphs illustrate the duration (A) and the frequency (B) of the coils of the zebrafish embryos between 21-47 hpf. Curves are predicted and fitted by the model. The columns depict the different treatments with solvent control (sc), 5 µM (c1), 10 µM (c2), 20 µM (c3) and 40 µM (c4) nicotine exposure. The three rows show all three replicates (r1-3) separately. The final solvent concentration was 0.1 % DMSO.
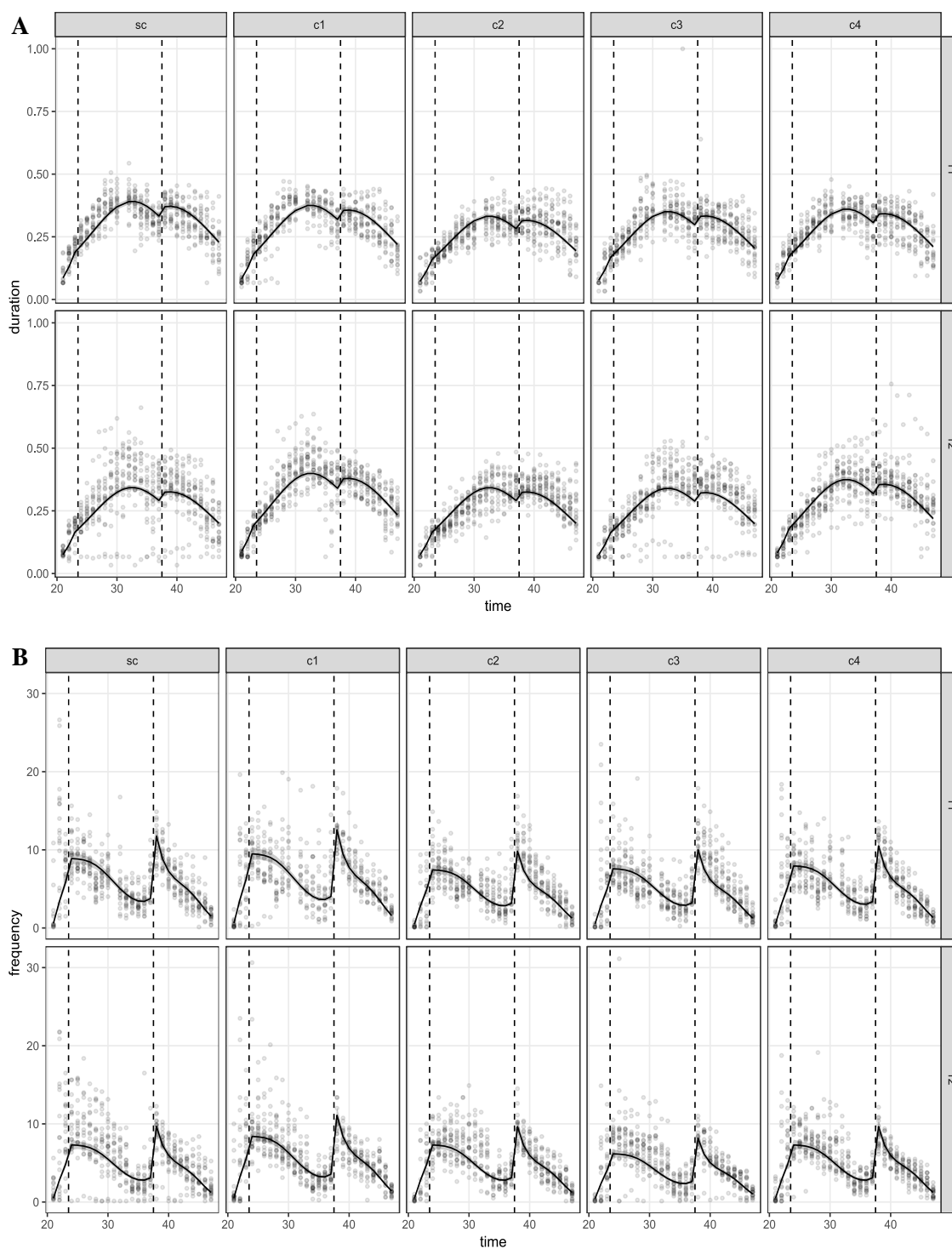
Figure B2: Coiling behavior analysis of the desnitro-imidacloprid (+DMSO) treatment experiment. The graphs illustrate the duration (A) and the frequency (B) of the coils of the zebrafish embryos between 21-47 hpf. Curves are predicted and fitted by the model. The columns depict the different treatments with solvent control (sc), 5 µM (c1), 10 µM (c2), 20 µM (c3) and 40 µM (c4) desnitro-imidacloprid exposure. The two rows show the two replicates (r1 und r2) separately. The final solvent concentration was 0.1 % DMSO.

APPENDIX C

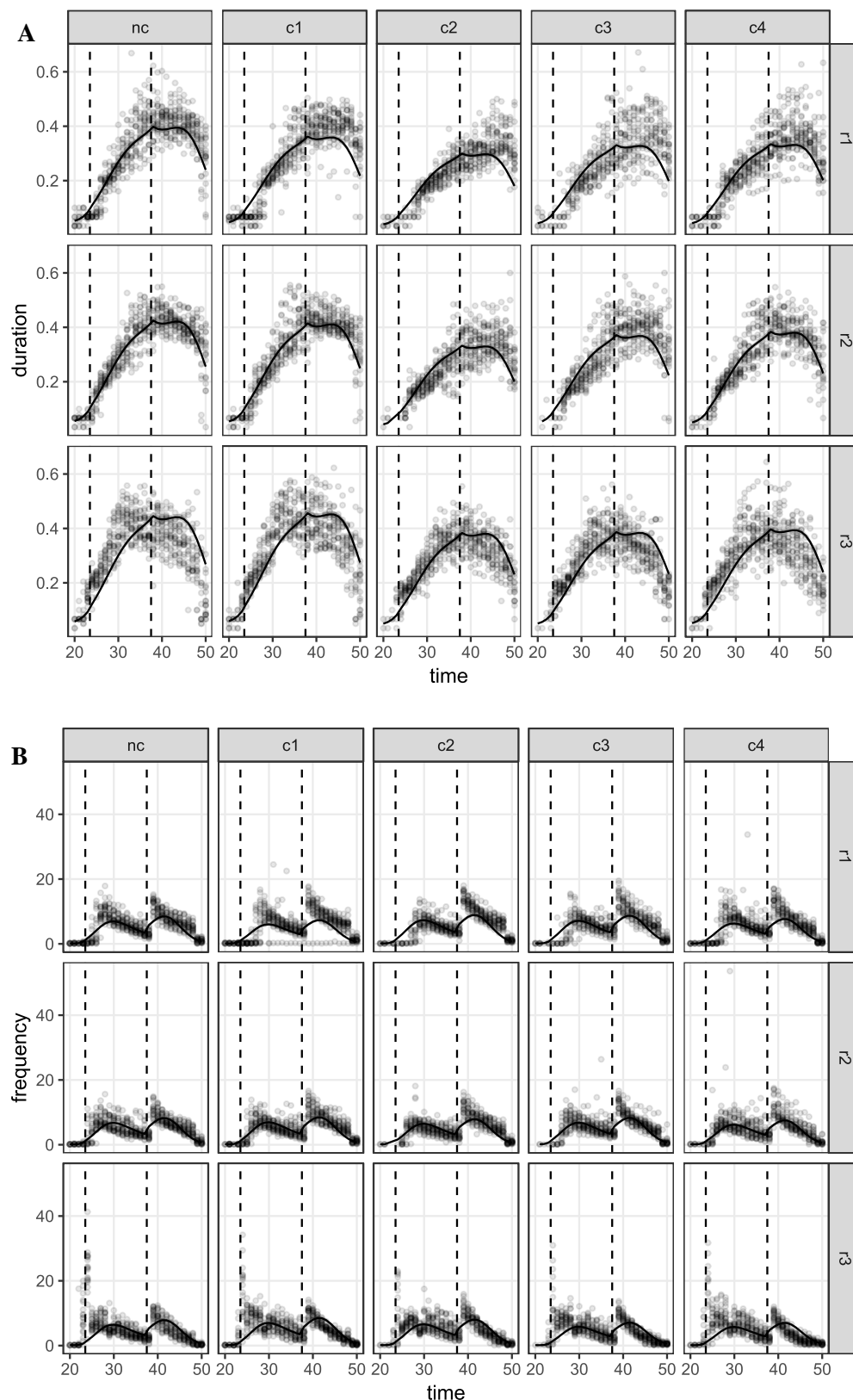## Impact on coiling behavior – sertraline, paroxetine and venlafaxine

Figure C1: Coiling behavior analysis of the sertraline (+DMSO) treatment experiment. The graphs illustrate the duration (A) and the frequency (B) of the coils of the zebrafish embryos between 21-47 hpf. Curves are predicted and fitted by the model. The columns depict the different treatments with solvent control (sc), 0.01 µg/L (c1), 0.1 µg/L (c2), 1 µg/L (c3) and 10 µg/L (c4) sertraline exposure.

The three rows show all three replicates (r1-3) separately. The final solvent concentration was 0.01 % DMSO.

A

Figure C2: Coiling behavior analysis of the paroxetine treatment experiment. The graphs illustrate the duration (A) and the frequency (B) of the coils of the zebrafish embryos between 21-47 hpf. Curves are predicted and fitted by the model. The columns depict the different treatments with negative control (nc), 0.01 µg/L (c1), 0.1 µg/L (c2), 1 µg/L (c3), 10 µg/L (c4), 100 µg/L (c5), 1000 µg/L (c6) and 2000 µg/L (c7) paroxetine exposure. The six rows show all replicates (r1-6) separately. The concentration c4 was involved in all replicates.

A

B

Figure C3: Coiling behavior analysis of the venlafaxine treatment experiment. The graphs illustrate the duration (A) and the frequency (B) of the coils of the zebrafish embryos between 21-47 hpf. Curves are predicted and fitted by the model. The columns depict the different treatments with negative control (nc), 0.1 mg/L (c1), 1 mg/L (c2), 10 mg/L (c3) and 25 mg/L (c4) venlafaxine

exposure. The three rows show all three replicates (r1-3) separately. The final solvent concentration was 0.01 % DMSO.

Impact on the visual-motor response

Recording and detection settings

Table C1: Detection settings for EthoVision XT 16.0 in the visual motor response assay

Sample rate	25 fps
Method	Differencing
Detection reference image	Background (Appendix)
Subject color compared to background	darker
Sensitivity	90
Background changes	very slow
Video pixel smoothing	none
Dropped frames correction	off

Heatmaps as a quality control for detection
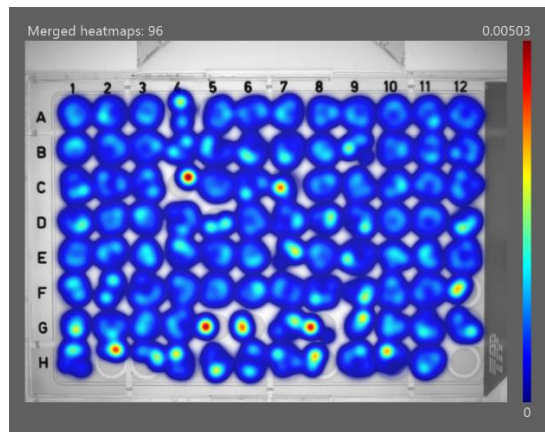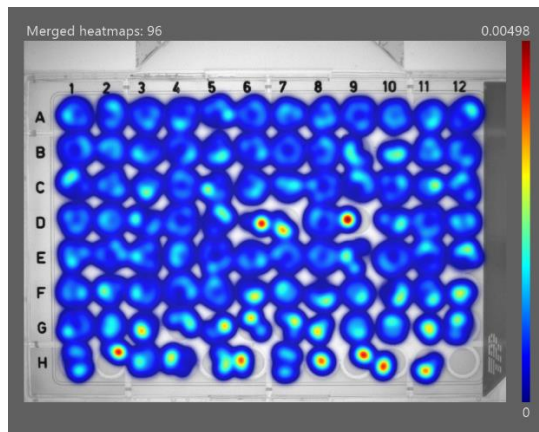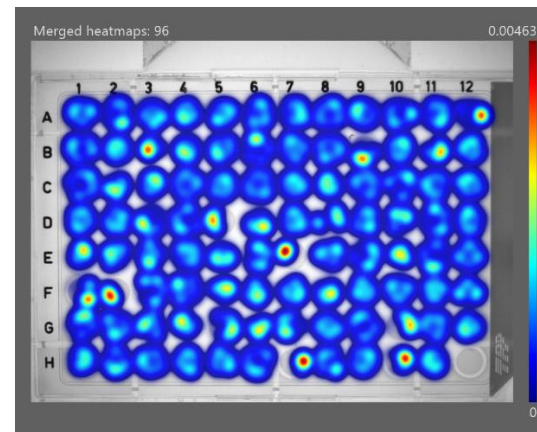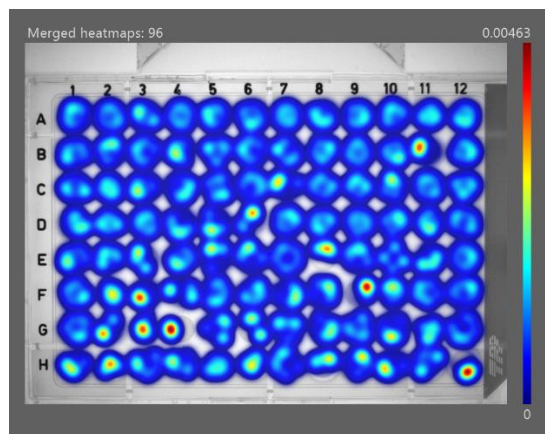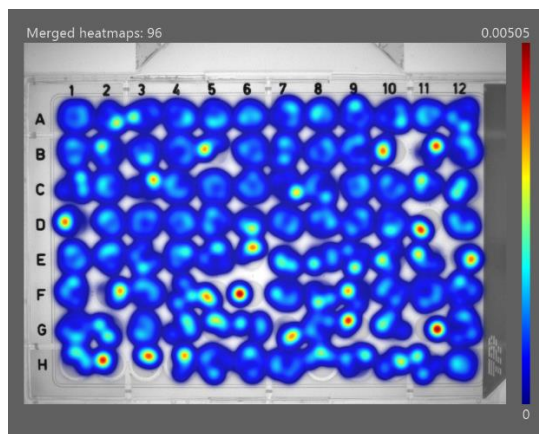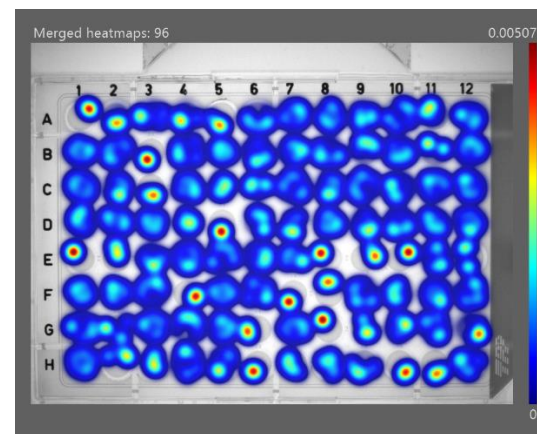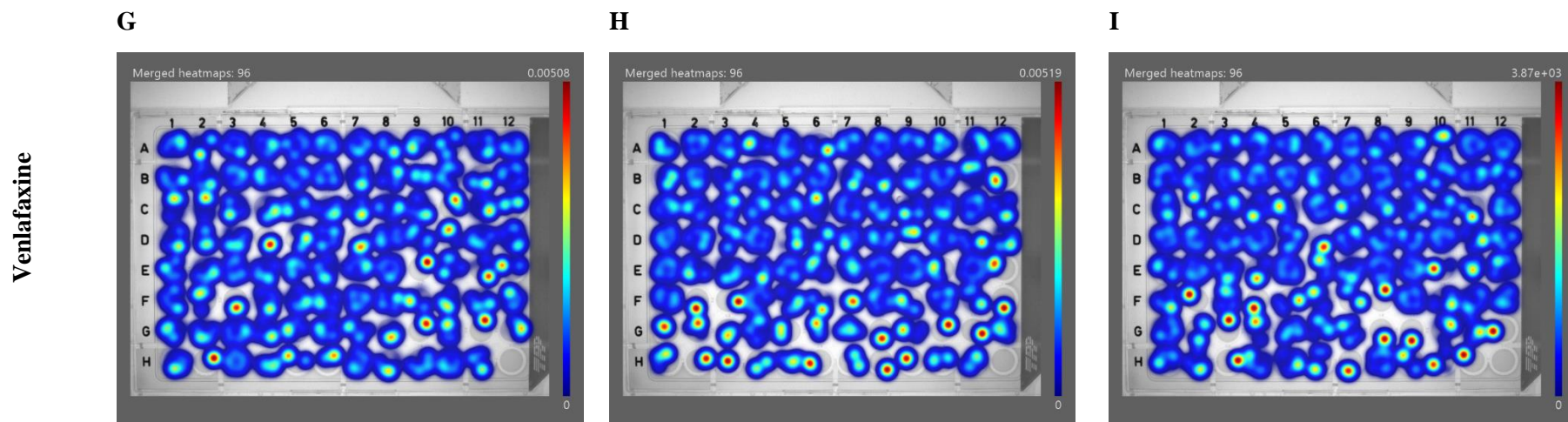
Figure C4: Cumulative distance moved of the VMR experiments as heatmaps. The images show a 96-well plate of zebrafish embryos previously treated with sertraline (A-C), paroxetine (D-F) or venlafaxine (G-I), each with three replicates. The maps show the activity of the zebrafish embryos over time in each well. Blue indicates the location where the embryos have not spent much time, while red to dark red indicates a location where the embryo has spent a long time.